SCUOLA NORMALE SUPERIORE

Pisa

CLASSE DI SCIENZE MATEMATICHE, FISICHE E NATURALI

CORSO DI PERFEZIONAMENTO IN NEUROBIOLOGIA

Triennio 2007-2009

Tesi di perfezionamento

ENVIRONMENTAL ENRICHMENT AND VISUAL SYSTEM: THALAMOCORTICAL AND CROSSMODAL PLASTICITY

Candidato: **MARCO MAINARDI**

Relatori: P**rof. Lamberto Maffei**

Dr. Matteo Caleo

TABLE OF CONTENTS

ABSTRACT

It has been demonstrated that the complex sensorimotor and social stimulation achieved by rearing animals in an enriched environment (EE) can reinstate juvenile-like plasticity in the adult cortex. However, it is not known whether EE can affect thalamocortical transmission. In the first part of this work, I investigated this problem by recording *in vivo* field potentials from the visual cortex evoked by electrical stimulation of the dorsal lateral geniculate nucleus (dLGN) in anaesthetized rats. I found that a period of EE during adulthood shifted the input-output curves and increased paired-pulse depression, suggesting an enhanced synaptic strength at thalamocortical terminals. Accordingly, EE animals showed an increased expression of the vesicular glutamate transporter 2 (vGluT-2) in geniculocortical afferents to layer IV. Rats reared in EE also showed an enhancement of thalamocortical long-term potentiation (LTP) triggered by theta-burst stimulation (TBS) of the dLGN. To monitor the functional consequences of increased LTP in EE rats, I recorded visual evoked potentials (VEPs) before and after application of TBS to the geniculocortical pathway. I found that responses to visual stimulation were enhanced across a range of contrasts in EE animals. This was accompanied by an upregulation of the intracortical excitatory synaptic marker vGluT-1 and a decrease in the expression of the vesicular GABA transporter (vGAT), indicating a shift in the excitation/inhibition ratio.

Thus, in the adult rat, EE enhances synaptic strength and plasticity of the thalamocortical pathway associated with specific changes in glutamatergic and GABAergic neurotransmission.

Another interesting problem connected to EE, is the possibility that the multimodal sensory stimulation provided by this rearing protocol can affect functional relationships among different cortical areas, thus contributing to the effect observed on visual cortical plasticity. In the second part of my work, I explored this problem by looking for cortical areas

monosynaptically connected with primary visual cortex (V1), using stererotaxic injections of cholera toxin β subunit. I found that primary visual cortex is connected with secondary motor cortex (M2, also known as frontal eye field), primary somatosensory cortex (S1) and primary auditory cortex (A1). These connections could explain how the sensorimotor stimulation provided by EE, which does not have a specific "visual" component, can affect visual function. Functional interactions between V1 and M2 or A1 were investigated using multichannel local field potential recordings in awake, freely moving mice, subjected to EE since birth. Quantitative analysis of LFP signals revealed that EE has opposite effects on V1-M2 and V1-A1 activity correlation, resulting in a decrease of functional coupling in the first case and in an increase in the second case.

These data provide novel insights into the mechanisms by which EE shapes the adult brain.

1. INTRODUCTION

1.1 THE PROBLEM OF ENVIRONMENT AND BRAIN

The initial development of the nervous system is controlled by a genetic program which defines the overall morphology, circuits and even the number of cells. For instance, *Hox* genes determine in Mammals the correct pattern of rhombomeres (Tumpel et al., 2009), whereas apoptosis regulates the cellular population, as it is demonstrated by brain enlargement in transgenic mice overexpressing the *Bcl2* antiapoptotic gene (Farlie et al., 1995).

Anyway, the structure created by genes action undergoes an experience-dependent maturation process, to adjust functioning of the central nervous system to interindividual differences in experience, which cannot be *a priori* determined. For this reason, the nervous system must be endowed with "plasticity" mechanisms for adapting itself to the environment.

The first evidence that experience could have a crucial role in directing development of the central nervous system came from studies in patients experiencing a prolonged sensory loss. The most interesting examples come from visual deprivation, caused, for instance, by congenital unilateral cataract. In this condition, the opacity of the lens results in low acuity of vision through the affected eye (*i.e.* amblyopia) and loss of stereopsis. Surgical treatment permits to restore normal vision only if correction of the defect is performed early in life; if not amblyopia persists (Lewis and Maurer, 2009). A similar situation is present in squint. In this pathology, the patient shows a preferential response to one eye and suppression amplyopia in the fellow eye develops, in addition to loss of stereopsis. Similarly to cataract, if surgical correction is performed in early postnatal life there is an almost complete recovery of visual function, whereas in case of late intervention, only aesthetic improvements are achieved (Schmucker et al., 2010). This suggests that the altered experience that derives from amblyopia is responsible for a loss of responsiveness to sensory input of visual brain areas, which can persist even after normal ocular function has been restored.

An interesting case is reported by Oliver Sacks, who narrates the experience with a fifty-year-old patient, Virgil, who could only perceive gross variations in luminance because he had been visually impaired since birth and at the age of six had also become affected by severe cataract. After surgery, he regained a certain degree of visual function; however, he still preferred to use the other sensory modalities, instead of "learning" to use the new one (Sacks, 1985). More recently, positive results have been obtained by a patient who had one eye blind and the other one suffering after a corneal thermal and chemical damage, both occurred at the age of three and a half. At 43, corneal transplantation to the spared eye was eventually successful and he was able to acquire a certain degree of low-acuity vision, orientation sensitivity and motion perception (Fine et al., 2003). The greater recovery of function in this latter patient may be explained by the fact that he became blind at a later age and his visual system had had more time to normally develop until lesion happened.

These clinical data highlight the importance of experience in defining the correct physiology of the central nervous system. Two cardinal concepts emerge from these studies: (i) the nervous system is "plastic", *i.e.* it has the capability to adapt its functioning to environmental stimuli and (ii) neural plasticity is temporally regulated, so the adaptive potential of neural circuits is not homogeneous over the animal's lifespan.

1.1.1 Fundamental studies on plasticity

Probably, the greatest contribution to understanding the functional basis of neural plasticity has been given by the studies of David Hubel and Thorsten Wiesel. Using the cat as a model system and by means of electrophysiological recordings at the single unit level, they first made an extensive description of the visual system physiology. Among the other results, they showed that neurons in the primary visual cortex (V1) are binocular and they can be sorted in seven

classes according to their preference to visual stimuli coming from the ipsilateral eye (class 1 and 2-3) , contralateral eye (class 5-6 and 7) or both eyes (class 4) (Hubel and Wiesel, 1962). They also found, in cats and monkeys, that thalamic afferent-receiving neurons in layer IV of V1 are arranged in ocular dominance (OD) columns, which respond alternatively to the ipsilateral or contralateral eye (Hubel and Wiesel, 1963, 1968; Wiesel et al., 1974).

To assess the cortical response to manipulations in visual experience, they deprived one eye of patterned vision in kittens by suturing the lids closed, then reopened it and measured the ocular dominance of neurons in the contralateral visual cortex. A period of this protocol, called monocular deprivation (MD), resulted in a marked shift of the ocular dominance distribution towards the open eye. Moreover, there was a reduction in the number of class 4 cells, which caused a decrease in binocularity of the striate cortex (Hubel and Wiesel, 1964; Hubel et al., 1977). Consistent results were found at the structural level by analyzing ocular dominance columns: the columns that received input from the deprived eye shrank, whereas the columns that were innervated by the open eye expanded (Hubel et al., 1977). Interestingly, these effects are present only during early postnatal development and are not observed if MD is performed in adult animals (Hubel and Wiesel, 1970).

During immediate postnatal development, ocular dominance column development is experience-independent, since their pattern in the ferret is not affected by total deprivation of visual input by binocular enucleation, starting as early as postnatal day 0 (Crowley and Katz, 1999). However, maintaining cortical column structure requires visual experience, since silencing input from both eyes with bilateral injections of tetrodotoxin (TTX) causes in the cat desegration of layer IV columns (Stryker and Harris, 1986).

Cortical column shrinkage is the macroscopical result of more subtle processes, acting on thalamocortical afferents. Indeed, it has been shown in cats that MD during early postnatal life

initially induces in layer IV of primary visual cortex retraction of thalamocortical axons conveying input from the deprived eye (after 4-7 days of MD), then an expansion of axons serving the non-deprived eye (after 5 weeks of MD) (Antonini and Stryker, 1996) . However, in mice, only expansion of open eye-guided axons is observed and this process requires MD for a period of at least 15 days (Antonini et al., 1999).

According to the fact that visual input enters V1 in layer IV, it has long been thought that this were the initial place of ocular dominance plasticity. Instead, it has been shown that remodelling of connections takes place first in supragranular layers, namely layer II-III, where horizontal connections between different ocular dominance columns are present (Trachtenberg et al., 2000).

Interestingly, all these effects on thalamocortical connectivity and primary visual cortex physiology take place only if one eye is deprived of experience, whereas binocular deprivation yelds no effect (Blakemore and Van Sluyters, 1974; Antonini and Stryker, 1998). This result can be explained by considering that binocular deprivation causes a reduction of cortical activity driven by *both* eyes, while MD creates an *imbalance* between one eye and its fellow. Thus, it appears that a crucial factor in developing the cortical response is the competition between sensory inputs.

The importance of activity for proper development of the central nervous system is remarked by studies on total deprivation of visual input, which is achieved by rearing the animal in darkness from birth (dark rearing, DR). Prolonged DR increases the number of binocular neurons and results in a lower visual acuity (Mower et al., 1981; Fagiolini et al., 1994). On the other hand, binocular deprivation does not totally block light from reaching retinae (but hinders patterned vision) and this explains the different effect on cortical development (Mower et al., 1981).

It must be pointed out, anyway, that visual experience is not entirely responsible for shaping visual system, as in non-human primates ocular dominance columns are fully formed at birth (Horton and Hocking, 1996). This process can be driven by spontaneous retinal ganglion waves of activity, which begin even before photoreceptor maturation (Galli and Maffei, 1988; Katz and Shatz, 1996).

The profound changes induced by MD can be reversed during early postnatal life by reopening the deprived eye and closing the fellow eye, a protocol known as reverse suture (RS) (Malenka et al., 1988). According to these data, the preferential response of cortical neurons is determined by competition between inputs and artificially favoring one eye through MD has the effect of shifting the cortical response towards this dominant input. Conversely, to induce recovery from MD, the deprived eye must made the dominant input with RS.

Surprisingly, also binocular vision after MD is able to restore normal vision even faster that RS (Mitchell et al., 2001). Moreover, if eyes are misaligned during MD, recovery through binocular vision is inferior (Kind et al., 2002). Thus it seems that cooperation between the input coming from the two eyes, coupled to sustained activity (*i.e.* light stimulation *vs.* dark rearing) can be even more effective than favoring the input coming from the formerly deprived eye with RS.

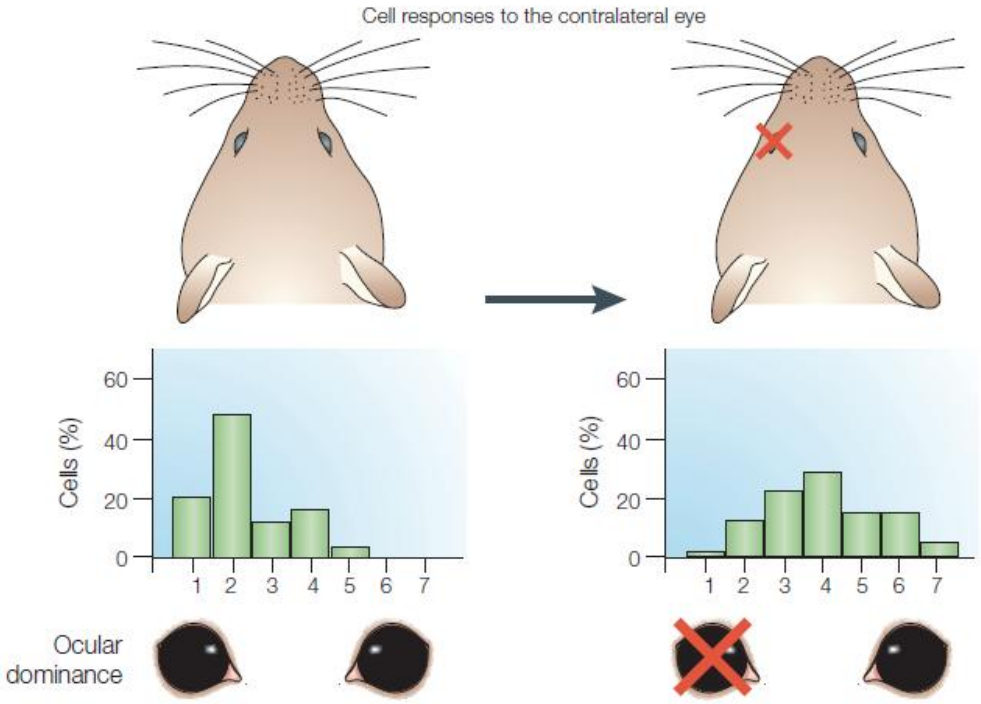

Figure 1.1 Ocular dominance shift of cortical neurons in response to monocular deprivation. Closure of one eye results in a shift in the response of cortical neurons towards the open eye, as demonstrated by single-cell electrophysiological recordings (from Hensch, 2005).

1.1.2 Age-dependent regulation of plasticity

MD does not have the same effect over the entire lifetime of the animal. In kittens, susceptibility to MD arises around the fourth postnatal week, remains constant until the eighth week and then declines towards the third month of life (Hubel and Wiesel, 1970). Besides, RS is effective in restoring binocularity only if performed within the same temporal boundaries described for susceptibility to MD (Hubel and Wiesel, 1970). These data agree with clinical reports (Polat, 2008) and it is possible to conclude that the visual system is sensitive to manipulations of experience, but only if this happens within a precise time window, that is called the "critical period". Further studies have shown that the critical period duration is correlated to the specific lifespan of a particular animal species and that, inside this time window, sensory systems mature their performance (Berardi et al., 2000). However, in rats it has been observed that, after DR from birth, P60 animals still respond to MD with an ocular

dominance shift and their visual performance is comparable to P19-21 controls (Fagiolini et al., 1994). Hence, a total lack of sensory experience is able to postpone the maturation of primary sensory cortex, which appears to be an activity-dependent process.

Analogous experiments have been performed in different sensory areas and it appears that each one has its critical period; moreover, different functions in the same area have different critical periods. For instance, the layer IV of primary somatosensory cortex (S1) of the rodent is characterized by an ordered somatotopic map of vibrissae, which resembles an array of "barrels". Analogously to development of ocular dominance columns, deprivation of input from one whisker impairs the correct formation of the corresponding barrel (Van der Loos and Woolsey, 1973; Wong-Riley and Welt, 1980). However, the critical period for sensitivity to whisker deprivation is much briefer, being restricted in the rodent to the first 4 postnatal days (Fox, 1992). Besides, in layer II-III of S1, whisker trimming leads to a potentiation of the response to the spared vibrissa and a depression of the response to the deprived vibrissae. (Glazewski and Fox, 1996). While depression of response is only observed in animals younger than 3 months, potentiation does not seem to be limited to a specific critical period (Glazewski and Fox, 1996; Glazewski, 1998).

Analogous results come from studies on the sound source localization circuit of the barn owl. This system is based on the alignment between interaural time difference (ITD) of sounds and visual receptive fields, in the optic tectum. For instance, a visual stimulus located right in front of the animal (azimuth = 0°) is associated to an ITD of 0μsec. The alignment of optical and auditory maps can be experimentally disrupted by displacing the visual field with optic prisms. Given that birds cannot rotate the eyes to compensate for this variation, brain circuits have to adjust to restore proper sound source localization. After 6 to 8 weeks of prism rearing, a neuron in the optic tectum with a visual receptive field of 0° has adjusted its optimal ITD to a value that

is consistent with the displacement imposed by prisms (Knudsen and Brainard, 1991). Young animals can adjust their sound map up to an ITD of 70μsec, while in adult barn owls, the maximal values are lower and adaptation ceases after 200 days of age, which marks the end of the critical period for this peculiar neural function and coincides with sexual maturation (Knudsen and Knudsen, 1990). A similar time window exists for recovering of accurate sound source localization after prism removal, with younger animals showing an almost complete re-alignment of auditory and spatial maps, whereas older animals have limited or no recovery (Knudsen and Knudsen, 1990).

More recent experiments are leading to a revision of the traditional view of plasticity as a process confined, plus or minus, to the developmental period. Chronic recordings of visually evoked potentials (VEPs) in mice have shown that MD effect during the critical period on the visual cortex is bi-phasic. The earlier step is represented by a depression of response to activity coming from the deprived eye, which takes place within the first 3 days of MD, then follows potentiation of response to inputs from the undeprived eye, after 5 days of MD (Frenkel and Bear, 2004). However, a similar experiment has demonstrated that MD in adulthood fails to induce depression of response to the deprived eye, but the enhancement of response to the spared eye is still present (Sawtell et al., 2003). Besides, the degree of adult plasticity can also be influenced by prior manipulations during the critical period. Imaging of intrinsic optical signals has shown that, if MD is performed for 4 days during the critical period and repeated in adulthood for 3 days, the visual cortex retains the capability to display an OD (Hofer et al., 2006). Interestingly, also 6-7 days of MD, without any prior manipulation, could still induce an OD shift in adult mice and complete recovery 8 days after the end of MD (Hofer et al., 2006). Moreover, facilitation of repeated MD on OD plasticity was also observed if the first MD

period was performed in adulthood, since the second MD period was able to induce an OD shift after only 3 days (Hofer et al., 2006).

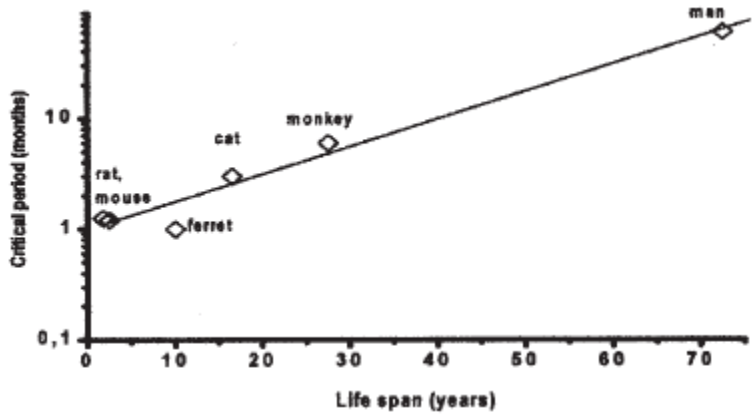

Figure 1.2 Duration critical period for ocular dominance plasticity in various animal species. A linear relationship links critical period duration and the entity of the animal lifespan (from Berardi et al., 2000).

1.2 FUNCTIONAL CORRELATES OF NEURAL PLASTICITY

A key issue in plasticity study is the search for the cellular mechanisms driving such large adaptive changes like ocular dominance shift, barrel cortex rearrangement and re-alignment of auditory and spatial maps. The leading idea of these experiments is the Hebbian postulate, which states that "neurons that fire together, wire together" (Hebb, 1949), that is, correlated activity between the pre- and postsynaptic terminals would lead to a selective strengthening of connections. Conversely, uncorrelated or sparse activity would cause depression at a given synapse.

1.2.1 Activity-dependent synaptic plasticity: long-term potentiation and depression

The first evidence that activity could be able to drive plastic phenomena came from the fundamental work by Bliss and Lømo, who found in the rabbit hippocampus that high-frequency repetitive stimulation of the perforant path could elicit a long lasting potentiation

(Long-Term Potentiation, LTP) of the postsynaptic field potential amplitude recorded in the dentate gyrus (Bliss and Gardner-Medwin, 1973; Bliss and Lomo, 1973), representing a form of activity-dependent synaptic plasticity (ADSP). Using chronic recording implants in unanaesthetized rats, LTP has been shown to last up to one year (Abraham et al., 2002). In the visual system, LTP has been observed in slices (Artola and Singer, 1987) and also in V1 *in vivo*, in response to stimulation of the visual thalamus (Heynen and Bear, 2001).

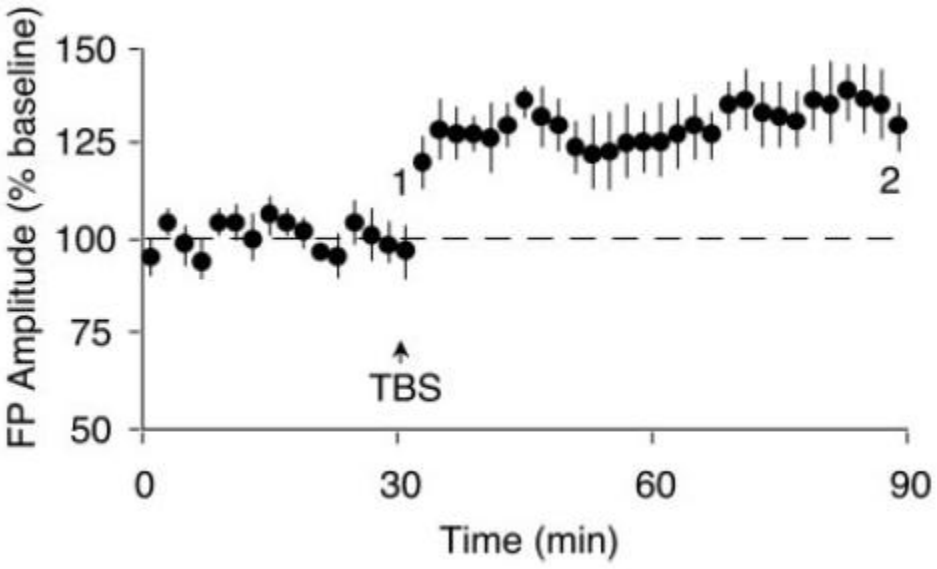

Figure 1.3 Long-term potentiation of synaptic transmission. This plot shows potentiation of cortical field potential amplitude after high-frequency stimulation (TBS) of the dLGN of the thalamus (from Heynen and Bear, 2001).

The first molecular mediator of LTP to be characterized has been the NMDA glutamate receptor (NMDAR), which is coupled to a Ca^{2+}-permeable channel. It was hypothesized to be involved in LTP when it was discovered that it coud specifically contribute to epileptiform activity in hippocampal preparations (Collingridge et al., 1983); subsequently it was demonstrated that pharmacological blockade with the selective agonist D-2-amino-5-phosphonovalerate (APV) inhibited LTP in response to tetanic stimulation without affecting basal synaptic transmission (Collingridge et al., 1983; Wigstrom and Gustafsson, 1986).The same NMDAR-mediated mechanism is shared by the neocortex, as it has been shown in visual

cortical slices; however, in some cases concurrent lowering of the inhibitory tone was required for LTP induction (Artola and Singer, 1987).

In its basal state, the ion channel associated to the NMDAR is obstructed by a Mg^{2+} ion (Herron et al., 1986), which is displaced only by postsynaptic depolarization concurrent with glutamate binding, thus allowing Ca^{2+} to enter the cell (Gustafsson et al., 1987; Huang et al., 1987). For this reason, the NMDAR is considered a detector of coincidence between stimuli and an ideal sensor of sustained presynaptic activity. Elevation of Ca^{2+} concentration inside the postsynaptic terminal is then responsible for activating the molecular cascades required for potentiation, which mainly depend on calcium/calmodulin-dependent kinase II (CaMKII) (Lisman et al., 2002), the cAMP-dependent protein kinase PKA (Lynch, 2004), protein kinase C (PKC) (O'Connor et al., 1995) and MAPK/ERK pathway (Kelleher et al., 2004b; Sweatt, 2004; Thomas and Huganir, 2004). Moreover, *in vitro* studies showed that LTP can be divided into different phases (i) an early phase, or E-LTP, which can be elicited by just one train of high frequency stimulation, resulting in a transient potentiation of postsynaptic response, lasting 30 to 60 min; (ii) a later phase or L-LTP, that is elicited only by repeated high-frequency stimulation and lasts several hours. In addition, it has been shown that: (i) blocking mRNA translation by means of bath perfusion with anisomycin converts L-LTP into E-LTP and (ii) blocking mRNA synthesis with actinomycin-D causes L-LTP to be maintained for a shorter time compared to control slices (Kelleher et al., 2004a). Thus, it appears that E-LTP relies on modifying an existent pool of proteins, whereas L-LTP requires first the synthesis of new peptides and then production of new mRNAs.

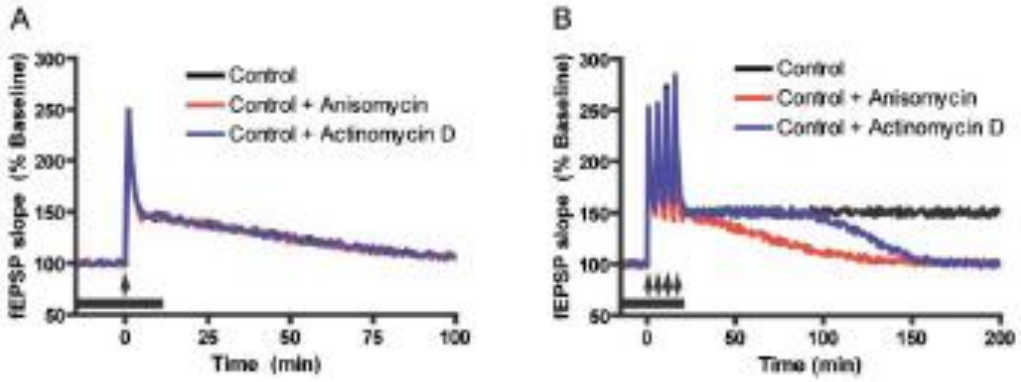

Figure 1.4 Different phases in LTP expression. A) E-LTP is a transient potentiation of synaptic response that takes place after a single cycle of high-frequency stimulation and does not depend on mRNA transcriptio nor translation. **B)** L-LTP is a persistent potentiation of synaptic response that is induced by sustained high-frequency stimulation. It can be further divided in an earlier phase, which is blocked by transcriptional inhibition (red trace) and a later phase, which is blocked by translational inhibition (blue trace) (from Kelleher et al., 2004).

The first change associated with LTP induction is the phosphorylation of AMPA glutamate receptors (AMPARs) subunit GluR1, that increases its insertion into the postsynaptic membrane; this can explain *per se* at least the initial phase of response potentiation (Barria et al., 1997; Lee et al., 2000). Subsequently, GluR1-containing AMPARs are substitued by receptors composed of GluR2 and GluR3 subunits due to constitutive receptor turnover (Shi et al., 2001). After LTP induction, insertion of new AMPARs can also convert sylent synapses –*i.e.* synapses that do not have AMPARs– into active synapses through the activation of NMDAR-mediated currents (Isaac et al., 1995). Later modifications include synthesis of new proteins and modulation of gene expression, which are essential for maintaining LTP on a longer timescale (Abraham and Williams, 2003).

In particular experimental conditions it is also possible to observe NMDAR-independent LTP. Indeed, it has been observed with intracellular recordings in rat visual cortex slices that, if $GABA_A$ receptor-associated chlorine channels are blocked with bicuculline, tetanic stimulation can induce an APV-insensitive potentiation (Artola and Singer, 1990). Further work performed in an analogous situation, obtained by bath perfusion with picrotoxin, demonstrated that a

"weak" tetanic stimulation protocol (basically consisting in a lower number of stimuli compared to the "standard" tetanic stimulation) was able to elict a slow-onset LTP that was not affected by the NMDAR-antagonist D(±)-2-amino-5-phosphonopentanoic acid (D-AP5), but was inhibited by the mGluR antagonist (S)-a-methyl-4-carboxyphenylglycine (MCPG) (Huemmeke et al., 2002). These data agree with previous work on freely moving rats, showing the involvement of group 1 mGluRs in LTP (Manahan-Vaughan, 1997).

In addition to LTP, long-term depression (LTD) has been observed as well, first at the hippocampal Schaffer collateral pathway (Dudek and Bear, 1992) and subsequently in visual cortex slices (Kirkwood and Bear, 1994b). LTD can be elicited by a prolonged, low-frequency stimulation of the circuit of interest and it is also dependent on NMDAR activation (Dudek and Bear, 1992; Mulkey and Malenka, 1992) and postsynaptic Ca^{2+} influx (Mulkey and Malenka, 1992). Moreover, electrophysiological recordings of field potential in freely moving rats, coupled to the use of the specific antagonists for group 1 mGluR [(S)4-carboxyphenylglycine (4CPG)], and for group 2 mGluR [(RS)-a-methylserine-O-phosphate monophenyl ester (MSOPPE) and (2S)-a-ethylglutamic acid (EGLU)], pointed to a role of both receptor subclasses in contributing to the later phase of LTD (Manahan-Vaughan, 1997).

The molecular cascade responsible for NMDAR-dependent LTD relies on phosphatase activity, namely phosphatases 1 and 2A (Mulkey et al., 1993). Phosphatase activity is required also for LTD maintenance, because their inhibition after LTD induction can reverse response depression (Mulkey et al., 1993). The target of phosphatases is, again, the GluR1 subunit of AMPARs, which have different phosphorylation sites mediating LTP or LTD. In particular, dephosphorylation of ser-845 is specifically associated with LTD and phosphorylation of both

ser-831 and -845 mediates LTP (Lee et al.). LTD induction also causes rapid, clathrin-dependent endocytosis of membrane AMPAR (Carroll et al., 2001).

On the other hand, LTD based on mGluRs appears to rely on activation of PKC (Nicoll et al., 1998). Anyway, the final effect is analogous to NMDAR-mediated LTD, given that it has been shown in hippocampal cultures that activation of group 1 mGluRs with (RS)-3,5-dihydroxyphenylglycine (DHPG) causes internalization of AMPARs (Xiao et al., 2001).

It is worth noting that these two different types of LTD involve different mechanisms, as NMDAR-mediated LTD decreases quantal size through the activation of protein phosphatases, while mGluR-mediated LTD decreases EPSP frequency through PKC activation (Nicoll et al., 1998).

LTD as well shows a late phase which is based on new protein synthesis (but not transcription of new mRNAs) (Manahan-Vaughan et al., 2000).

According to this "classical" view, LTP and LTD are considere to be mainly postsynaptic processes. Anyway, newer studies are beginning to clarify the role of presynaptic terminals in establishing potentiation. For instance, experiments combining calcium imaging and electrophysiology at the Schaffer collateral pathway in adult mice have demonstrated that individual synapses can undergo multiple transitions between potentiation and depression (Enoki et al., 2009). Instead of relying on modifications of postsynaptic response, plasticity was associated with changes in neurotransmitter release probability (Enoki et al., 2009).

An indirect proof of the involvement of NMDAR –and thus presumably LTP– in cortical plasticity came from the regulation in rat visual cortex of the expression of different isoforms of the subunit 2 of this protein. During the initial phase of postnatal life, the NR2B isoform is predominant but at eye opening (*i.e.* at the beginning of the critical period for ocular dominance plasticity) the NR2A isoform becomes prominent (Quinlan et al., 1999a). Moreover, dark

rearing impairs the shift in the NR2A/NR2B relative abundance ratio (Carmignoto and Vicini, 1992) and exposing dark-reared animals to light, even just for two hours, can restore the normal situation (Quinlan et al., 1999b). The reason for this developmental switch is that NR2B-mediated currents have a slower decay time compared to NR2A (Flint et al., 1997). Persistent currents would be necessary before eye opening to sustain correct development of connections in the absence of visual stimulation, while during the critical period the increase in sensory stimulation would require a fast-kinetic receptor to correctly shape the cortical structure.

Another important evidence is the existence of a critical period for LTP of layer III synapses of primary visual cortex, induced *in vitro* by stimulation of the white matter, which closely parallels the time course of the critical period for ocular dominance plasticity and can be analogously preserved by dark rearing (Kirkwood et al., 1995).

Concerning MD experiments, NMDAR appears to be essential, because pharmacological blockade (Bear et al., 1990; Daw et al., 1999) prevents the OD shift. A major problem of this experimental approach is that it also deeply affects basal visual function. However, blockade of the OD shift without effects on basal cell responsiveness has been found with inhibition of translation of the NR1 subunit via antisense oligonucleotides delivered into the visual cortex (Roberts et al., 1998). More recently, it has been shown that response potentiation to non-deprived eye inputs relies on NMDAR (Sawtell et al., 2003).

Whisker deprivation experiments support the link between LTP and plasticity as well. Indeed, when only one whisker is left intact, the potentiation in the cortical response to its sensory input is correlated to an increase in the AMPAR/NMDAR ratio and AMPA-mediated current rectification (Clem and Barth, 2006). Response potentiation can also be blocked by genetically knocking out the GluR1 subunit of the AMPAR (Hardingham and Fox, 2006).

On the other hand, the hypothesis that LTD can account for depression of cortical response to the deprived eye, is supported by the fact that MD reduces AMPAR surface expression and GluR1 phosphorylation (Heynen et al., 2003). Additional support for activity-dependent mechanisms comes from the fact that monocular injection of TTX is less effective than monocular lid suture in inducing depression of response to the deprived eye (Rittenhouse et al., 1999). This can happen because TTX injection almost totally silences activity driven by the treated eye, while with lid suture the eye evokes a residual amount of decorrelated and low-frequency activity which would in turn cause cortical LTD (Rittenhouse et al., 1999). Moreover, viral transduction of a sequence coding for a peptide competing with the GluR2 subunit for binding to AP2 adaptor complex impairs NMDA-dependent internalization of AMPARs (Yoon et al., 2009). This, in turn, blocks LTD in visual cortex slices from infected animals and, following MD, selectively affects depression of response to the deprived eye (Yoon et al., 2009).

Whether ADSP can also regulate recovery from MD is less clear. RS in kittens after one week of MD during the critical period is ineffective if coupled to inhibition of NMDARs by cortical infusion of APV (Gu et al., 1989), which would support a role for ADSP. However, at least for short periods of MD (6 days) during the critical period, intrinsic optical imaging and single-unit recordings in ferrets have shown that restoring binocular vision allows for a fast recovery of response to the contralateral, deprived eye within a few hours from eye reopening (Krahe et al., 2005). This partially excludes the involvement of Hebbian plasticity mechanisms, that RS may trigger by favoring the input from the formerly deprived eye. Interestingly, recovery is not influenced by inhibition of protein translation with cortical infusion of cycloheximide or rapamycin, whereas it is prevented by blocking neuronal activity with tetrodotoxin (TTX) (Krahe et al., 2005). On the other hand, recovery in the hemisphere ipsilateral to the deprived eye relies on protein synthesis (Krahe et al., 2005). Hence, in contrast

to RS, it seems unlikely that long-lasting plasticity phenomena are involved in binocular vision-mediated recovery from MD, because it is known that L-LTP depends on proteic synthesis (Frey et al., 1988).

1.2.1 Regulation of activity-dependent plasticity: metaplasticity

An additional feature of neural circuits is their capability to regulate their plasticity as a function of average activity, usually termed "plasticity of plasticity" or, in one word, "metaplasticity" (Abraham, 2008). This represents an important regulatory step, as it can avoid unwanted potentiation or depression in case of a prolonged and widespread increase or decrease in inputs.

The rules of metaplasticity have been theoretically described by Bienenstock, Cooper and Munro, who elaborated the so-called "BCM theory" (Bienenstock et al., 1982). It is based on a function (θ) that expresses the change in synaptic strength according to the degree of postsynaptic activity in reponse to presynaptic stimulation. Hence, if the afferent can elicit a low level of activity at the postsynaptic terminal, then that connection will undergo depression and viceversa (Bienenstock et al., 1982). Moreover, the threshold (θ_m) which separates induction of depression from potentiation can be shifted as average activity changes, thus facilitating LTP if activity is scarce and LTD in the opposite situation (Bienenstock et al., 1982).

Subsequent experimental work, mainly in hippocampus preparations, has shown that metaplasticity can result from a priming event, in the form of either electrical or behavioural activity, that is able to influence the expression of LTP or LTD; it can be distinguished from a simple modulation of plasticity because its effect persists for a certain time after it the priming stimulus has ended (Abraham, 2008). A complication for studying metaplasticity is that protocols for plasticity induction can simultanously cause metaplasticity. For instance, repeatet

cycles of LTP-inducing stimuli can apparently impair further potentiation: this can be actually due to a transient increase in θ_m,, because allowing the preparation to "rest" for a certain time restores LTP susceptibility (Frey et al., 1995). The same situation is observed for LTD, whose magnitude is proportional to the duration of the low-frequency stimulation induction protocol (Mockett et al., 2002). Hence, the first stimuli act as primers by facilitating the expression of subsequent LTD (Mockett et al., 2002).

The fact that the same molecules can mediate both LTP and LTD in different conditions leads to hypothesize that they are subject to metaplastic regulation. In fact, previous activation of the NMDAR facilitates the induction of LTD at the expense of LTP (Huang et al., 1992). Moreover, increasing the strength of the induction stimulus restores LTP, which indicates that priming increases θ_m, rather than completely abolishing potentiation (Huang et al., 1992). Conversely, prior NMDAR activation facilitates LTD (Christie and Abraham, 1992).

Another interesting mediator of metaplasticity is the metabotropic glutamate receptor (mGluR), whose slower kinetic of action, comapred to ionotropic receptors, makes it an ideal candidate for long-lasting regulatory processes. Indeed, prior activation of mGluRs with the agonist 1-amino-cyclopentane-1S,3R-dicarboxylic acid (ACPD) is able to facilitate LTP induction and to increase its magnitude in response to weak stimulation (Cohen and Abraham, 1996); this property is displayed by both group 1 and group 2 mGluRs (O'Leary and O'Connor, 1998). It must be pointed out that, even in presence of priming facilitation by mGluRs, LTP expression is still dependent on NMDARs activation (Cohen and Abraham, 1996).

Moreover, pharmacological priming of group 1 mGluRs can convert E-LTP, triggered by only one train of high frequency stimulation, into L-LTP (which normally would require a stronger stimulation protocol), using a translation- (but not transcription-) dependent mechanism (Raymond et al., 2000). Moreover, a cycle of low-frequency stimulation can wipe

away the priming effect of mGluRs activation (Bortolotto et al., 1994). For these reasons, mGluRs activation represents a molecular switch to facilitate and enhance subsequent LTP (Bortolotto et al., 1994).

The main mechanisms of mGluR priming are (i) the reduction in slow afterhyperpolarization caused by downregulation of Ca^{2+}-activated K^+ channels (Cohen et al., 1999a), that enhances membrane depolarization; (ii) an increase in AMPARs delivery to the extrasynaptic membrane, via their phosphorylation on ser-845 (Oh et al., 2006), to create a pool ready to be inserted in the postsynaptic membrane at LTP induction.

Metaplasticity can be invoked to interpret some aspects of visual cortex plasticity. First of all, during MD, the overall decrease in cortical activity caused by reduction in the dominant input, coming from the contralateral, deprived eye would in turn lower the threshold value of θ_m. Therefore, the cortex would be in a potentiation-prone status, which would facilitate potentiation of response to the non-dominant input coming from the ipsilateral, open eye (Smith et al., 2009). Accordingly, previous DR causes a prolonged reduction in cortical activity and lowers θ_m so that in visual cortex slices LTP can be induced more easily at the expense of LTD (Kirkwood et al., 1996). These changes appear to involve bidirectional changes in the NR2A/NR2B NMDAR subunit ratio, which resembles the critical period situation (Quinlan et al., 1999b). In particular, DR causes a transient increase in NR2B, then the expression of this protein goes back to the basal level and NR2A expression decreases (Chen and Bear, 2007): thus, the net effect is an increase in the NR2B/NR2A ratio. Reduction of NR2A level plays a critical role, because its genetic deletion occludes the effect of DR on θ_m modulation (Philpot et al., 2007). Further support to this model comes from the fact that MD increases the NR2B/NR2A ratio (Chen and Bear, 2007), but only after 5 days of treatment, which parallels the delayed time course for response potentiation to non-deprived eye (Frenkel and Bear, 2004). Following these

directions, the possibility to restore OD plasticity in adult rats through a period of DR (He et al., 2007) might again result from the increase in the relative abundance of NR2B, which has been shown to take place in adult ferrets (Corson et al., 2009).

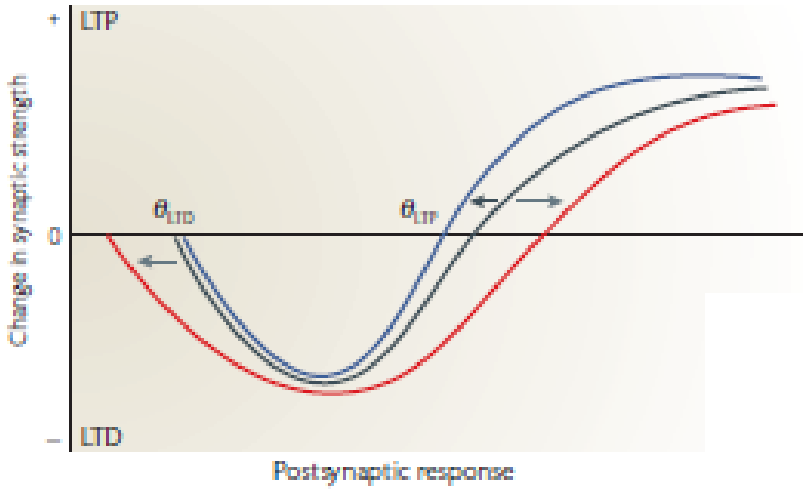

Figure 1.5 Schematic diagram of metaplasticity. Modulation of plasticity affect the activity thresholds for LTP and LTD induction (θ_{LTP} and θ_{LTD}) (from Abraham, 2008).

1.2.3 Spike timing-dependent plasticity

The experimental protocols used to elicit ADSP (activity-dependent synaptic plasticity, see above) consist of long periods of repetitive stimulation, which are not likely to be observed during genuine physiological activity. This opens the possibility that other plasticity mechanisms exist. Indeed, Calcium imaging experiments on layer IV neurons of rat barrel cortex, have shown that the amplitude of the Ca^{2+} transient evoked at single synapses by coupling EPSPs with backpropagating action potentials (BAPs) originating in the soma varies according to the temporal order of these stimuli (Nevian and Sakmann, 2004). In particular, when synaptic activity (EPSP) preceded postsynaptic depolarization (BAP) a supralinear summation of the evoked Ca^{2+} transient was observed, whereas inverting the order of the stimuli led to sublinear summation (Nevian and Sakmann, 2004). This was true for a time

window comprised between 10 and 50msec (Nevian and Sakmann, 2004) and represents an example of "spike-timing dependent synaptic plasticity" (STDP). An analogous phenomenon had been previously observed *in vivo* in the retinotectal pathway of the toad *X. laevis*, where potentiation or depression of postsynaptic response was observed when EPSP preceded postsynaptic depolarization and *vice versa* within a 20msec time window (Zhang et al., 1998).

STDP could be important *in vivo* for improving the sensitivity of postsynaptic response to the presynaptic activity pattern; moreover, it could select and favour inputs with higher correlation (Song et al., 2000).

STDP thus responds to a true Hebbian rule, based on the temporal order between EPSP evoked by presynaptic activity and postsynaptic depolarization, which can arise from backpropagating action potentials (BAPs). The transducer for STDP could be again NMDAR (Zhang et al., 1998). BAPs could facilitate Mg^{2+} dissociation from the channel pore, and the fast kinetic of this process could explain the narrow time window for plasticity induction (Kampa et al., 2004).

Induction of potentiation *versus* depression could be determined by the different levels of Ca^{2+} entering the cell. Leading of presynaptic ("pre leading post") input causes opening of the NMDAR-associated channel and a high Ca^{2+} influx, while postsynaptic leading ("post leading pre") would activate voltage-dependent Ca^{2+} channels and a lower but sustained increase in Ca^{2+} concentration (Dan and Poo, 2004). Indeed, the Ca^{2+} transient evoked at single synapses by coupling subthreshold EPSP and postsynaptic depolarization through backpropagating action potentials, was greater when "pre led post", showing supralinear summation (Koester and Sakmann, 1998). Consistently, partial inactivation of NMDAR with low doses (1-3μM) of APV during the "pre leading post" protocol resulted in LTD at the Schaffer collateral pathway (Nishiyama et al., 2000).

In some cases, STDP-mediated LTD is independent from NMDAR activation. For instance, at layer IV to layer II/III of the barrel cortex, LTD requires activation of group 1 mGluRs, Ca^{2+} influx-induced phospholipase C (PLC) activation and further release of Ca^{2+} mediated by IP3, together with retrograde endocannabinoid signaling (Bender et al., 2006). This accounts for a model based on two coincidence detectors, NMDAR for LTP and PLC for LTD (Bender et al., 2006; Caporale and Dan, 2008).

Anyway, different cell types appear to actuate STDP in different ways. CaMKII activation in excitatory neurons of the dorsal cochlear nucleus causes STDP LTP, whereas in inihibitory neurons the same signaling pathway (coupled with endocannabinoid retrograde signaling) induces LTD (Tzounopoulos et al., 2007).

Interestingly, the rules for STD-LTP or –LTD seems to vary also across the dendritic tree. At the layer II/III to layer V synapse of the somatosensory cortex, low-frequency EPSPs paired to BAP bursts elicited in layer V neuronal somata have opposite effects at proximal and distal dendritic sites. Indeed, when "post leads pre" proximal sites exhibit the expected LTD, but distal sites respond with LTP (Letzkus et al., 2006). The reversal in STDP rule can be explained by the induction of dendritic Ca^{2+} spikes during the BAP burst, which would cause a peak in postsynaptic depolarization coincident with EPSP (Caporale and Dan, 2008).

Beyond a certain level of activity, the fine tuning of STDP seems to be replaced by conventional ADSP, at least in synaptically connected pairs of layer V neurons in visual cortex slices and using a protocol of EPSPs leading postsynaptic bursts of action potentials at 10msec intervals. Up to a burst frequency of 40Hz, the classical rule for STDP was respected, but a higher intersimulus intervals, LTP was invariably induced regardless of pre-leading-post or post-leading-pre patterns (Sjostrom et al., 2001). This may happen because, for instance, at 50Hz and "post leading pre", the presynaptic stimulus is equally spaced in time from the preceding

and following postsynaptic stimuli: in this ambigous situation, potentiation can be favoured over depression.

The involvement of STDP in cortical plasticity *in vivo* is only beginning to be clarified. Interesting results come from whole-cell recordings of layer II-III neurons of the barrel cortex, where pairing whisker deflection to postsynaptic spikes generated by current injection in a "post leading pre" manner and within a 33msec time window, generated LTD (Jacob et al., 2007).

STDP can also mediate orientation map plasticity in kitten visual cortex. Indeed, pairing of visual stimuli with extracellular stimulation at 7Hz for 3-4hrs induces in extragranular layers a shift towards or away the stimulus orientation of the cortical map if this preceded or followed the stimulation (Schuett et al., 2001). The lack of effect of the pairing protocol on layer IV maps could imply that spike-timing dependence is typical of intracortical connections (Schuett et al., 2001), while thalamocortical connections would either not be affected by this activity pattern or require stronger stimulation paradigms, like the ones used in ADSP experiments.

Concerning OD plasticity during MD, STDP can model the peculiar behaviour of fast-spiking inhibitory interneurons (see below). These cells display a paradoxical shift after 3 days of MD, which, after two weeks, reverts to the expected shift towards the open eye (Yazaki-Sugiyama et al., 2009). These bidirectional plasticity fits with a computational STDP model based on an initial increased drive of the interneuron by the deprived eye, which is later reversed by pruning of inactive synapses (Yazaki-Sugiyama et al., 2009).

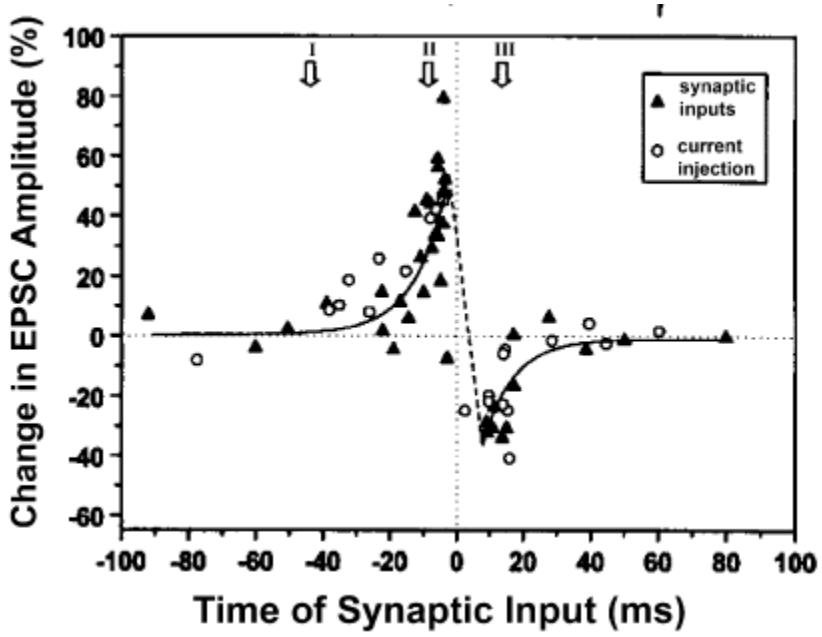

Figure 1.6 Spike timing-dependent plasticity. The relative timing between postsynaptic depolarization and synaptic input results in potentiation or depression of postsynaptic response within a critical window of about 20msec (from Dan and Poo, 2004).

1.2.4 Homeostatic plasticity

An intrinsic problem of Hebbian plasticity rules is that they trend to destabilize the balance of neuronal networks, dramatically increasing or decreasing their activity (Turrigiano and Nelson, 2004; Turrigiano, 2008). Even in basal conditions transmission of information from sensory organs to subcortical stations and, eventually, to the cortex must be finely adjusted to achieve a nearly unitary gain; if the gain is inferior, activity will extinguish before reaching the final stages of processing, vice versa, it will eventually saturate the response (Turrigiano and Nelson, 2004). For this reason, there must be a homeostatic system to preserve the average activity level on neural circuits. Experimentally, this was first shown in hippocampal cultures, where blocking excitatory activity had the effect of raising spontaneous postsynaptic activity (miniature EPSCs, mEPSCs) and, conversely, impairment of inhibition caused a decrease in mEPSCs (Turrigiano et al., 1998). The global increase or decrease of activity in response to

overall blocking or enhancement of excitation was termed "synaptic scaling" and is considered the manifestation of homeostatic plasticity (Turrigiano et al., 1998).

Synaptic scaling involves regulation of AMPAR clustering at synaptic sites. Indeed, selective blocking somatic excitatory activity by means of TTX microperfusion increases AMPAR accumulation, peaking after 4.5hrs, whereas no effect emerged when microperfusion was applied to block presynaptic glutamate release or postsynaptic receptor activation (Ibata et al., 2008). Thus, it appears that synaptic scaling results from a reduction in postsynaptic firing (Ibata et al., 2008). Moreover, synaptic scaling depends on mRNA transcription, as it is blocked by actinomycin-D (Ibata et al., 2008).

Local mechanisms for homeostatic plasticity at single synapes have been described in hippocampal neurons after NMDAR inhibition with APV, with concomitant TTX application (Sutton et al., 2006). Under these conditions, the increase in mEPSCs was faster than with somatic activity blockade and was dependent on protein synthesis of GluR1 AMPAR subunit (Sutton et al., 2006). Moreover, local perfusion of APV in dendrites, combined with somatic AP block with TTX, demonstrated single-synapse homeostatic plasticity (Sutton et al., 2006). These data indicate the existence of two homeostatic plasticity mechanisms: (i) a global increase in mEPSCs amplitude induced by a drop in postsynaptic firing and (ii) a local and faster upregulation of single-synapse activity when both glutamate receptors and postsynaptic firing are blocked. In particular, the local scaling would permit a differential response among the various dendritic branches of the same neuron (Turrigiano, 2008), while the global scaling would preserve homeostasis of whole-neuron activity.

Two interesting features of synaptic scaling is its slower kinetic, compared to STDP and LTP/LTD, and the immediate requirement for transcription (Ibata et al., 2008). This could allow a period for consolidating response potentiation or depression and then synaptic scaling would

restore the physiological range of activity. Indeed, given that with synaptic scaling all synapses are modified according to the same multiplying or dividing factor, strength ratios between different synapses are preserved, without overloading or dampening activity levels (Turrigiano and Nelson, 2004).

Actuation of homeostatic plasticity depends on variations in Ca^{2+} concentration, as inhibition of calcium channels with $NiCl_2$ to abolish somatic spikes is sufficient to induce an increase in AMPARs-containing puncta (Ibata et al., 2008). The intracellular sensor of this drop in Ca^{2+} influx is probably CaMKIV, because transfecting cultures to express a dominant-negative mutant induces an increase in mEPSCs amplitude similat to the effect of somatic TTX microperfusion (Ibata et al., 2008). A different transduction pathway seems to be involved during scaling down of high activity, obtained in hippocampal neurons with PTX perfusion (Seeburg et al., 2008). Interfering with polo-like kinase 2 (Plk2) activity by means of transfection with a truncated form competing for binding Plk-2 targets or by suppression of endogenous Plk2 synthesis with RNAi, prevented the expected decrease in mEPSC amplitude ("scaling down") otherwise observed in mock-transfected cultures (Seeburg et al., 2008). Moreover, overexpression of Plk2 was *per se* capable of inducing scaling down of mEPSCs (Seeburg et al., 2008). However, this effect requires also cyclin-dependent kinase 5 (CDK5) activity, as transfection with a dominant negative construct lacking kinasic activity blocked mEPSC scalign down in response to PTX administration (Seeburg et al., 2008). Both CDK5 and Plk2 converge on the SPAR scaffolding protein at the postsynaptic density to trigger its ubiquitinilation-mediated degradation; indeed, transfection with a mutant lacking the Plk2 binding site rendered cells insensitive to PTX-induced scaling down, and RNAi to suppress endogenous SPAR synthesis is able to induce scaling down in a similar manner to kinase activation (Seeburg et al., 2008).

The existence of *in vivo* synaptic scaling has been shown in slices from the visual cortex, where it appears to be involved in postnatal circuit maturation. From postnatal day 12 (P12) to P23 in layer IV there is an increase in mEPSC frequency that is accompanied by a decrease in their amplitude (Desai et al., 2002). Conversely, slowing down visual system development with dark rearing also prevents this age-dependent modification (Desai et al., 2002).

Different cortical layers have their own critical period for displaying synaptic scaling. Indeed, MD can induce scaling up of mEPSC in layer IV until P18 (*i.e.*one week after eye opening), when this phenomenon begins to be observed in layer II-III, where it persists until adulthood (Desai et al., 2002).

Blocking ganglion cell activity with intraocular injection of TTX and MD both yield a scaling up of mEPSCs in layer II-III of the visual cortex which involves an increase in single-cell excitability (Maffei and Turrigiano, 2008). However, TTX treatment increased the excitatory spontaneous activity and decreases the inhibitory spontaneous activity on layer II-III neurons, thus resulting in a net increase in the excitation/inhibition ratio, whereas MD reduces mEPSCs without affecting mIPSCs, which causes a decrease in the excitation/inhibition ratio (Maffei and Turrigiano, 2008). Besides, TTX increases mEPSCs amplitude without affecting their frequency; on the other hand MD decreases both amplitude and frequency of mEPSCs, but increases intrinsic cell excitability (Maffei and Turrigiano, 2008). The final effect in both cases is an increase in spontaneous firing which, however, depends on different mechanisms. Total activity blockade with TTX activates canonical synaptic scaling, whereas the residual, uncorrelated input left after MD induces acts mainly through an increase in intrinsic cell excitability (Maffei and Turrigiano, 2008).

Homeostatic plasticity could also explain the paradoxical increase of response to deprived-eye input observed with *in vivo* calcium imaging in neurons which were guided predominantly

by the deprived eye (Mrsic-Flogel et al., 2007). This could be due to a mechanism of preservation of the net sensory drive to cortical neurons, and consistent with this interpretation is the increase in response to both eyes after a period of binocular deprivation (Mrsic-Flogel et al., 2007). According to the results obtained in slices by Maffei and Turrigiano (Maffei and Turrigiano, 2008), this situation could depend on the increase in intrinsic cell excitability, rather than to synaptic scaling (Turrigiano, 2008).

1.3 CRITICAL FACTORS CONTROLLING PLASTICITY

It can be easily imagined that such a comprehensive process like plasticity involves a wide number of changes, most of which take place at the gene expression level. Microarray analysis has permitted to appreciate the high number of genes which are regulated after manipulation of visual experience through MD and DR (Majdan and Shatz, 2006; Tropea et al., 2006). Virtually every class of gene is influenced by visual deprivation; among them, particularly interesting are modifications in the expression of mRNAs related to signaling pathways, inhibitory transmission, and neurotrophins (Majdan and Shatz, 2006; Tropea et al., 2006).

One key signaling pathway for visual plasticity is the molecular cascade that relies on the MAP kinase ERK. Indeed, pharmacological inhibition of the ERK pathway is able to prevent the OD shift caused by MD during the critical period (Di Cristo et al., 2001) and visual stimulation after a brief period of DR activates ERK through PKA-dependent phosphorylation, which in turn upregulates transcription of genes controlled by the CRE promoter (Cancedda et al., 2003).

During the critical period, ERK activation results in histone H3 acetylation and phosphorylation, a modification that is associated to the remodeling of chromatin structure towards a more transcription-permissive status, coupled to increased CRE-mediated gene expression (Putignano et al., 2007). In adult animals well beyond the critical period, visually-

induced ERK activation is still present, but CRE-dependent transcriptional activation is lower compared to juvenile mice (Putignano et al., 2007). This implies that downregulation of cortical plasticity after closure of the critical period can involve a widespread repression of gene transcription. Indeed, pharmacological inhibition of histone deacetylases with trichostatin A to promote histone acetylation is able to restore OD plasticity in adult mice (Putignano et al., 2007).

1.3.1 Neurotrophins

The pioneering experiments by Rita Levi-Montalcini and Stanley-Cohen led to the discovery of Nerve Growth Factor (NGF), the first member of the neurotrophin family (Levi-Montalcini, 1965). Subequently, gene cloning permitted to identify Brain-Derived Neurotrophic Factor (BDNF), NT3 and NT4/5 (Lewin and Barde, 1996). The main class of receptors for neurotrophins is represented by the tyrosine kinase receptor family "Trk". NGF binds specifically to TrkA, BDNF and NT4/5 to TrkB, while NT3 can interact with both TrkC and – with lower affinity- TrkB (Reichardt, 2006). A supplementary common co-receptor for all neurotrophins is p75NTR, which works as a helper of TrkA, by presenting the ligand to this receptor via the formation of a transient heteromer (Reichardt, 2006).

Neurotrophins are usually considered for their involvement in neuronal survival, and their role in plasticity was first revealed with pioneering experiments by Lamberto Maffei and colleagues. They showed that infusion of NGF prevents in the rat the OD shift that would have been induced by monocular deprivation (Maffei et al., 1992). Further work demonstrated that TrkB ligands, BDNF and NT4/5, determine the correct segregation of thalamocortical connections, since a dramatic increase in their availability by means of osmotic micropumps infusion desgregates ocular dominance columns (Cabelli et al., 1995). Moreover, during

development, *Bdnf* mRNA in layer IV of the visual cortex appears at eye opening and peaks at the end of the critical period (Lein et al., 2000). The definitive proof of the involvement of neurotrophins in visual system development comes from *Bdnf* overexpression. This manipulation has interesting effects on cortical maturation, causing an accelerated development of visual acuity and a precocious closure of the critical period for OD plasticity (Huang et al., 1999). Conversely, blocking NGF action through continuous administration of monoclonal antibodies produced by implanted hybridoma cells, dramatically alters visual system development at the functional and anatomical levels (Berardi et al., 1994).

Bdnf transcription is activity-dependent, as can be observed by the progressive increase of its mRNA during postnatal development which parallels development of vision (Castren et al., 1992). Indeed, MD causes in rats a decrease in BDNF synthesis, both at the mRNA and protein levels (Bozzi et al., 1995; Rossi et al., 1999). Moreover, DR and blockade of retinal activity with TTX injection causes a decrease in *Bdnf* mRNA (Castren et al., 1992).

Exogenous manipulation of cortical levels of neurotrophins has interesting consequences on plasticity. Intraventricular infusion of NGF and NT4 prevents in rats the OD shift in response to MD during the whole critical period (Maffei et al., 1992; Lodovichi et al., 2000). The effect of BDNF infusion is more peculiar, because it counteracts the OD shift only if used a higher concentration compared to NGF and NT4 (Lodovichi et al., 2000). Moreover, it is the only neurotrophin that can also modify spontaneous cell activity and induce a paradoxical shift of OD towards the deprived eye in close proximity to the infusion site (Lodovichi et al., 2000).

BDNF and NGF infusion are also able to prevent the delay in visual system development caused by DR (Fagiolini et al., 1997). It must be pointed out that the action of neurotrophins necessitates a certain amount of electrical activity to be present, because completely blocking

afferent activity with intraocular injections of TTX abolishes the OD shift-preventing effect of NGF infusion (Caleo et al., 1999).

The role of activity in regulating neurotrophin release has been studied more in detail for BDNF, which is secreted in response to Ca^{2+} influx after activation of NMDARs and voltage-gated calcium channels (Lu et al., 2008). The role of NMDAR in BDNF release suggests a role in LTP induction and maintenance. Indeed, in hippocampal slices, BDNF secretion increases or decreases after LTP and LTD induction, respectively (Aicardi et al., 2004). Besides, *Bdnf*$^{-/-}$ and *Bdnf*$^{+/-}$ transgenic mice do not show hippocampal CA1 L-LTP in response to theta-burst stimulation (Korte et al., 1995), a deficit that can be rescued by bath application of BDNF (Patterson et al., 1996).

According to this evidence, neurotrophins would act as a stabilizing and strengthening factor for geniculocortical connections. They are released in a limiting amount and are taken up by thalamocortical afferents in an activity-dependent manner. Thus, when an afference decreases its activity, as during MD, it cannot efficiently compete for neurotrophin uptake and depotentiates. Conversely, exogenous supply of neurotrophins prevents the effect of MD because it can support also low-activity, deprived inputs (Caleo and Maffei, 2002). In addition, specific neurotrophins, such as BDNF, can affect cortical plasticity via an effect on intracortical inhibition (Huang et al., 1999).

1.3.2 Cortical inhibition

Inhibitory circuits fulfil the important task of regulating in time and space the information flow carried to the cortex by excitation (Huang et al., 2007). Hence, it is not suprising that interfering with GABAergic activity yelds profound effects on cortical physiology. Knocking-out the *Gad65* gene reduces neuronal GABA synthesis; this class of transgenic mice lack the

typical OD shift induced by MD during the critical period (Hensch et al., 1998). This deficit can be restored by local infusion of the $GABA_A$ agonist diazepam (Hensch et al., 1998), an effect that persists even in adult animals, well outside the canonical critical period (Fagiolini and Hensch, 2000). Moreover, diazepam administration to *Gad65*$^{-/-}$ animals between P23 and P33 is able to restore a normal OD development, including the lack of OD shift in response to MD in adulthood (Fagiolini and Hensch, 2000). Finally, MD in wild-type mice is ineffective if performed before P20-21 (*i.e.* "opening" of the critical period), but enhancing cortical inhibition with diazepam induces susceptibility to MD at P16 (Fagiolini and Hensch, 2000). In addition, varying cortical inhibition is sufficient to define the visual cortex morphology, as in kitten V1 direct infusion of $GABA_A$ receptor agonists (diazepam) or inverse agonists (methyl-6,7-dimethoxy-4-ethyl-β-carboline, DMCM), makes OD columns wider or more shallow, respectively (Hensch and Stryker, 2004). Taken together, these data indicate that the level of cortical inhibition regulates the onset of the critical period and the maturation of the visual cortex.

Work on visual cortex slices has described that maturation of inhibition results in a layer-specific restriction of ADSP. Indeed, stimulation of the white matter can elicit LTP in layer III only within the critical period (Kirkwood and Bear, 1994a; Kirkwood et al., 1995), whereas stimulation of layer IV gives rise to LTP in layer III even in adult animals (Kirkwood and Bear, 1994a). However, lowering cortical inhibition with bicuculline methiodide (BMI) restores white matter to layer III LTP (Kirkwood and Bear, 1994a). These results led to the "plasticity gate hypothesis", according to which development of inhibition in layer IV at the end of the critical period establishes a band-pass filter that allows only certain activity patterns to reach the highly plastic layer III synapses (Kirkwood and Bear, 1994a).

The specific role of inhibition in visual cortex plasticity has been explored with patch clamp recordings at layer IV connections between principal cells and fast-spiking (FS) interneurons. Between P18 and P21, a brief period of MD induces a potentiation of both the excitatory input on FS cells and the inhibitory input of FS neurons on principal cells in the monocular portion of the primary visual cortex, which results in a net increase of the inhibitory feedback (Maffei et al., 2006). Performing MD before opening of the critical period, between P15 and P17, yelds an exactly opposite picture: layer IV pyramidal neurons increase their spontaneous activity as a result of increased excitatory drive, whereas the opposite happens to the inhibitory input, thus causing an increase in layer IV excitability (Maffei et al., 2004). The same situation has been very recently described in the binocular portion of primary visual cortex as well (Maffei et al., 2010), which is the precise site of ocular dominance plasticity.

Gene knock-out of $GABA_A$ receptor ($GABA_AR$) subunits has helped in understanding the specific circuits involved in plasticity regulation. In particular, a point mutation in the $\alpha 1$ subunit determines a loss of sensitivity to diazepam, which in turn abolishes the capability of this drug to trigger a premature critical period (Fagiolini et al., 2004). Interestingly, $GABA_AR$ $\alpha 1$ subunits are preferentially expressed at perisomatic synapses receiving input from parvalbumin (PV)-expressing large basket interneurons (Klausberger et al., 2002), which have been shown in the cat to span with their axonal arbor an entire cortical column (Buzas et al., 2001) and preferentially display a fast-spiking discharge pattern (Markram et al., 2004). Labeling of specific interneuron subpopulations with genetically-encoded GFP has demonstrated that PV cell-originated perisomatic inhibitory synapses increase in number during the critical period, and that this maturation depends on visual activity, being impaired by contralateral intraocular TTX injection (Chattopadhyaya et al., 2004).

Calcium imaging experiments have revealed that, during the initial phase of MD, inhibitory interneurons show a retarded shift of their response towards the spared eye, compared to principal cells (Gandhi et al., 2008). Fast-spiking interneurons could be the main cause of this peculiar situation. Indeed, a brief period (2 days) of MD during the critical period induces in fast-spiking neurons a peculiar shift of their response *in favour* of the closed eye, a phenomenon that disappears after long-term (two weeks) MD (Yazaki-Sugiyama et al., 2009). By an increase in fast-spiking neuron-mediated feedforward inhibition, thalamic input from the deprived eye could suppress itself, to cause the loss of responsiveness to deprived-eye input during the initial phase of MD (Yazaki-Sugiyama et al., 2009). A peculiar behaviour of PV cells has also been observed in adult rats (age > P120) after long-term MD initiated in the critical period, when the previously deprived eye was reopened and its fellow concomitantly closed (Mainardi et al., 2009). Indeed, immunostaining for the product of the activity-dependent immediate-early gene *cFos* demonstrated a higher level of activation in long-term MD rats, compared to the global inhibitory population and to the other main cortical interneuron subclasses –expressing calbindin and calretinin, respectively- (Mainardi et al., 2009). According to the model proposed by Yazaki-Sugiyama and colleagues (Yazaki-Sugiyama et al., 2009), this situation could result from activation of a feedforward inhibitory circuit aimed at maintaining the preferential response of the visual cortex towards the formerly undeprived eye, which had shaped cortical response during the critical period. Thus, the previous interpretation that PV cells would not respond to long-term MD and maintain their response to the contralateral eye even during deprivation (Mainardi et al., 2009) can be corrected and reconciled with electrophysiological data obtained by Yazaki-Sugiyama *et al.* (Yazaki-Sugiyama et al., 2009).

This is in agreement with results from another model system, the sound source localization pathway in the optic tectum of the barn owl. Indeed, the creation of a new visuo-acustic map

after displacing the visual receptive field with optic prisms does not erase the old map, but inactivates the underlying circuitry by $GABA_A$ receptor-mediated inhibition (Zheng and Knudsen, 1999). It is woth noting that PV interneurons represent a link between inhibition and neurotrophins; indeed, *Bdnf*-overexpressing mice have an accelerated development of this cellular type, which parallels the precocious visual system development (Huang et al., 1999). This implies that BDNF could regulate the critical period primarily through the maturation of parvalbumin fast-spiking neurons.

Conclusive evidence about the negative regulation of neural plasticity by inhibition comes from a recent study that used minipump infusion of 3-mercaptoproprionic acid (MPA) or PTX (at doses that did not interfere with normal physiology) in the visual cortex of adult rats (Harauzov et al., 2010). Both treatments are able to restore the capability of MD to induce a persistent OD shift towards the deprived eye (Harauzov et al., 2010). Besides, *in vitro* electrophysiology on slices from treated animals demonstrated the presence of white matter to layer II/III LTP, but not LTD (Harauzov et al., 2010), which is known to be normally limited to the critical period (Kirkwood and Bear, 1994a). This (i) confirms that OD plasticity in adult animals primarily involves response potentiation to the spared eye through an LTP-like mechanism (Sawtell et al., 2003) and (ii) suggests that lowering intracortical inhibition can reopen the "plasticity gate" situated in layer IV (Kirkwood and Bear, 1994a).

1.3.3 Dendritic spines, the structural substrate of plasticity

Examination of a cerebral cortex section stained with the Golgi method reveals that dendritic arbors are not smooth, but have many tiny processes, called "dendritic spines", that receive the majority of excitatory inputs (Gray, 1959). Their size is within the order 0.1μm and their morphology is variegate, ranging from thin protrusions ("filopodia"), to short spines

("stubby spines"), to spines with identifiable neck and head ("mushroom spines") (Holtmaat and Svoboda, 2009). Spine shape is related to the stability of their contact with the corresponding presynaptic density; in particular, time-lapse imaging experiments in slices from GFP-expressing mice have elucidated that filopodia have a high motility and mediate transient synaptic contacts, whereas canonical spines are less motile and their contacts more persistent (Konur and Yuste, 2004).

Initially, dendritic spines have thought to be a way to increase the plasmatic membrane surface available for synaptic contacts. This superficial view has been widened and it now appears that each spine represents an individual subcellular biochemical and electrical compartment, which is consistent with the induction of synapse-specific long-term plasticity (Tsay and Yuste, 2004). The spine neck has a high electrical resistance compared to the dendritic shaft. This creates an "impedance mismatch" which attenuates EPSPs reaching the dendrite body (whereas depolarization entering the neck from the dendrite would not be attenuated), creating a filter to allow only a subset of synaptic inputs to reach the dendritic shaft (Tsay and Yuste, 2004). Besides these passive cable properties, spines can actively amplify the EPSP, because their head has a high density of voltage-dependent Ca^{2+} channels, in addition to NMDARs and AMPARs (Tsay and Yuste, 2004).

The decay of Calcium concentration in the spine following synapse activation has an initial fast phase, that is mediated by active extrusion and buffered diffusion towards the dendrite, and a later slow phase, that relies on simple diffusion (Majewska et al., 2000b). Spine morphology influences Ca^{2+} kinetics, because a small neck reflects in a diminished passage to the dendrite and in a protracted increase in Ca^{2+} concentration (Noguchi et al., 2005) and modification of spine neck length consistently affects Ca^{2+} diffusion (Majewska et al., 2000a). This could favor (i) activation of Ca^{2+}-mediated signaling pathways and (ii) summation between

sequential EPSCs, compared to larger spines, thus facilitating plasticity at thinner spines, which are thought to be more "immature" (Holtmaat and Svoboda, 2009).

As expected, long-term plasticity generates changes in spine structure. LTP induction through glutamate uncaging leads to an enlargement of spine head and to an increase in AMPAR-mediated currents; interestingly, this effect is present only in small, thin-necked spines (Matsuzaki et al., 2004). Conversely, low-frequency electrical stimulation induces in slices from rat hippocampus LTD and spine head shrinkage (Zhou et al., 2004). On the other hand, long-term imaging studies in rodent somatosensory cortex have revealed that larger spines last in time (Trachtenberg et al., 2002), leading to the hypothesis that small spines are involved in learning and large spines in memory (Matsuzaki, 2007).

Given the invovement of LTP and LTD in experience-induced plasticity, it is not surprising that manipulations in sensory experience reflect on dendritic spine dynamics. Whisker deprivation causes in the rat somatosensory cortex a reduction of motility and an increase in thin, transient spines in the barrel serving trimmed vibrissae, without affecting their density (Lendvai et al., 2000; Trachtenberg et al., 2002). In the visual cortex, DR causes a decrease in spine density that cannot be reversed by light exposure, coupled to a reversible increase in spine diameter, with a net preservation of the total synaptic area (Wallace and Bear, 2004). This has been interpreted to be a structural correlate of homeostatic plasticity (Wallace and Bear, 2004). Two to three days of MD induce an increase in spine motility in supragranular and extragranular layers -with layer IV remaining unaffected, without altering spine dimensions (Oray et al., 2004). In layer II-III, 4 days of MD produce a decrease in spine density (Mataga et al., 2004). Interestingly, this process is limited to the binocular portion of the visual cortex, which reinforces its involvement in competitive rearrangements of connectivity following MD (Mataga et al., 2004; Oray et al., 2004).

Dendritic spine appearance in the visual cortex closely parallels the opening of the critical period; indeed, before eye opening layer II-III dendrites are smooth and spines begin to appear and increase in number after eye opening, with their density peaking during the critical period (first apical segment) or at about P60 (superior branching orders) (Mataga et al., 2004). Analogously, the effects of MD on spine density and motility are restricted to the critical period, whereas in adulthood it only induces a (slight) decrease in spine dynamics, which also suggests an opposite effect of MD outside the critical period, aimed at stabilizing synapses (Mataga et al., 2004; Oray et al., 2004). Similarly to the visual cortex, in the barrel cortex spine motility in response to whisker deprivation is higher between P8 and P12, and a decline is apparent starting from P16, together with a decrease in filopodia abundance (which, however, retain their high motility) (Lendvai et al., 2000). Indeed, between P16 and P25 the dynamic equilibrium of spine dynamics is shifted to favor retraction, resulting in a net pruning that is accompanied by an increase in persistent spines (Holtmaat et al., 2005). It is worth noting that the crucial factor controlling spine rearrangement could be the the balance between excitation and inhibition. MD on *Gad65*$^{-/-}$ mice (which fail to enter the critical period because of a lower level of GABA synthesis, see above) between P25 and P29 causes an increase in spine density, which is exactly opposite to what observed in wild-type animals (Mataga et al., 2004). This situation is normalized by triggering a normal critical period with diazepam treatment (Mataga et al., 2004).

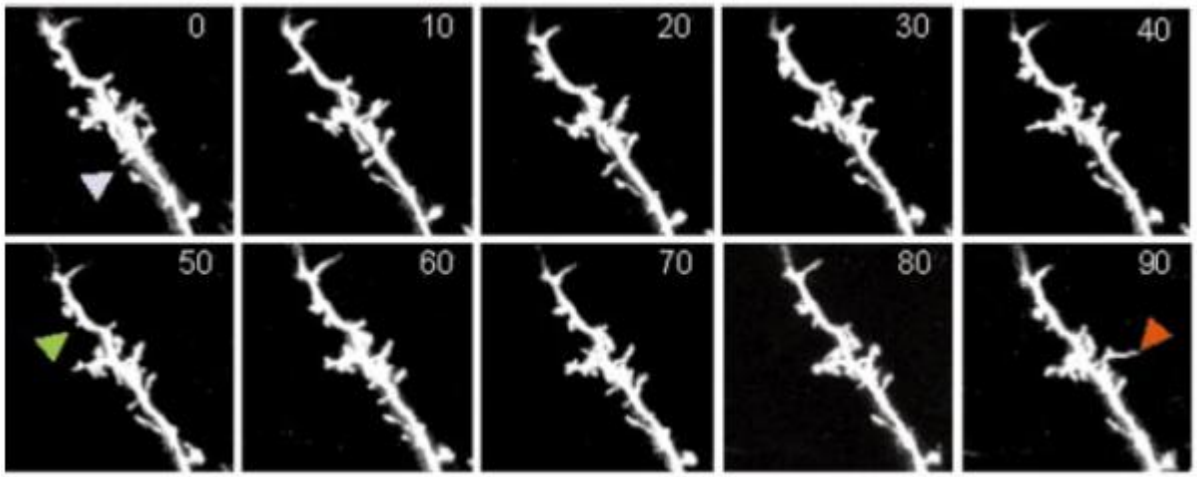

Figure 1.7 Dendritic spine dynamics in barrel cortex. Time-lapse imaging (time in minutes is reported in each frame) reveals motility and shape variation of dendritic spines (from Lendvai et al., 2000).

The effect of MD in adulthood has been recently addressed using chronic *in vivo* imaging of EGFP-expressing transgenic mice, revealing that spine turnover is more pronounced than indicated by previous works (Mataga et al., 2004; Holtmaat et al., 2005). Four days of MD increased spine gain in layer V of the binocular region in the primary visual cortex, suggesting a structural substrate for potentiation of spared-eye responses during adult MD (Sawtell et al., 2003); however, no significant effect was found in layer II-III (Hofer et al., 2009). Interestingly, restoring normal visual experience caused returning to baseline of spine gain, but spines acquired during MD were maintained, leaving a lasting trace in the binocular visual cortex (Hofer et al., 2009). Anyway, repeating MD –which is known to induce a more rapid OD shift (Hofer et al., 2006)- did not have any effect in spine turnover, which has been interpreted as a reactivation of spines acquired during the first MD period, after their silencing during normal vision (Hofer et al., 2009).

Taken together, these data indicate that dendritic spines represent a correlate at a single-synapse scale of all the experience-dependent processes that have been observed with

electrophysiology, providing a structural substrate for functional changes triggered by experience.

1.3.4 Extracellular matrix, a cage for synapses

As the vast majority of animal tissues, also the central nervous system possess an extracellular matrix (ECM), whose supporting function is particularly important to give at least a minimal mechanical resistance to this delicate tissue. However, ECM has something more to do than acting like a simple scaffold for neurons and glia. Studies on axonal lesion, have described the secretion of ECM molecules by astrocytes to form a "glial scar" that inhibits regeneration of neuronal processes (Fawcett and Asher, 1999). Anyway, ECM is also important in normal nervous physiology. This was already apparent from the first observations by Camillo Golgi, who noted a reticular structure covering the neuronal soma and dendrites up to the third branching order, which was later named "perineuronal net" (PNN) (Celio et al., 1998). Interestingly, PNNs begin to form during postnatal development, suggesting that they could contribute to maturation of the CNS (Celio and Blumcke, 1994). Moreover, PNN abundance is activity-dependent, as it has been demonstrated by immunohistochemical studies using antibodies recognising isoforms of chondroitin-sulphate proteoglycans (CSPG) (Guimaraes et al., 1990). In particular, rearing kittens in the dark from birth reduces PNN density in the visual cortex, reinforcing the idea that their appearance correlates with visual experience-induced regulation of plasticity during and after the critical period (Guimaraes et al., 1990). Consistently, manipulating visual experience in adulthood does not affect the expression of these PNN-specific antigens (Hockfield et al., 1990).

Disruption of interaction between neurons and ECM affects ADSP. For instance, treating hippocampal slices with disintegrins, a class of snake toxins, inhibits the binding of the

membrane proteins integrin β1 and β3 to ECM, thus impairing LTP consolidation (Chun et al., 2001). Conversely, application of reelin –an ECM component that interacts with integrins- to slices increases LTP magnitude, without affecting basal synaptic transmission (Weeber et al., 2002).

Interestingly, ECM components could also modulate the excitation-inhibition balance, as knock-out mice deficient for the gene encoding the secreted protein Tenascin-R (TN-R) have a reduced LTP, an increase in basal excitation in tha CA1 area of the hippocampus and smaller perisomatic mIPSCs (Saghatelyan et al., 2001). These functional effects could be due to an impairment in perisomatic inhibition, as TN-R is present in PNNs, and the increase in basal excitability would then occlude the possibility for further activity-dependent potentiation (Bruckner et al., 2000).

Given the effect of artificial manipulation of ECM components on plasticity, it is not surprising that the brain itself can act on their structure, namely through proteolytic mechanisms. For instance, neuropsin is a serine-protease that neurons secrete as a proenzyme and that is converted into the active form to cleave fibronectin (Shimizu et al., 1998). Perfusion of hippocampal slices with recombinant neuropsin increases the early phase of LTP at the Schaffer collateral pathway, an action that is inhibited by concomitant application on a neutralizing antibody or by prior *in vivo* infusion of antisense oligos (Komai et al., 2000). Similar results have been observed for plasmin, a protease that degrades laminin, whose application to hippocampal slices enhances E-LTP in response to weak high-frequency stimulation (Mizutani et al., 1996). Another important family of nervous system proteases is the matrix metalloprotease one (MMPs), which are present in several isoforms (Ethell and Ethell, 2007). Gene knock-out for *MMP-9* results in impaired hippocampal LTP, a deficit that can be reversed by bath perfusion of MMP-9 (Nagy et al., 2006). This effect is mediated by integrins, as their

blockade impairs the LTP-facilitating action of MMP-9 (Nagy et al., 2006). It is worth mentioning that among the substrates of MMPs are NGF and BDNF, which are secreted as inactive profactors (Lee et al., 2001b).

As expected, ECM dynamics are also involved in experience-dependent plasticity. For instance, proteolysis mediated by tissue-type plasminogen activator (tPA) is upregulated during MD within the critical period (Mataga et al., 2002). Conversely, transgenic mice deficient for the gene encoding tPA do not exhibit any OD shift following MD; this deficit can be restored by direct infusion of tPA (Mataga et al., 2002). However, tPA activity requires a normally-developing visual system, because its activity upregulation is not observed if MD is performed in *Gad65*$^{-/-}$ mice (Mataga et al., 2002).

The ultimate target of ECM degradation by proteases appear to be dendritic spines. Indeed, loss of dendritic spines of layer II-III neurons in response to MD during the critical period is impaired in *tPA* knock-out mice (Mataga et al., 2004), that is an interesting correlation with the loss of OD shift displayed by this transgenic line (Mataga et al., 2002). Normal spine dynamics are restored by infusion of tPA in the visual cortex, starting 3 days before and continuing during the MD period (Mataga et al., 2004). It must be pointed out that tPA acts primarily on extragranular layers, as the naturally high motility of these spines during MD occludes an additional effect of exogenous application of plasmin (whose proactive form, plasminogen, is activated by tPA) (Oray et al., 2004). On the opposite side, layer IV dendrites, which normally show reduced motility during MD, display the higher increase after exogenous tPA application (Oray et al., 2004). It has been hypothesized that spine mobilization by proteolysis could represent the main event explaining the initial, fast phase of OD plasticity, that can not rely on thalamocortical axon rearrangement (Hensch, 2005).

ECM degradation can also influence adult cortical plasticity. This topic has been explored using the bacterial protease Chondroitinase ABC (ChABC), synthesized by *Proteus vulgaris*, that acts on chondroitin-sulphate proteoglycans (CSPGs) by separating the glucydic component from the core protein (Ulrich et al., 1979). Interestingly, CSPG are the main component of PNNs and their degradation by ChABC is transient, presumably because of the physiological turnover of ECM components, so that the normal cortical immunoreactivity profile is restored within a few months from treatment (Bruckner et al., 1998). Treating adult rats with ChABC injections in the visual cortex degrades PNNs and yelds dramatic effects on plasticity (Pizzorusso et al., 2002). Indeed, PNN digestion permits to restore susceptibility to MD in adulthood (Pizzorusso et al., 2002). Besides, this experimental approach can also favor recovery from long-term MD started in the critical period, when coupled to RS, to the extent that the OD distribution of treated animals does not differ from controls with normal visual experience (Pizzorusso et al., 2006). Besides, long-term MD persistently decreases dendritic spine density in the binocular area of the visual cortex contralateral to the deprived eye (Pizzorusso et al., 2006). ChABC treatment restores spine density of formerly long-term MD animals to the normal value (Pizzorusso et al., 2006).

The rationale from these studies is that ECM development parallels the decline in plasticity due to closure of the critical period. Thus, increasing its degradation by endogenous or exogenous proteases quickly enhances cortical plasticity, mainly by freeing synapses (*i.e.* dendritic spines) from their molecular cage.

1.4 A COMPREHENSIVE RECAPITULATION OF FACTORS CONTROLLING PLASTICITY: ENVIRONMENTAL ENRICHMENT

1.4.1 Environmental enrichment action on neural physiology and pathology

Canonical experimental paradigms for studying plasticity, such as MD, DR or whisker trimming, are based upon sensory deprivation and favoring the spared sensory input (the open eye, intact whiskers). However, it is equally important to know whether the brain can also react in some way to an *enhancement* of sensory inputs. This problem began to be explored a few years after Hubel and Wiesel's studies on MD, by the group of Rosenzweig (Rosenzweig et al., 1962). They turned into an experimental protocol previous anecdotical evidence by Hebb, who was used to carry home rats and reported them to be somehow "smarter", compared to their littermates reared in the laboratory (Hebb, 1947). This led to the definition of a new rearing condition, characterized by "a combination of complex inanimate and social stimulation" (Rosenzweig et al., 1978), which is currently referred to as "environmental enrichment" (EE) (Sale et al., 2009). EE is achieved by rearing animals in large cages containing several objects (which are frequently changed), multiple decks, tunnels, ladders and running wheels; moreover, animals are reared in large groups (Sale et al., 2009). This results in a complex sensory stimulation and the opportunity for spatial and cognitive exploration, coupled to voluntary physical activity and social interaction, all factors that are obviously absent in standard condition rearing (SC) (Sale et al., 2009). Tests have been done to determine the selective contribution of each single factor to the general effect of EE; the results show that each component can partially account for the general effect, but their combination is fairly more effective, showing synergism (van Praag et al., 2000).

The first effects of EE were shown at the anatomical level, as an increase in cortical thickness, brain weight, perikarional and nuclear size of neurons (Rosenzweig et al., 1964; Diamond et al., 1967; Beaulieu and Colonnier, 1987). EE also increases dendritic arbor complexity and synaptogenesis (Globus et al., 1973; Greenough and Volkmar, 1973; Greenough et al., 1973). Similar results have been found in the cat visual cortex, where EE increases dendritic spine density (Beaulieu and Colonnier, 1987). At the molecular level, this corresponds to an increase in the neurotransmitter vesicle-associated protein synaptophysin and in the postsynaptic protein PSD-95 (Frick and Fernandez, 2003; Nithianantharajah et al., 2004).

Physical exercise appears to be a very important component of EE; indeed, voluntary exercise alone is able to increase adult hippocampal cell proliferation and recruitment to the dentate gyrus (van Praag et al., 1999). The existence of a similar effect in response to cognitive stimulation alone is more controversial (Gould et al., 1999; van Praag et al., 1999); it has been proposed that these variations can arise from differences in the timing at which neurogenesis was assessed (Greenough et al., 1999). Further studies have demonstrated that motor activity and cognitive stimulation can affect neurogenesis in different ways, with the former acting on progenitor proliferation and the latter on survival of newborn neurons (Olson et al., 2006).

At the functional level, EE induces the expression of genes related to synaptic plasticity and transmission (Rampon et al., 2000b). Another very important target are neurotrophins, as NGF gene expression and protein level synthesis are increased in the hippocampus of EE rats (Pham et al., 2002). Consistently, BDNF, NGF and NT-3 protein levels are increased in the cerebral cortex of rats enriched for one year, starting at the age of two months (Ickes et al., 2000).

The main outcome of EE is an improvement of cognitive capabilities, as demonstrated by behavioural tests for spatial learning, such as the Morris water maze (Rampon et al., 2000a). Interestingly, EE rats performed better than rats subjected to physical exercise in isolation,

which supports the importance of the contribution of the other components of EE, such as social interaction and cognitive stimulation (Bernstein, 1973).

Besides its action on brain physiology, EE has been shown also to have a beneficial influence on various neuropathological conditions, both in animal models and in humans (Nithianantharajah and Hannan, 2006). In different mouse transgenic models of Huntington disease, EE delays cerebral tissue degeneration (van Dellen et al., 2000; Hockly et al., 2002; Schilling et al., 2004), and improvement of neurological function has also been observed in human patients (Sullivan et al., 2001). However, when EE was applied to the *APP*/*PS1* mouse models of Alzheimer disease, contrasting results were obtained, reflecting differences in the enrichment protocol and in the sex of the experimental animals (Jankowsky et al., 2003; Lazarov et al., 2005). On the other hand, when AD11 transgenic mice –which synthesize endogenous anti-NGF antibodies and reproduce the histopathological and behavioural signs of Alzheimer disease- were subjected to EE, they showed an improvement in visuospatial memory and a reduction in neural tissue alterations (Berardi et al., 2007). In addition to the improvement of neurodegenerative conditions, EE can also exert a therapeutical effect on pharmacological models of epilepsy and stroke (Nithianantharajah and Hannan, 2006). A possible mechanism mediating recovery from pathological conditions could involve plastic changes of spared neural inputs and tissues, since it has been shown that, after partial retinal lesion, EE promotes sprouting of undamaged retinal inputs reaching the superior colliculus and the recovery of synaptic contacts (Caleo et al., 2009).

The usual criticism about EE is that it could just be a condition that approximates animal life in a natural setting; thus, it is not EE that is better, but SC that is worse, being an impoverishment respect to ideal rearing conditions (van Praag et al., 2000). However, re-creating a natural setting for laboratory animals is not the primary aim of EE. Indeed, EE

provides potential interesting stimuli and challenges, both at the social, physical and cognitive levels, that the animal can *volountarily choose* to undergo or not (Sale et al., 2009). The importance of voluntary action is underlined by the fact that passive observation of an enriched environment does not produce any effect comparable to active EE (Ferchmin and Bennett, 1975).

Another important issue about EE is whether its effects can persist after the animal has been transferred to standard rearing, which is particularly crucial when this protocol is used to ameliorate pathological deficits. Some studies have demonstrated that a period of EE does not exert a permanent action on the brain, but that anatomical and biochemical changes are reversed (Bennett et al., 1974; Green and Greenough, 1986). However, it appears that the longer EE rearing period has been, the more time its effects will last after transferring to standard rearing (Bennett et al., 1974).

1.4.2 Environmental enrichment and visual system plasticity during development and adulthood

The action of EE on brain is not limited to a general increase in cognitive performance: indeed, it has a much deeper impact on neural development, in particular on the visual system. Rearing rats in EE since birth results in a precocious development of visual acuity, detectable with both electrophysiological and behavioural methodologies (Cancedda et al., 2004). Also activity-dependent plasticity shows a faster maturation, since induction of white matter to layer II/III LTP disappears earlier than controls (Bartoletti et al., 2004).

At the molecular level, acceleration of visual system development reflects on an increased synthesis of BDNF, a faster establishment of the mature inhibitory tone (*i.e.* expression of both isoforms of the GABA-synthesizing enzyme, GAD65 and GAD67) and of CSPG perineuronal

nets (Cancedda et al., 2004; Ciucci et al., 2007). This is striking, because it means that a non-specific manipulation of the rearing environment that is simply aimed at providing the animals with increases socio-cognitive stimuli and physical exercise, can profoundly affect the development of a single sensory modality. Moreover, rodents do not preferentially use vision to explore the external world, but rather tactile and olfactory informations: nevertheless, visual function turns out to be highly stimulated by EE. This effect is so strong that vision can even become dispensable for proper development of visual system, since combining EE with dark rearing results in a normal time-course of the critical period, indicating that lack of visual experience is counterbalanced by enrichment (Bartoletti et al., 2004). It is interesting to note that the similarity of this situation with the accelerated visual development of *Bdnf*-overexpressing mice (Huang et al., 1999), that are not sensitive to DR in early postnatal life as well (Gianfranceschi et al., 2003).

It could seem paradoxical that newborn pups can benefit from EE, given that they spend most of the time in their nest. Specific work has clarified that EE pups receive a sort of "indirect" enrichment from their mother and from other females of the same cage, in the form of increased parental care (Sale et al., 2004). After this initial phase, when they begin the exit the nest, they begin to actively benefit from the EE condition.

An additional growth factor playing a crucial role in EE is insulin-like growth factor 1 (IGF-1), the main mediator of the effects of growth hormone (Bidlingmaier and Strasburger). IGF-1 expression is higher in the primary visual cortex of enriched rats, compared to age-matched standard-reared animals and direct infusion of IGF-1 in the visual cortex entirely mimics EE, resulting in precocious visual acuity and inhibitory system development (Ciucci et al., 2007).

Recently, the benefits of using perinatal enrichment to improve central nervous system maturation have also been extended to humans (Guzzetta et al., 2009). Indeed, artificially

increasing maternal care via a massage stimulation protocol, significantly accelerated maturation of visual function of preterm infants, an effect that correlated with higher serum levels of IGF-1; moreover, an analogous protocol in rats yelded comparable results (Guzzetta et al., 2009).

The visual system is not affected by EE only at the cortical level: indeed, this manipulation also acts on retinal development. Maternal enrichment is able to accelerate retinal development of the fetus and, again, this action is mediated by IGF-1, whose concentration is higher in the milk of enriched dams and their offspring (Sale et al., 2007a). Moreover, neutralization of IGF-1 by means of antibody infusion abolishes EE effect on retinal development and, conversely, IGF-1 administration to standard-reared pregnant dams mimicks EE (Sale et al., 2007a). Further studies have elucidated that prenatal and perinatal EE cause an accelerated maturation of retinal visual acuity assessed with pattern electroretinogram, which is correlated to a precocious increase in retinal BDNF immunoreactivity (Landi et al., 2007b). Finally, these effect can be reproduced in standard-reared pups using intravitreal injections of IGF-1 from P1 to P7 and can be blocked in EE pups with intravitreal injections of JB-1, an IGF-1 antagonist (Landi et al., 2009).

Thus, EE appears to involve all the crucial factors acting on cortical plasticity during the critical period, since it relies on neurotrophins, inhibition and extracellular matrix, with the additional participation of IGF-1 (Cancedda et al., 2004; Ciucci et al., 2007).

Another fascinating question concerning EE is whether it can also affect the adult central nervous system, which is traditionally thought to be scarcely sensitive to modifications in sensory experience. This point has been addressed by using the experimental paradigm of MD. Rats underwent MD during the critical period, then subjected to EE coupled with RS. The combination of enhanced sensorimotor experience with favoring visual experience through the

formerly deprived eye was able to induce complete recovery from MD-induced ambylopia, assessed with electrophysiology and behaviour (Sale et al., 2007b). Restoring of OD plasticity in the adult visual system appears to be mediated by an increase in BDNF content, reduction of GABA levels and disruption of PNNs (Sale et al., 2007b). Another striking effect was the re-appearance of white matter to layer II/III LTP (Sale et al., 2007b), which would indicate the reopening of the inhibitory plasticity gate in layer IV that closes together with the critical period (Kirkwood and Bear, 1994a). The essential role of inhibition is confirmed by the fact that artificially increasing inhibition by means of diazepam infusion, completely abolishes recovery from ambliopya after EE during adulthood (Sale et al., 2007b).

These findings indicate that EE has different effects during development and adulthood: (i) in the precocious phases of life, it accelerates maturation of neural circuits so that they reach faster adult performance, (ii) in adulthood, it enhances plasticity by inducing a juvenile-like state, primarily through a reduction of inhibition, that tips the excitation to inhibition balance towards the former. In both cases, the net result is a better capability of brain to undergo adaptive changes to experience.

An interesting clinical correlate of EE may be represented by the effectiveness of specific perceptual training to improve recovery from lately-treated ambylopia (Levi and Li, 2009b). Indeed, the use of challenging visual tasks to stimulate activity in the deprived eye induces an enhancement in visual performance that ultimately reflects on visual acuity, possibly through experience-dependent plasticity mechanisms (Levi and Li, 2009a).

1.5 CROSSMODAL PLASTICITY: INTERACTIONS BETWEEN PRIMARY SENSORY CORTICES IN PATHOLOGY AND PHYSIOLOGY

The vast majority of studies on neural plasticity are focused on a single sensory modality or cortical area. On the other hand, the possibility that induction of plasticity using a given sensory modality (*e.g.* vision) can instead affect a cortical area that receives its primary input from another sensory system (*e.g.* hearing) has been scarcely investigated. This so-called "crossmodal plasticity" has a relevant interest also for clinicians, because it seems to be involved in the functional peculiarities of blind and deaf patients. For example, the somatosensory input associated with Braille reading causes activation of the occipital (visual) cortex in early blind persons (Sadato et al., 1996). This activation has functional consequences, as inferfering with visual cortex functioning by means of transcranial magnetic stimulation (TMS), negatively affects tactile discrimination of Braille in blind. (Cohen et al., 1997), in addition to inducing an illusory tactile sensation in the fingers (Ptito et al., 2008). TMS of the occipital lobe does not impair tactile performance in sighted individuals but, as expected, interferes with visual function, generating phosphenes (Cohen et al., 1997). Analogously, in early deafs, the primary auditory cortex (A1) is activated by visual stimuli (Finney et al., 2001). Anyway, it should be pointed out the high interindividual variability of these functional reorganizations (Bavelier and Neville, 2002). Moreover, crossmodal plasticity does not affect basic sensory properties such as pure tone threshold (Niemeyer and Starlinger, 1981), but rather more complex functions like speech processing, sound localization and spatial tuning (Lessard et al., 1998; Roder et al., 1999; Roder et al., 2002).

In animals models, a correlate of human clinical studies is represented by the improvement in somatosensory function in rats after early binocular enucleation. Indeed, neurons in the barrel cortex of enucleated animals had larger receptive fields and a higher angular sensitivity

to whisker deflection and this correlated with a better behavioural performance, assessed with the rectangular maze test (Toldi et al., 1994). Concerning visuo-acustic interaction, auditory responses are observed in about a third of the neurons in the V1 of early deprived rats (Piche et al., 2007).

The extent of recruitment of deprived area by a different sensory modality differs across ages. This has been demonstrated with imaging studies in the human visual system, with the occipital cortex being strongly activated by somatosensory stimuli only in early blind (Cohen et al., 1999b). Interestingly, late blind people (who lack a strong activation of the occipital cortex during Braille reading) did not show a worsening of their Braille reading performance during TMS of the visual cortex, which is different from the situation of early blind (Cohen et al., 1999b). This suggests fundamentally different mechanisms for crossmodal plasticity during and after the critical period, a situation that could share a common basis with ocular dominance plasticity in the immature and adult animal (Sawtell et al., 2003; Frenkel and Bear, 2004). A similar result has been obtained in rodents, with a reduced effect of binocular deprivation on the improvement of somatosensory performance (Volgyi et al., 1993). These differences seem to find a structural correlate, in the remarkable degree of adaptability to a change in the quality of sensory input that is typical of the immature cortex. In neonatal ferrets, disruption of the auditory pathways by severing the neural input to the medial geniculate nucleus and and damaging the superior colliculus causes retinal inputs to redirect and colonize the auditory thalamus (Angelucci et al., 1997). This is turn, causes the appearance of visual features – including a retinotopic map- in A1 neurons (Sur et al., 1988), an adaptation that also appears to mediate visual behaviour, assessed with a grating discrimination test (von Melchner et al., 2000). Circuit rewiring appears to occur also in physiological conditions, namely in animals with a light-deprived lifestyle such as moles. Even if the occipital cortex is partly degenerated,

the spared portion has auditory and somatosensory responses which, in the first case, are due to a projection from the inferior colliculus to the undegenerated visual thalamus (Doron and Wollberg, 1994; Kudo et al., 1997). An analogous circuit ha also been described in congenitally anophtalmic mice (Chabot et al., 2008).

Cortical function redirection could arise from a transient state of multimodal connectivity during early development, since it has been shown in kittens that the primary and secondary auditory cortices project to the V1 until P38 (Innocenti and Clarke, 1984). Later these connections are lost, possibly through an axon pruning process driven by sensory experience (Innocenti and Clarke, 1984) and competition between the "elective" and secondary sensory modalities. Sensory deafferentation could instead preserve and even enhance these crossmodal projections, hence the survival of this pathway could be responsible for the superior functional outcome of early deafferented patients, compared to late deafferented.

In physiological conditions, auditory, frequency-tuned, responses in visual cortex neurons, with alignment of receptive fields between the two different sensory operating modalities have described in cats (Morrell, 1972; Fishman and Michael, 1973), which could indicate a partial retaining in the mature central nervous system of crossmodal connectivity mediated by subcortical structures. Moreover, a behavioural task in which a monkey had, sequentially, to activate a bar in response to the occurrence of a visual cue, hear a tone and release the same bar in response to another visual cue to gain a reward, indicates that neurons in primary auditory cortex show activity also during the non-acustical phases of the test (Brosch et al., 2005).

Studies in humans also have pointed to role of corticocortical connectivity in crossmodal plasticity, in addition to subcortical pathways. For instance, imaging by means of PET has demonstrated in early blind subjects the recruitment of the ventral occipital pathway –usually devoted to shape recognition- during a non-Braille tactile discrimination task (Sadato et al.,

1998). The existence of a direct connection between primary sensory areas has been demonstrated with anatomical tracing experiments in primates, showing a direct pathway between the A1 and the portion of the V1 serving the peripheral visual field (Falchier et al., 2002). On the other hand, connections between V1 and S1 have been described so far only in the rodent model represented by the prairie vole (Campi et al., 2009).

Finally, it is worth noting that extensive reorganization of the cortex serving a given sensory modality is not necessarily a positive event. Indeed, an fMRI study has shown that in prelingually deaf patients, subjects with the highest metabolic activity in primary auditory cortex –which is a sign of crossmodal recruitment by other sensory modalities- had the smallest hearing improvement after a cochlear implant (Lee et al., 2001a).

A relatively unexplored problem is the effect of cognitive stimulation on crossmodal plasticity. Only one report (Piche et al., 2004) has described an effect of environmental enrichment on anophtalmic mice. In this model, EE was responsible for an enhancement in the activation of the occipital cortex by auditory stimuli (Piche et al., 2004). Moreover, an unanswered question is whether non-invasive manipulations such as EE can affect functional interactions between primary sensory areas also in physiological conditions.

1.6 AIM OF THE PRESENT WORK

The purpose of this work is to evaluate the influence of environmental enrichment (EE) on central nervous system plasticity, using different approaches and techniques.

In the first part, I analyzed the effect of EE in adulthood on the plasticity of the visual thalamocortical pathway. This issue is important because previous studies have only examined the effects of EE during adulthood on cortical plasticity, and it is not known whether subcortical structures are also responsive to this rearing condition.

Rats were reared either in standard condition (non-EE) until postnatal day 120 (P120), or in EE starting from P105 and ending at P120. After the EE period, *in vivo* electrophysiological experiments were performed, stimulating the visual thalamus (dorsal nucleus of the lateral geniculate body, dLGN) and recording the evoked field potential in primary visual cortex . Using this experimental setup, I measured both short term plastic phenomena, namely paired-pulse depression of response, and long-term potentiation triggered by tetanic stimulation of the dLGN. I also did an assessment of the impact of EE on visual function, by recording visual evoked potentials (VEPs) in response to sinusoidal gratings across a range of contrasts, before and after LTP induction. Based on the known effect of EE on the excitation to inhibition ratio (Sale et al., 2009), I quantified the expression of the neurotransmitter transporters for glutamate (vGluT-1 and -2) and GABA (vGAT), which are, respectively, markers of the excitatory and inhibitory cortical tones.

In the second part of my experimental work, I investigated whether EE could also influence crossmodal plasticity in different cortical areas. In this case, I performed experiments on mice, reared in EE from birth. To search for cortical areas that are monosynaptically connected with the primary visual cortex –and thus more likely to show crossmodal plasticity- I did anatomical tracing experiments, by injecting minimal amounts of cholera toxin β subunit into the

monocular and binocular portions of the primary visual cortex. These studies provide the first description of long range cortico-cortical connections from mouse primary visual cortex. They are important because mouse is the elective model for visual plasticity studies.

Then, I simultaneously recorded local field potentials in freely moving animals, using chronically-implanted EEG electrodes, in V1 and in other cortical regions that anatomical experiments had shown to be connected with the former area. Computational analysis was then used as a quantitative measurement of activity correlation between the recorded areas, in EE and non-EE mice.

2. MATERIALS AND METHODS

2.1 Animals and Surgery

All procedures were performed according to the guidelines of the Italian Ministry of Health for care and maintenance of laboratory animals (law 116/92), and in strict compliance with the European Communities Council Directive n° 86/609/EEC. N=15 non-EE and N=15 EE rats were used for electrophysiological experiments. For western blots analysis I processed N=9 non-EE and N=9 EE brains. For immunohistochemistry I analyzed N=5 non-EE and N=4 EE brains. A total of 57 animals were used.

Adult Long Evans hooded rats were housed in an animal room with a 12h/12h light/dark cycle, and food and water available *ad libitum*. Animals were reared either in a Standard Environment (non-EE; 3 adult rats in 30X40X20 cm laboratory cages) or Enriched Environment (EE) for 15 days starting at P90. The EE condition (60X50X80cm cages) consists of a large and three-deck cage containing several foodhoppers, one running wheel for voluntary physical exercise, and differently shaped objects (tunnels, shelters, stairs) that were repositioned twice a week and completely substituted with others once a week.

For experiments using mice, C57Bl6/J mice were housed in an animal room with a 12h/12h light/dark cycle, with food and water available *ad libitum*. Pregnant dams, together with two to three helper females, were put either in non-EE or EE condition about one week before delivery and pups were hatched at P25. The standard rearing condition consisted of a 26 X 18 X 18cm cage housing 3 animals. The EE condition was achieved using a large cage (44 X 62 X 28cm) containing several foodhoppers, one running wheel for voluntary physical exercise, and differently shaped objects (tunnels, shelters, stairs) that were repositioned twice a week and completely substituted with others once a week. A total of 30 mice were used.

2.2 Acute electrophysiology

Rats were anaesthetized with an intraperitoneal injection of 20% urethane (ethyl carbamate, Sigma, USA) in saline solution (0.7ml/hg). Experiments were performed blind to the rearing condition of the animals.

Body temperature was held constant at 37.0°C with a thermostatic pad, while heartbeat and breathing were monitored throughout the experiment. To ensure preparation stability, the cortical electroencephalogram was continuously monitored. After anaesthesia stabilization, a craniotomy was performed with a dental drill through the parietal bone at 3.6mm mediolateral and 2.6mm anterior to lambda to create a burr hole to reach the lateral geniculate nucleus (dLGN), allowing the penetration of a stimulating electrode. A second craniotomy was made in correspondence of the primary visual cortex in the hemisphere ipsilateral to the stimulated dLGN. Care was taken to expose the visual cortex by removing a bone window (3mm X 1.5mm) centered at 3.6mm lateral and in correspondence with lambda. The dura mater was carefully removed with #5 tweezers (Fine Science Tools, Germany) and the exposed cortex was covered with saline solution to prevent drying. To stimulate the thalamus, a custom-made bipolar stimulating electrode (made of a teflon-coated, nichrome steel wire) was used. To accurately position the tip of the stimulating electrode in the dLGN, visually-driven multiunit activity was monitored as this electrode was slowly tracked down through neocortex and overlying hippocampus. The final depth of the stimulating electrode tip was typically within 100–200μm of the point at which visually responsive neurons were first encountered. The recording electrode consisted of a glass pipette filled with 3M NaCl and having an impedance of 2MΩ. In most experiments, except for laminar profile analysis (see below), the recording electrode was positioned at a depth of 400μm in the cortex. This position allows sampling of the major and earliest current sink associated with thalamocortical input activity and is consistent with

previous studies in rat visual cortex by other groups (Heynen and Bear, 2001; Kuo and Dringenberg, 2008).

At the end of the experiment, to label the position of the recording electrode, the tip of the recording pipette was gently brushed with a saturated solution of the lypophilic dye DiI (Invitrogen, USA), then reinserted into the cortex at the same coordinates and depth. Coronal sections from the visual cortex were cut, counterstained with the nuclear dye YoYo-1 (Invitrogen, USA) and examined with epifluorescence microscopy. To confirm the correct location of the stimulating electrode, coronal sections comprising the dLGN were cut and processed for Nissl staining. Representative images of Nissl-stained dLGN sections were acquired using a 1.25X objective mounted on a Zeiss Axioskop (Zeiss, Germany) microscope with a 1.6X optical zoom and digitized using a Zeiss Axiovision CCD camera. Analysis of histological sections (Fig. 1A) confirmed that the stimulating electrode tip was typically positioned in the dorsal part of the dLGN and near its anterior pole, where optic radiation fibers are bundled in close proximity (Hughes, 1977; Molnar et al., 1998). Stimulation of the dLGN was provided via a stimulus insulator (WPI, USA), with 100μsec pulses whose timing was controlled through a custom-made software based on the LabView platform. Cortically-evoked field potentials were filtered at 0.3-1,000Hz, amplified with a 10,000X gain and digitized at 10,000Hz with a National Instruments card.

At the beginning of each experiment a plot of the response amplitude to different stimulus intensities was calculated; the stimulation intensity which achieved a response amounting to the 60% of the maximal response recorded was then chosen as a test stimulus for the subsequent trials. In most experiments, the test stimulus intensity was 200-300μA, while a full range of intensities (from 50 to 900μA) were used to determine the input-output relationship, as described in previous studies (Heynen and Bear, 2001).

For current source density (CSD) analysis, I recorded field potentials evoked by dLGN electrical stimulation at different depths in the cortex (from 0μm to 800μm, in steps of 100μm). For each recording depth, 3 stimuli were delivered and the resulting field potentials were averaged. Using these data, I computed the one-dimensional CSD profile using a spatial differentiation grid of 100μm, following the theoretical directions of Mitzdorf (Mitzdorf, 1985). The corresponding color map was generated by means of the MatLab toolbox CSDplotter, using a continuous Gaussian spatial filter (kindly provided to us by Dr. Klas Pettersen, Norwegian University of Life Sciences, Ås, Norway).

To evaluate both short-term and long-term plastic effects induced in the visual cortex after stimulation of the thalamus, I performed the following measurements:

1) analysis of paired-pulse depression: paired-pulse stimulation was delivered with two identical stimuli, spaced by 1000, 100 or 40msec;

2) analysis of long-term potentiation: baseline responses were collected every 30 sec at least 30 minutes after field potential stabilization and before application of theta-burst stimulation (TBS). TBS consisted of 10 trains of stimuli at 5Hz, each one composed of 5 stimuli at 100Hz, repeated 4 times with an interval of 10sec. After TBS induction, the response to test stimulus was recorded for at least 60 minutes.

For visual evoked potential (VEP) recording, the eye contralateral to the recording site was kept open by means of an adjustable metal ring. The recording electrode was positioned at a depth of 400μm within the cortex, and VEPs were recorded before and after application of TBS to the dLGN. We chose to use steady-state VEPs, in which the grating contrast reverses sinusoidally at a relatively high temporal frequency. VEPs were recorded in response to reversal (4Hz) of a horizontal sinusoidal grating (spatial frequency, 0.07 cycles/degree; contrast 0, 6, 10, 15, 20, 30, 90%), generated by computer on a display (Sony; 40 x 30 cm; mean luminance

15 cd/m2) by a VSG card (Cambridge Research System). Signals were amplified (1000-2000-fold), bandpass filtered (0.1–500 Hz), and fed to a computer for storage and analysis. At least 100 events were averaged in synchrony with the stimulus contrast reversal. VEP amplitude was quantified by measuring the amplitude of the second harmonic of the Fourier transform computed from the recorded signal, which yields most of the response energy (Porciatti et al., 1992; Caleo et al., 2003), using a custom-made application based on the LabView software. The response to a blank stimulus (0% contrast) was also frequently recorded to estimate noise. When computing the contrast threshold curve, the response amplitude was expressed as the ratio between the VEP amplitude at a given contrast and the VEP amplitude at 90% contrast before TBS delivery.

2.3 Western Blot

Rats where anaesthetized with an overdose of chloral hydrate, then decapitated. The brain was quickly removed from the skull and the primary visual cortex was dissected out, paying attention not to remove the underlying white matter. Tissue explants were quickly frozen in dry ice and stored at -80°C for further processing. Samples were homogenated and proteins were extracted with lysis buffer (1% Triton X-100, 10% glycerol, 20 mM TrisHCl, pH 7.5, 150mM NaCl, 10mM EDTA, 0.1 mM Na_3VO_4, 10 μg/ml leupeptin, 10 μg/ml aprotinin, and 1mM PMSF), and the total concentration of samples was assessed with a Bradford assay kit (Bio-Rad, USA) using a bovine serum albumin-based standard curve. Fifteen microgram of non-boiled proteins extracts were loaded on Tris-HCl 12% precast gels (Bio-Rad) and separated using SDS-PAGE (1hr at 200V), then blotted on nitrocellulose membrane (Bio-Rad). Blots were blocked using a solution of 4% milk and 0.2% Tween-20 in TBS, for 2h at RT. The primary antibody solution contained 2% milk, 0.1 Tween-20 and either 1:2,500 anti-vGluT1 rabbit polyclonal

antibody (Synaptic Systems, Germany) or 1:2,500 anti-vGluT2 rabbit polyclonal antibody (Synaptic Systems) or 1:1,000 anti-vGAT rabbit polyclonal antibody (Synaptic Systems), in TBS. Incubation lasted overnight at 4°C. Blots were then incubated with 1:20,000 HRP-conjugated goat anti–rabbit secondary antibody (Jackson Laboratories, USA), for 2h at RT. The signal was detected by enhanced chemiluminescence (ECL), using the luminol/enhancer system (Immun-Star western C, Bio-Rad) and autoradiography films (HyperFilm, GE Healthcare, USA). As an internal quantification standard, blots were also probed for α-tubulin. To do this, blots were blocked again for 30min at RT with 4% milk, 0.2% Tween-20 in TBS, added with 0.05% sodium azide to extinguish the peroxidase activity of the anti-rabbit secondary antibody. The primary antibody solution contained 2% milk, 0.1% Tween-20 and 1:8,000 anti-α-tubulin mouse monoclonal antibody (Sigma, Germany) in TBS; incubation lasted 45min at RT. Then, blots were reacted with 1:20,000 HRP-conjugated goat anti-mouse secondary antibody (Sigma-Aldrich, Germany) in 2% milk, 0.1% Tween-20 and TBS, for 45min at RT and developed with the same ECL method. In these experimental conditions, all the antibodies gave rise to a single band at the appropriate molecular weight on the immunoblots, and the staining was abolished by incubation with the respective control peptide (Synaptic Systems). In the figures, we show this single band rather than the entire nitrocellulose sheet for reasons of space.

2.4 Immunohistochemistry

After terminal anaesthesia with an overdose of chloral hydrate, the thoracic cavity was open to expose the heart. A needle was inserted in the left ventricle, while the right atrium was cut open. By means of a peristaltic pump, vessels were washed with PBS, then the animal was perfused in a 4% w/v solution of freshly prepared paraformaldehyde (PFA) in 0.1M phosphate buffer (PB), pH 7.4. The brain was then quickly removed from the skull, postfixed by

immersion in the same fixative solution for 3h, then overnight cryoprotected in 30% w/v sucrose in 0.1M PB. Finally, brains were frozen by immersion in isopenthane and stored at -80°C; 12h before cutting, samples were put at -20°C. Coronal sections comprising the primary visual cortex were cut at 50μm thickness using a cryostat (Leica Microsystems, Germany) and collected in PBS. Free-floating sections were blocked in 10% BSA, 0.3% Triton X-100 in PBS for 2h at room temperature, then incubated overnight at 4°C in 1% BSA, 0.1% Triton X-100 and 1:1000 rabbit anti-vGluT-2 primary antibody (Synaptic Systems, Germany) in PBS. The signal was detected by incubation in 1% BSA, 0.1% Triton X-100 and 1:400 anti-rabbit secondary antibody conjugated to Alexa Fluor-488 fluorophore (Molecular Probes, USA) for 2.5h at room temperature. Sections were mounted on glass slides using VectaShield mounting medium (Vector Laboratories, USA).

Images of vGluT-2 immunoreactivity in layer IV of primary visual cortex were acquired using an Olympus confocal laser-scanning microscope (Olympus, Japan), using a 60X oil immersion objective (numerical aperture 1.42) and a 2X digital zoom. A preliminary analysis of the fluorescence intensity of the samples was done and the acquisition parameters (photomultiplier gain and offset, laser intensity) were set to avoid signal saturation at either end of the pixel intensity range (0-255). An intensity scan along the z axis was done to select the brightest focal plane, which was acquired together with the underlying and overlying focal planes (1μm z-step), then the resulting images were stacked and saved as 8-bit TIFFs. At least 12 images from 4 sections were acquired for each experimental case.

Signal quantification was done using the MetaMorph software (Molecular Devices, USA) as previously described (Caleo et al., 2007; Caleo et al., 2009). For each image, four rectangles comprising neuronal somata and representing the background were drawn and their mean fluorescence intensity was calculated, then the values were averaged. vGluT-2 positive pixels

were discriminated from background by applying a threshold (mean background signal in the cell somas multiplied by two). The expression level of vGluT-2 was then calculated as the percentage of pixels in the field whose intensity was over threshold (Caleo et al., 2007; Caleo et al., 2009).

2.5 Anatomical tracing experiments in mice

To identify cortical areas monosynaptically connected with the primary visual cortex (V1), I took advantage of the retrograde tracing capability of Cholera Toxin β subunit (CTB, Sigma, USA). Mice were mounted on a custom-made stereotaxical apparatus, then a burr hole was done in the skull overlying V1. In separate experiments, injections were performed at two different sites, whose stereotaxical coordinates were identified from literature (Paxinos, 2008): (i) 0.0mm anteroposterior and 2.5mm mediolateral to the lambda point, corresponding to the monocular portion of V1; (ii) 0.0mm anteroposterior and 3.0mm mediolateral to the lambda point, corresponding to the border between V1 and secondary visual cortex, the binocular portion of V1. To maximize the spatial specificity of the injection, thus avoiding unwanted labeling of connections impinging on different areas from V1, only 50nl of CTB solution at a depth of 600μm were delivered. This was achieved by using a 1μl Hamilton syringe (Hamilton, USA) filled with mineral oil and plugged to a glass injection pipette. After allowing 3 days for transport of CTB to neuronal somata and processes, animals were transcardially perfused (see above, histology section) with 50ml of 4% PFA, then processed for histology to obtain 50μm-thick coronal sections. CTB labeling was visualized by means of immunohistochemistry. Free-floating sections were blocked in 5% normal rabbit serum (NRS), 2.5% bovine serum albumin (BSA), 0.3% Triton X-100 in PBS for 2 hours at RT. Incubation with primary antibody was performed with 1:4000 anti-CTB made in goat (Calbiochem, USA), 2% NRS, 2.5% BSA, 0.1% Triton X-100 in PBS, overnight at 4°C. The signal was revealed using 1:400 donkey anti-goat

secondary antibody conjugated to Alexa-568 (Molecular Probes, USA), 2% NRS, 2.5% BSA, 0.1% Triton in PBS. Incubation lasted 2.5h at RT, then cellular nuclei were counterstained with 1:5000 YoYo-1 (Invitrogen, USA) in PBS. Sections were mounted on glass slides and protected with VectaShiel mounting medium (Vector Labs, USA). For double immunohistochemistry, 1:1000 anti-vGluT-2 rabbit primary antibody (Synaptic Systems, Germany) and 1:400 donkey anti-rabbit secondary antibody conjugated to Alexa-488 (Molecular Probes, USA) were added to the primary and secondary antibody solutions, respectively. To allow for a finer detection of CTB-labeled neuronal processes, signal detection with diaminobenzidine (DAB) was also performed. After incubation with the primary antibody, sections were transferred in a solution containing 2% NRS, 2.5% BSA, 1% Triton X-100 and 1:500 anti-goat biotinilated secondary antibody in PBS, for 2h at RT. This was followed by incubation for 1h in ABC kit (Vector Labs) and final detection with DAB reaction kit (Vector Labs). Sections were finally mounted on glass slides, dehydrated and sealed with DPX mounting medium (VWR International, UK). Immunofluorescence images were acquired with a confocal microscope (Leica) and merged in a mosaic using Photoshop software (Adobe, USA). DAB images were acquired using a CCD camera (Zeiss, Germany) mounted on an Axioskop microscope (Zeiss).

2.6 Local field potential recording in freely moving mice

Local field potential (LFP) recordings were performed in awake, freely moving mice using an adaptation of the protocol described by Antonucci *et al.* (Antonucci et al., 2008). Low-impedance recording electrodes made of nichrome steel wire (120μm thick) were thin-soldered to a multipin socket to create an array comprising four electrodes; the fifth position of the socket received a an insulated copper ground cable. Under avertin anaesthesia (0.01ml /g) and after placement in a stereotaxic apparatus, the skull was exposed and four burr holes were

drilled in the skull at given positions (see below), paying attention not to damage the undeerlying dural surface. The multipin socket was held by an adjustable manipulator and the electrodes were put in place, establishing an electrical contact without lesioning the dura mater. LFPs were sampled by placing a couple of electrodes in the same cortical area, spaced by 1.0mm to achieve detection of local electrical activity confined between the two sites. A ground screw was positioned on the occipital bone and connected with the ground cable, while an additional screw was installed on the frontal bone to provide further strength to the implant. The whole device was secured in place by means of dentistry acrylic cement (Paladur, Pala, Germany). Stereotaxical coordinates were (i) between 2.0mm and 3.0mm lateral (L) and 0.0mm anteroposterior (AP) to lambda for V1; (ii) 0.8mm L and between -0.8mm and -1.8mm AP to bregma for secondary motor cortex (M2); (iii) 3.9mm L and between - 2.0mm and -3.0mm AP to bregma for primary auditory cortex (A1) (Fig. 10B, C) (Paxinos, 2008).

Animals were returned to their home cage and recordings were done after allowing 3 to 5 days for recovery from surgery; the animal was habituated for 1h to the test cage, then a 1h recording session was performed, using a digital acquisition system. The hardware component was composed of a custom-made buffer to eliminate movement artifact from the signal, an amplifier and an acquisition card (National Instruments, USA), plugged via USB to a personal computer. The custom-made acquisition software was based on the LabView platform (National Instruments). Cortical LFP signals were acquired with a sampling rate of 100Hz as the differential between two adjacent electrode sites, 10000X amplified and 0.3-30Hz band-passed.

2.7 LFP signal analysis

The interaction between local activities between the recorded areas was quantified using the linear cross correlation and mutual information indexes.

The former analysis was performed as described in (Antonucci et al., 2008). The linear cross correlation function between two signals $s_a(t)$ and $s_b(t)$ is defined as:

$$corr(s_a, s_b)(\tau) = \int_{-\infty}^{+\infty} s_a(t+\tau) s_b(t) dt$$

Where τ is the time lag shift of one signal respect to the other. Hence, the function has its maximum at a given value of τ.

To compensate for differences in the mean amplitude and variance of each signal, which can vary because of experimental variability in electrode placement, the cross correlation function was normalized according to the equation:

$$C(s_a, s_b)(\tau) = \left| \frac{corr(s_a, s_b)(\tau)}{\sqrt{corr(s_a, s_a)(0) \cdot corr(s_b, s_b)(0)}} \right|$$

Where $corr(s_a, s_a)(0)$ and $corr(s_b, s_b)(0)$ are the linear autocorrelation values at a time lag of 0, which limits the range of cross correlation function between 0 and 1.

The maximum value of the cross correlation function was calculated as:

$$C_{\max} = \max_{\tau} C(s_a, s_b)(\tau)$$

Therefore, $C_{\max}$ is comprised between 0 (no cross correlation) and 1 (total cross correlation).

In my experimental case, I calculated $C_{\max}$ for values of τ comprised within 0 and 150msec, which is in line with previous literature (Mormann et al., 2003).

To include also non linear signal dynamics in the analysis, also the mutual information index was calculated, following the directions described in Kraskov *et al.* (Kraskov et al., 2004).

The first sted is represented by determining the Shannon's entropy associated with each recording channel, which is defined as:

$$H(X) = -\sum_i p_i \ln p_i$$

Where p_i is the probability that the signal assume the i-th state, that is a given amplitude value comprised in its discrete range. This is considered to be a measure of the information amount to specify the value assumed by the signal once the probability of occurrence of all the possible values are known (Kraskov et al., 2004).

In this case, we have a couple of variables (signals) X and Y and their joint Shannon's entropy is calculated as:

$$H(X,Y) = -\sum_{i,j} p_{i,j} \ln p_{i,j}$$

where p_{ij} is the joint probability that X is in state *i* and Y in state *j*.

Finally, the Mutual Information (MI) between X and Y is calculated as:

$$\Phi(X,Y) = H(X) + H(Y) - H(X,Y)$$

This value is always positive; moreover $\Phi(X,Y) = \Phi(Y,X)$ and, in case X and Y are statistically independent, $\Phi(X,Y) = 0$ (Kraskov et al., 2004).

To calculate cross correlation and mutual information indexes, custom-made applications were computed using the FORTRAN language. Both functions binned EEG signals in half-overlapping time windows of 5000 points -which corresponds to 50sec of acquisition. Cross correlation and mutual information were calculated for each time window, then averaged to obtain the mean values for each experimental case.

3. RESULTS

3.1 EE EFFECT ON PLASTICITY OF THE THALAMOCORTICAL PATHWAY IN THE ADULT RAT

Long Evans hooded rats (age P90) were placed in EE for 15 days; another group of rats were left in standard rearing condition (non-EE) and examined at P105 (Fig. 3.1A). I recorded extracellular field potentials following electrical stimulation of the dLGN (Fig. 3.1B). I also compared VEP recordings before and after application of theta-burst stimulation (TBS) to the dLGN (Fig. 3.1B). A second group of age-matched EE and non-EE animals were used for quantification of vesicular neurotransmitter transporter proteins. A third group of animals were used for immunohistochemistry experiments.

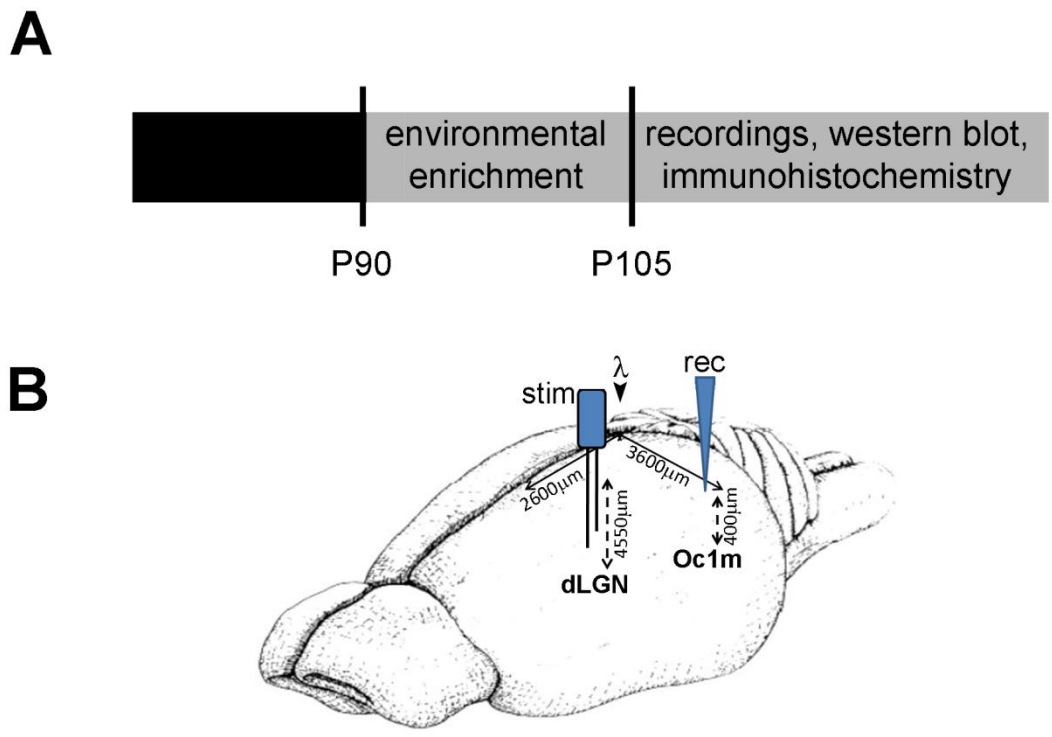

Figure 3.1 Experimental protocol for EE experiments on adult rats. A) Schematic diagram of EE protocol. B) Drawing showing the placement of stimulating (stim) and recording (rec) electrodes for *in vivo* LTP experiments.

3.1.1 Field potentials evoked in the visual cortex by stimulation of the dLGN

A bipolar stimulating electrode was placed into the dLGN and evoked field potentials were recorded in the ipsilateral primary visual cortex. In each animal, the correct location of the stimulating and recording electrodes was verified by histological analysis in coronal brain sections (Fig. 3.2A, B). In initial experiments, I recorded field potentials at different depths in the cortex to obtain a laminar profile of the field potential response. Fig. 3.2C reports a typical example of such profile, obtained by moving the recording electrode ventrally in steps of 100μm. Stimulation of the dLGN with a single test stimulus evoked in the cortex a primarily negative-going field potential (Heynen and Bear, 2001; Jiang et al., 2001; Jia et al., 2004; Kuo and Dringenberg, 2008), that displayed the shortest latency and maximal amplitude at a depth corresponding to layer IV - layer III (400-700μm; Fig. 3.2C). This profile is consistent with previous reports in the literature (Heynen and Bear, 2001). I performed a CSD analysis to examine the inward (sinks) and outward currents (sources) that generate the field potential responses (Fig. 3.2D). The CSD analysis demonstrated a major, short latency sink in layer IV-layer III, corresponding to excitatory postsynaptic currents elicited directly by the geniculocortical afferents (Mitzdorf, 1985; Heynen and Bear, 2001). Based on these data, I performed most of the experiments with the recording electrode positioned at a depth of 400μm, in proximity of this major sink. No differences in laminar and CSD profiles were observed between EE and non-EE rats.

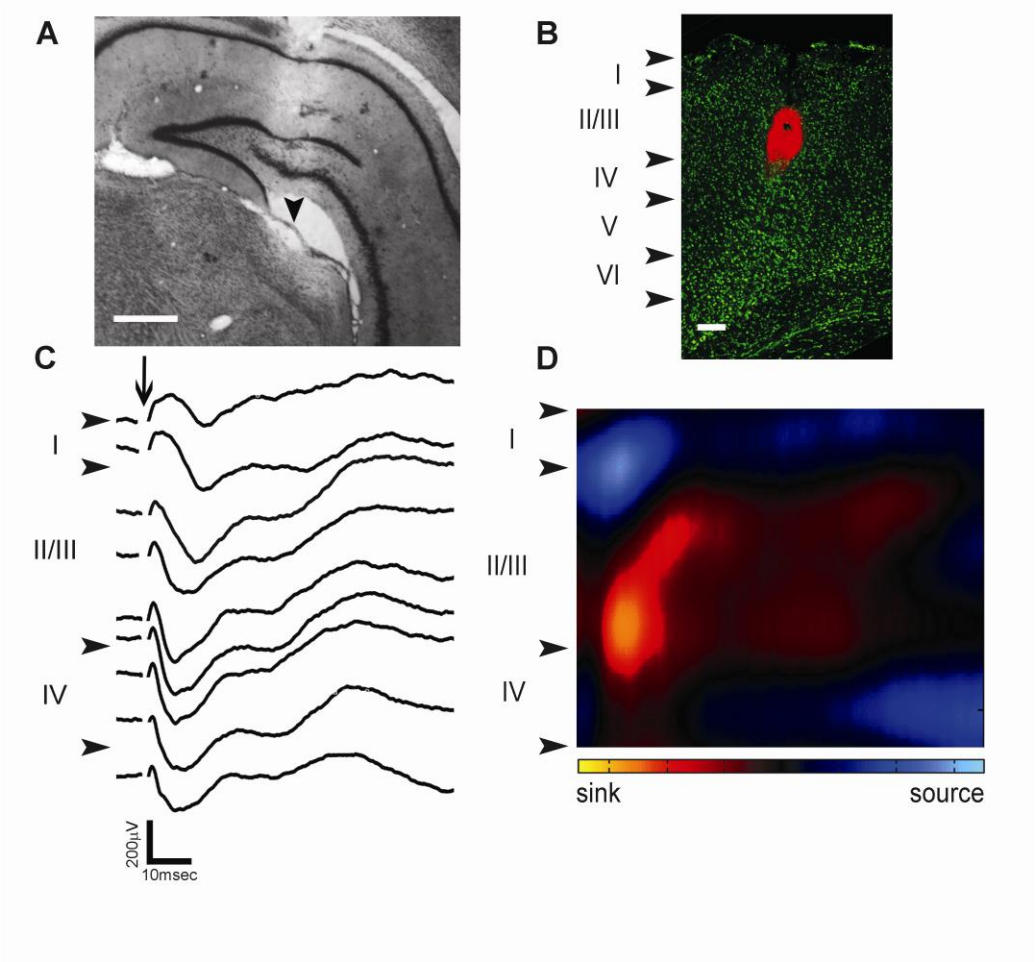

Figure 3.2 Cortical field potential responses evoked by dLGN stimulation. A) Nissl-stained section comprising the dLGN and overlying hippocampus, showing the correct placement of the stimulating electrode (scale bar = 0.5mm). The arrowhead indicates the site where the electrode touches the dLGN. B) Representative coronal section of the visual cortex demonstrating the placement of the recording electrode (DiI, red). Cortical layers were identified by cellular counterstaining with YoYo-1 (green). The lower boundary of the red staining identifies the position of the electrode tip, which appears to be in deep layer III. Scale bar = 100μm. C) Laminar profile of the field potential elicited in the primary visual cortex by electrical stimulation of the dLGN. Recordings were done in 100μm steps across the cortical depth, starting at 0μm and ending at 800μm. Cortical layers and boundaries (arrowheads) are indicated on the left. The vertical arrow indicates timing of dLGN stimulation. D) Current source density (CSD) analysis of the cortical field potential response to electrical stimulation of the dLGN. The figure depicts the interpolated CSD color map calculated using a continuous Gaussian filter from field potential recordings at different depths, using a spatial differentiation grid of 100μm. Hot colors (yellow and red) represent current sinks and cool colors (dark and light blue) represent current sources, while neutral areas are in black.

3.1.2 Enhanced efficacy of thalamocortical transmission in EE animals

I first compared the characteristics of basal geniculocortical transmission in non-EE and EE rats. I found that the mean negative peak latency of the field potential response was 8.8±1.2msec (non-EE) and 10.0±0.5msec (EE) and was not significantly different between the two experimental groups (Student's *t* test, P=0.317). Next, I examined the input-output curves and,

as expected, the amplitude of the response progressively increased with current strength in both groups. Remarkably, the curve of EE animals was shifted upwards and was significantly different from that in non-EE rats (Fig. 3.3A, two-way repeated measures ANOVA, P=0.039). This suggests that the responses of EE rats reach the saturation level at lower stimulation intensity. Indeed, while in 9 out of 11 enriched animals the input-output curve came to its asymptotic value at 600μA, this was true only for 3 out of 11 standard-reared animals (*z* test, P=0.032). Thus, EE increases the efficacy of thalamocortical transmission.

To further investigate whether the strength of thalamocortical input was altered after EE, I used a protocol of paired-pulse stimulation, that is widely used to measure changes in the probability of neurotransmitter release from presynaptic terminals (Thomson, 2000). Specifically, I stimulated the dLGN with two electrical pulses separated by various interstimulus intervals (ISIs), namely 1000, 100 and 40msec. In this range of ISIs, a decrease in the magnitude of the synaptic response to the second stimulus was invariably observed, indicating paired-pulse depression (PPD, Fig. 3.3B). I calculated the ratio between the amplitude of the second and first cortically-evoked field potential (PPD ratio) as a function of interstimulus pulse for control and EE rats. At 1Hz, we observed a moderate depression, and the PPD ratio was not significantly different between animals reared in control cages or EE (two-way repeated measures ANOVA followed by Tukey *post-hoc* test P=0.906, Fig. 3.3C). However, I observed an enhanced PPD in enriched rats compared to controls at shorter ISIs. PPD ratios of enriched rats were significantly lower than in controls at ISI=100msec (two-way repeated measures ANOVA followed by Tukey *post-hoc* test, P=0.035, Fig. 3.3C) and the effect became even more prominent at ISI=40msec (two-way repeated measures ANOVA followed by Tukey *post-hoc* test, P=0.002; Fig. 3.3C). Thus, response depression caused by paired stimulation

at short ISIs is enhanced in EE animals, pointing to an increased release probability (Amitai, 2001) at thalamocortical terminals following EE.

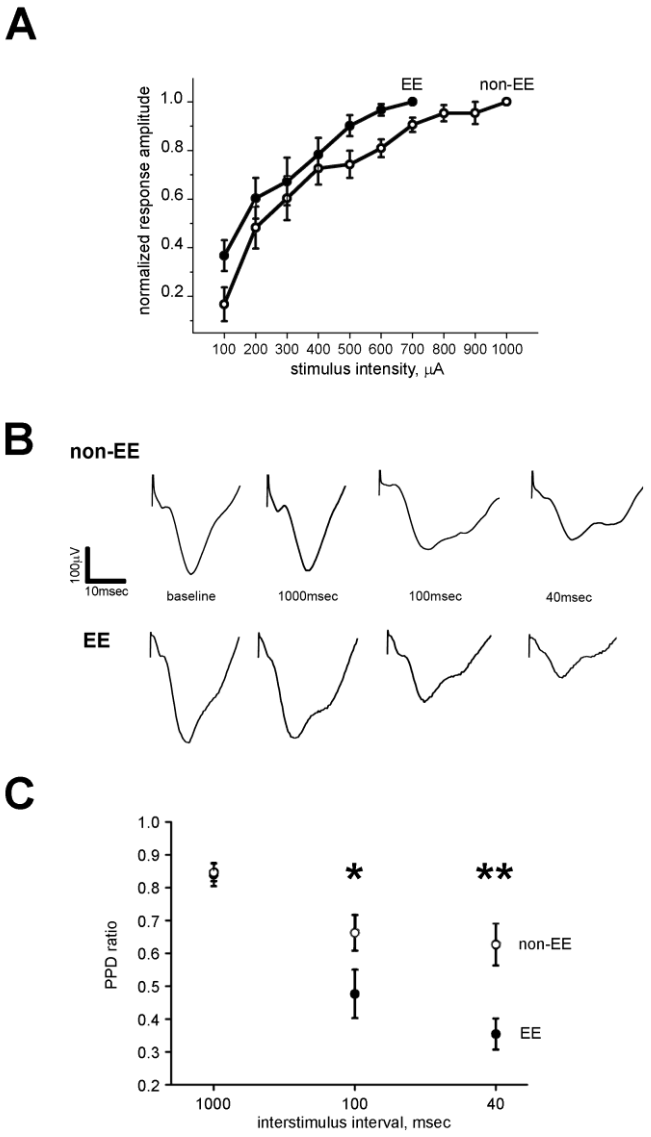

Figure 3.3 Enhanced thalamocortical transmission in EE animals. A) Plot showing the amplitude of cortical field potentials, normalized to the maximal response amplitude, as a function of stimulation intensity of the dLGN for standard-reared (non-EE, N=11, hollow circles) and EE animals (N=11, filled circles). The two curves are significantly different (two-way repeated measures ANOVA, P=0.039). **B)** Representative field potentials recorded in standard-reared (non-EE) and EE animals in response to paired-pulse stimulation at ISIs of 1000, 100 and 40 msec. For each ISI only the second response is shown. Scale bars represent 100μV and 10msec. **C)** Plots of PPD ratio as a function of ISI for standard-reared (non-EE, hollow circles, N=8) and enriched animals (EE, filled circles, N=8). No significant difference in PPD ratio can be observed with an ISI of 1sec (two-way repeated measures ANOVA followed by Tukey *post-hoc* test, P=0.906). However, a significant decrease in the PPD ratio is apparent for EE animals at shorter pulse intervals (two-way repeated measures ANOVA followed by Tukey *post-hoc* test, P=0.035 at ISI=100msec; P=0.002 at ISI=40msec).

3.1.3 Increased expression of the thalamocortical glutamate transporter vGluT2 in EE rats

I hypothesized that the functional changes in thalamocortical transmission might be associated with specific neurochemical changes affecting the neurotransmitter release machinery. To investigate this issue, I quantified by Western blot the expression of the vesicular glutamate transporter isoform-2 (vGluT-2), which is mainly expressed in thalamocortical afferents reaching layer IV of primary visual cortex (Nakamura et al., 2005).

As a preliminary control, I validated our vGluT-2 quantification method by loading increasing amounts of the same protein sample from the primary visual cortex (Fig. 3.4A). I found that the optical density (OD) of the vGlut-2 band increases in proportion to the amount of loaded sample, and the increase was almost linear in the range 5-20μg of total protein (Fig. 3.4B). Importantly, the ratio between the ODs of vGluT-2 and α-tubulin (internal control) bands remained constant (Fig. 3.4C). Thus, these experimental conditions and quantification method are reliable means to measure the expression of vGluT-2 in visual cortex.

A representative immunoblotting for vGluT-2 in non-EE and EE samples is shown in Fig. 3.4D, where each lane represents the visual cortex of one animal. The quantitative analysis demonstrated a remarkable upregulation of vGluT-2 in enriched rats (Student's *t* test, P=0.015; Fig. 4E).

vGluT-2 is mainly expressed at layer IV thalamocortical synapses, but some synapses in layer I and VI are also immunoreactive for this neurotransmitter transporter (Nahmani and Erisir, 2005). Thus, I performed immunohistochemistry experiments to support the conclusion of an enhanced vGluT-2 expression in thalamocortical layer IV afferents. I acquired with a confocal microscope images from layer IV of the primary visual cortex of non-EE and EE rats (Fig. 3.5A). Measurement of the area occupied by immunoreactive puncta indicated that EE rats had an increased density of vGluT-2 terminals in the neuropil (Student's *t* test, P<0.001; Fig.

3.5B). This finding is consistent with the specific enhancement of geniculocortical transmission induced by EE that was observed electrophysiologically.

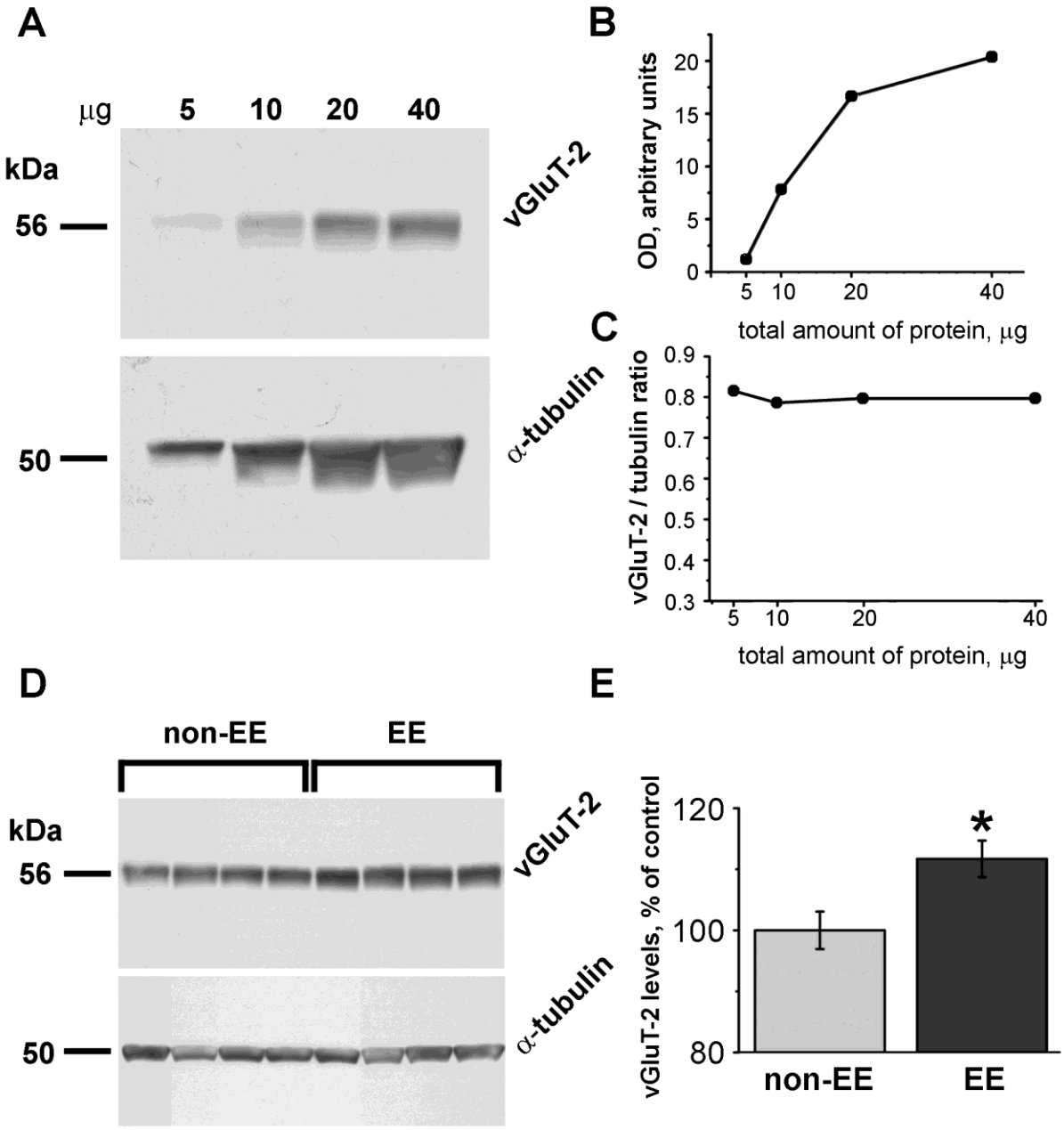

Figure 3.4 Increased expression of vGluT-2 in the primary visual cortex of EE rats. A) Representative immunoblottings for vGluT-2 and α-tubulin after loading increasing amounts of the same protein extract; B) Plot showing the relationship between the optical density (OD) of the vGluT-2 band and the total amount of protein loaded; note the linear relationship between OD and amount of loaded protein in the range 5-20 μg of total protein, with y-intercept at about 0; C) Plot displaying the ratio between the ODs of the vGluT-2 and α-tubulin bands as a function of total protein loaded; D) Western blot analysis of the glutamate transporter vGluT-2 in the visual cortex of rats reared in standard conditions (non-EE) or enriched environment (EE). Each lane represents the visual cortex of one animal. E) Quantification of vGluT-2 expression. Data are expressed as mean ± SEM of vGluT-2 optical density divided by α-tubulin (α-tubul) optical density of the corresponding sample. EE results in a higher expression of vGluT-2 (Student's *t* test, P=0.015; non-EE, N=9; EE, N=9).

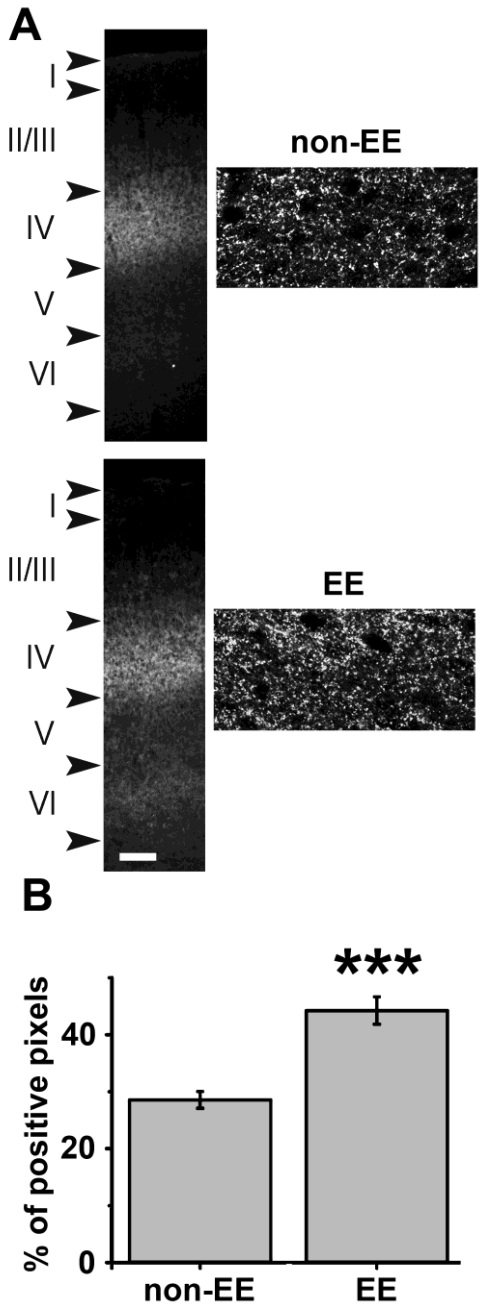

Figure 3.5 EE enhances vGluT-2 expression in thalamic afferents in layer IV of the primary visual cortex. A) Representative vGluT-2 immunoreactivity in primary visual cortex. Left, low-magnification images (10X) of the entire primary visual cortex in non-EE (top) and EE (bottom) rats, demonstrating a major band of vGluT-2-positive terminals in layer IV. Scale bar is 100μm. Right, high-magnification images acquired in layer IV from non-EE (top) and EE (bottom) rats (60X magnification, 2X digital zoom, scale bar = 20μm). B) Quantification of vGluT-2 expression. Data are expressed as mean ± SEM of the percentage of pixels with intensity above threshold. EE causes a higher expression of vGluT-2 in thalamic terminals reaching layer IV of the primary visual cortex (Student's *t* test, P<0.001; non-EE, N=5; EE, N=4).

3.1.4 Increased long-term potentiation in EE rats

To compare long-term potentiation (LTP) of the thalamocortical pathway in enriched and control rats, I applied theta-burst stimulation (TBS) to the dLGN after at least 30min of stable baseline field potential recording. In non-EE adult rats, TBS induced a significant potentiation of the response to the test stimulus compared to pre-TBS baseline (one-way ANOVA, $P<0.001$). This enhancement reached an average value of 9.6±1.1% between 43.5 and 84min after TBS delivery (Fig. 3.6). Compared to non-EE rats, animals reared in EE exhibited a 2.5-fold higher potentiation of cortical field potentials, which reached 23.5±0.8% relative to pre-TBS baseline 43.5-84 min following TBS (one-way ANOVA, $P<0.001$; Fig. 3.6). Statistical analysis indicated that the LTP curve of the EE group was significantly different from that of the standard group (two-way repeated measures ANOVA followed by Tukey *post-hoc* test, $P=0.017$; Fig. 3.6). Thus, 15 days of exposure to EE are capable of enhancing cortical plasticity in adult rats.

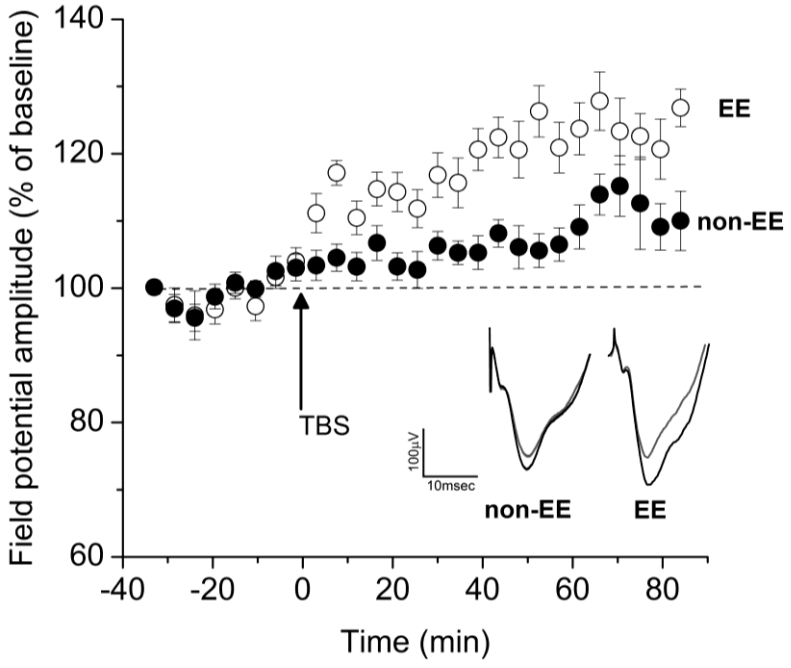

Figure 3.6 EE enhances thalamocortical LTP. LTP of thalamocortical transmission in the visual cortex of rats reared in standard conditions (non-EE, N=8, filled circles) or in an enriched environment (EE, N=8, hollow circles). Application of theta-burst stimulation (TBS, indicated by an arrow) after 30min of baseline recording induced a significant potentiation of field potential amplitude. LTP was significantly more pronounced in the EE group (two-way repeated measures ANOVA followed by Tukey *post-hoc* test, $P=0.017$). Traces illustrate representative recordings obtained in the two experimental groups before (grey trace) and after TBS (62 min, black trace). Scale bars represent 100µV and 10msec.

3.1.5 LTP induction enhances responses to visual stimulation

It was of interest to determine whether LTP induction can modify cortical responses to visual stimuli in non-EE and EE animals. Since cortical gain control can be reliably quantified by measuring responses to stimuli of different contrasts (Porciatti et al., 2000), I recorded steady-state VEPs evoked by grating of variable contrasts before and after application of TBS to the geniculate. In non-EE rats, high-frequency electrical stimulation of the dLGN was able to induce a potentiation of the VEP amplitude only in response to optimal contrast gratings (90% contrast; two-way ANOVA followed by Tukey *post-hoc* test, $P=0.004$; Fig. 3.7A, C). Interestingly, the same stimulation protocol in EE animals elicited a potentiation of the VEP amplitude across a wide range of contrasts (10-90%; two-way repeated measures ANOVA followed by Tukey *post-hoc* test; $P<0.05$ for all comparisons; Fig. 3.7B, D).

These data lead to conclude that the higher LTP shown by adult EE rats is paralleled by an enhancement of natural responses to grating stimuli across a range of contrasts.

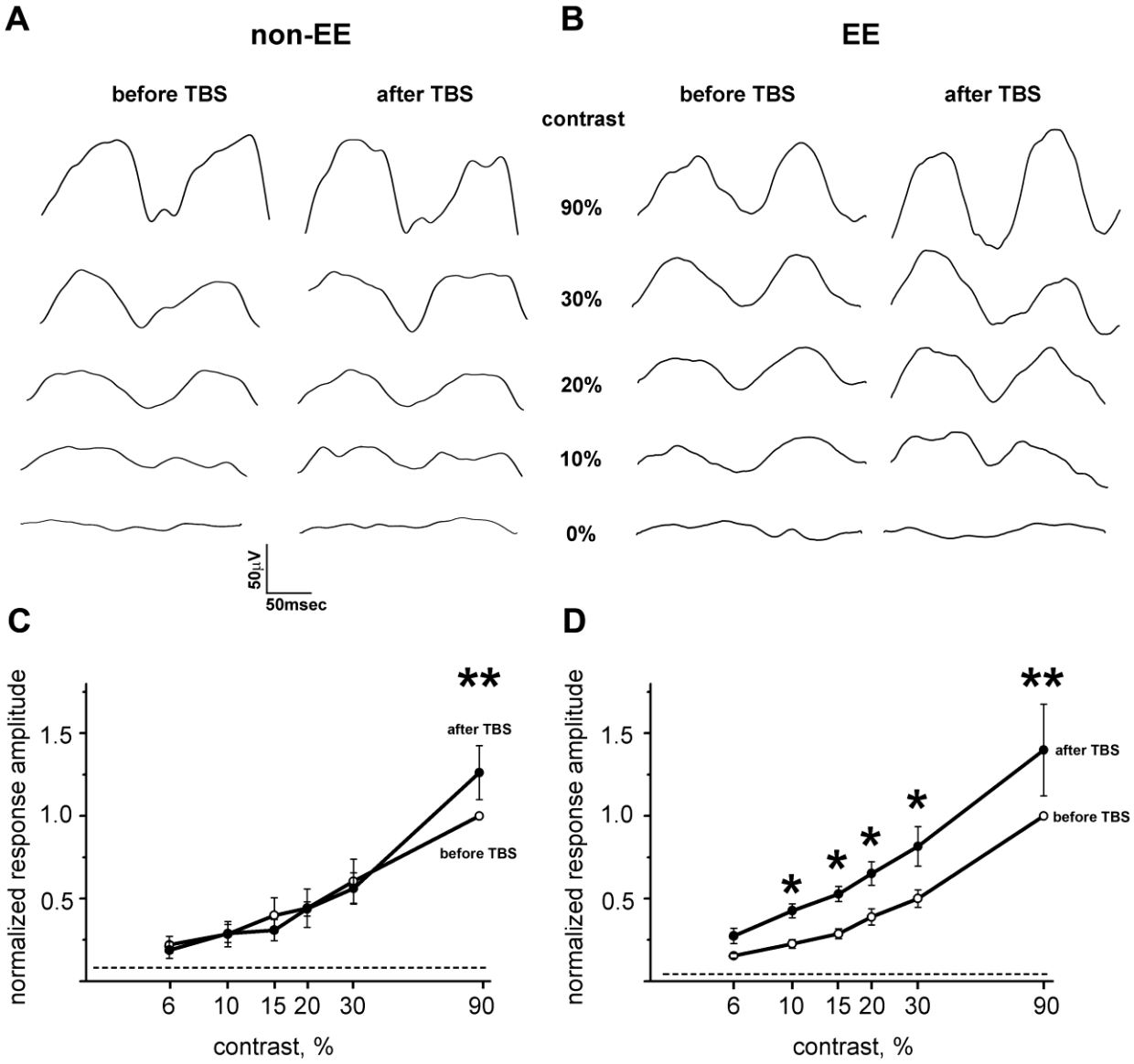

Figure 3.7 Increased response to grating stimuli in EE animals after TBS stimulation of the dLGN. A) and B) Representative steady-state VEP responses at different contrast intensities, before and after TBS stimulation of the dLGN in non-EE (A) and EE (B) rats. Visual stimulus: horizontal sinusoidal grating alternating at 4Hz, spatial frequency 0.07 c/deg, variable contrast. C) and D) Contrast threshold curves of non-EE (N=4) and EE (N=3) animals, before and after TBS stimulation of the dLGN. The VEP amplitude for each contrast value was normalized to the amplitude of the response at contrast = 90% before TBS. Dashed lines correspond to the noise level, measured as the VEP response to a blank stimulus (0% contrast). Data are presented as mean ± SEM. High-frequency stimulation of the visual thalamus in standard-reared animals (panel C) caused a significant potentiation of the VEP response only to 90% contrast gratings (two-way repeated measures ANOVA followed by Tukey *post-hoc* test, P=0.004). In enriched rats (panel D), the same stimulation protocol triggered a potentiation of the VEP response also to mid- and low-contrast gratings (two-way repeated measures ANOVA followed by Tukey *post-hoc* test, P<0.05 for all comparisons).

3.1.6 Changes in the cortical excitation/inhibition balance associated with EE

Then, I investigated whether the enhanced LTP of EE rats had a correlate in neurochemical changes in excitatory versus inhibitory transmission. I quantified by Western blot the expression of the intracortical vesicular transporter proteins for glutamate and GABA (vGluT-1 and vGAT, respectively). I first demonstrated for both proteins the reliability of the quantification method (Fig. 3.8), as described above for vGluT-2. I then compared expression levels in non-EE vs. EE rats. In enriched animals, a significant upregulation of vGluT-1 was detected (Student's *t* test, P=0.039; Fig. 3.9A, B); it is worth noting that this vesicular glutamate transporter is highly expressed in intracortical excitatory terminals (Nakamura et al., 2005). Examination of the expression of the vesicular GABA transporter (vGAT) revealed an opposite situation. EE-treated rats showed a clear downregulation of vGAT to about half of the levels found in standard-reared animals (Student's *t* test, P=0.040; Fig. 3.9C, D). Thus, EE acts in opposite directions on excitatory and inhibitory neurotransmission, resulting in a net shift of the excitation/inhibition balance towards the former.

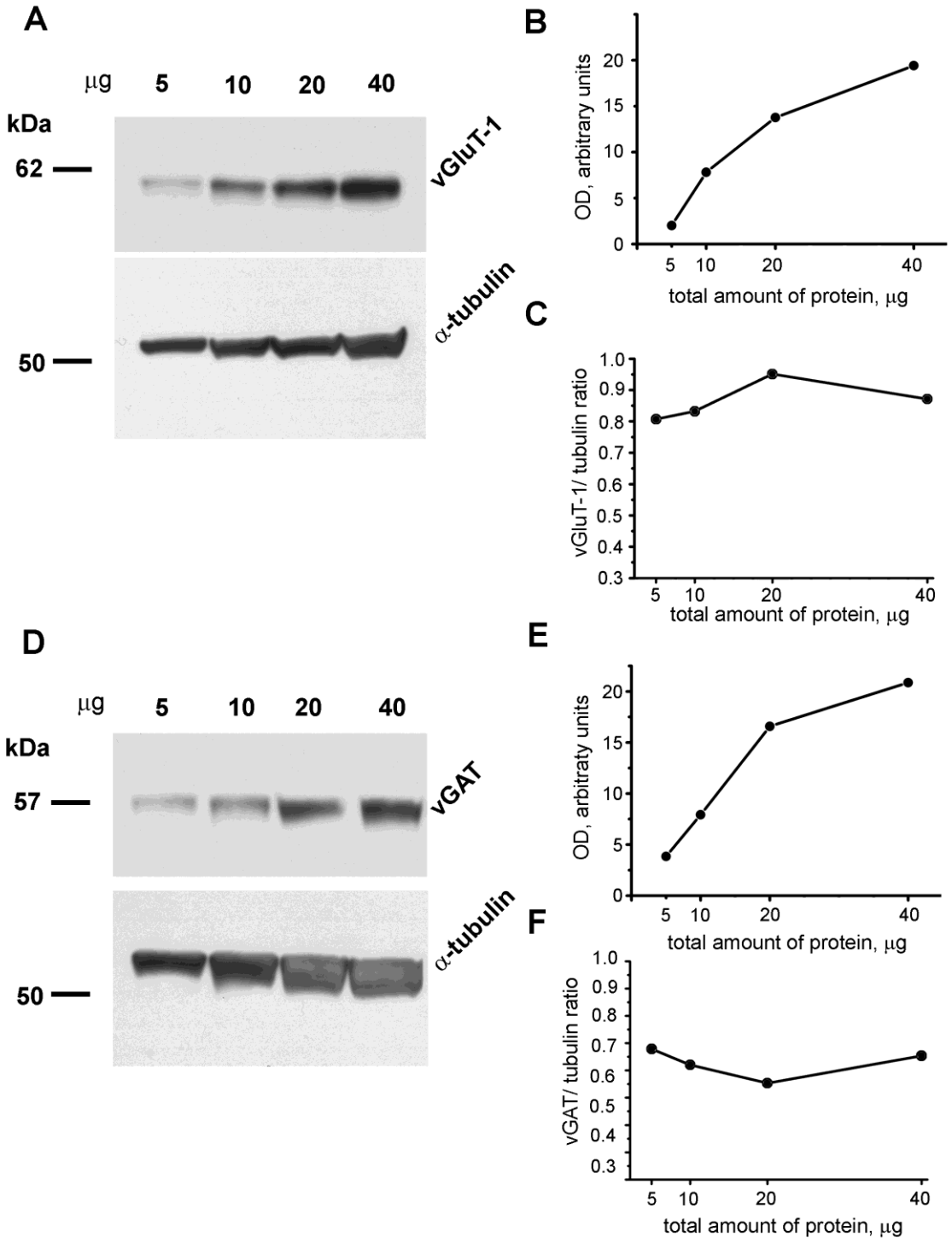

Figure 3.8 Assessment of the linearity of the method for evaluating the level of vGluT-1 and vGAT expression in rat primary visual cortex. A) Representative immunoblottings for vGluT-1 and α-tubulin after loading increasing amounts of the same protein extract; B) Plot showing the relationship between the optical density (OD) of the vGluT-1 band and the total amount of protein loaded note the linear relationship between OD and amount of loaded protein in the range 5-20μg of total protein, with y-intercept at about 0; C) Plot displaying the ratio between the ODs of the vGluT-1 and α-tubulin bands as a function of total protein loaded; D) Representative immunoblottings for vGAT and α-tubulin after loading increasing amounts of the same protein extract; E) Plot showing the relationship between the optical density (OD) of the vGAT band and the total amount of protein loaded; note the linear relationship between OD and amount of loaded protein in the range 5-20μg of total protein, with y-intercept at about 0; F) Plot displaying the ratio between the ODs of the vGAT and α-tubulin bands as a function of total protein loaded.

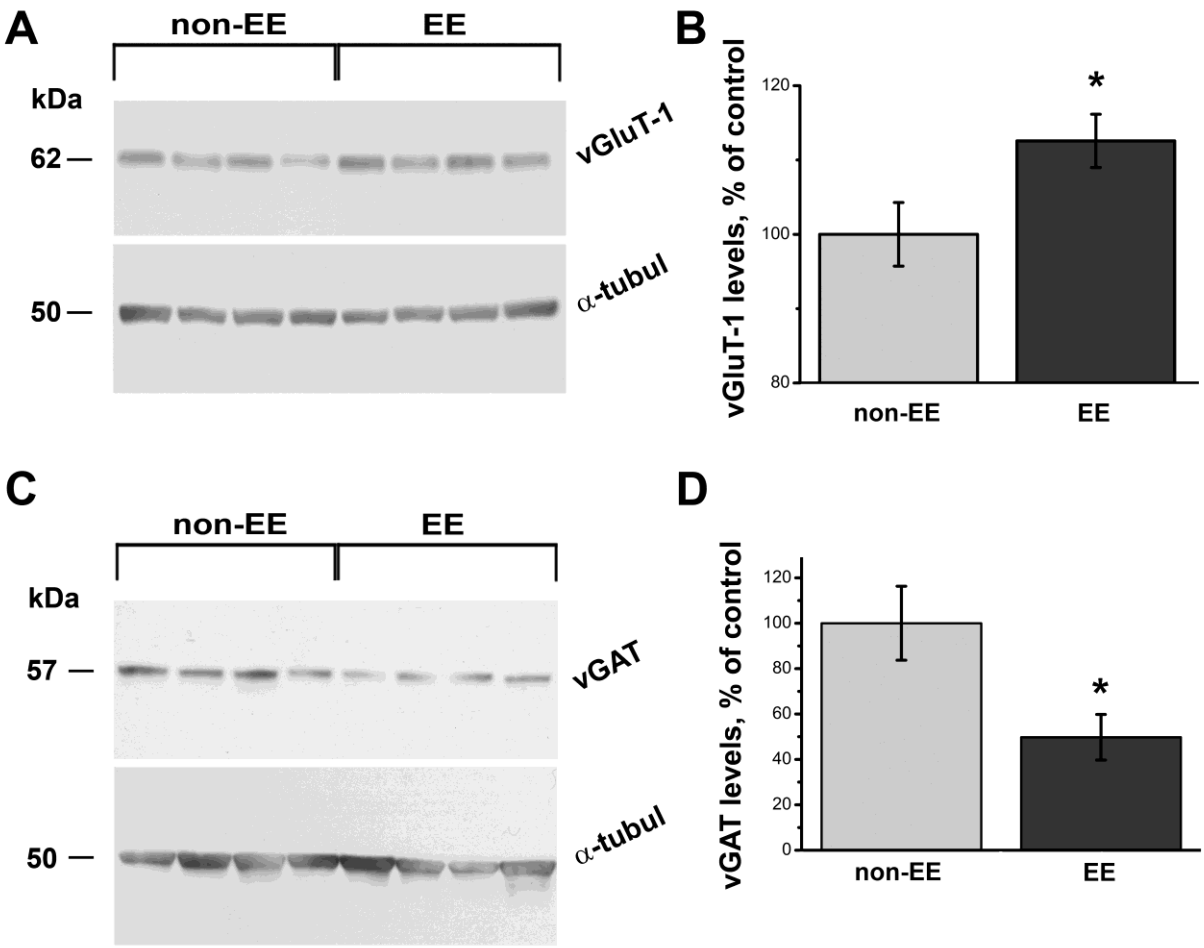

Figure 3.9 Upregulation of vGluT-1 and downregulation of vGAT in EE rats. Western blot analysis of neurotransmitter transporter expression in the visual cortex of adult rats reared in standard conditions (non-EE) or in enriched environment (EE). Panels A and C are representative immunoblottings for vGluT-1 (A) and vGAT (C), with each lane representing the visual cortex of one animal; panels B and D are the corresponding quantifications. Data are expressed as mean ± SEM of vGluT-1 and vGAT optical density divided by α-tubulin (α-tubul) optical density of the corresponding sample. EE results in a higher expression of vGluT-1 (Student's *t* test, P=0.039), while causing a decreased expression of the GABA transporter (vGAT, Student's *t* test, P=0.040). For each histogram, EE, N=9, non-EE, N=9 rats.

3.2 EE EFFECTS ON CROSSMODAL PLASTICITY IN THE ADULT MOUSE

The issue of the influence of the complex sensorimotor stimulation provided by EE on crossmodal plasticity between cortical areas was addressed using local field potential (LFP) recordings in adult, freely moving mice. To maximize a possible effect of EE on cortical activity, animals were raised since birth in EE, then implanted with EEG electrodes and recorded at P60 (Fig. 3.10).

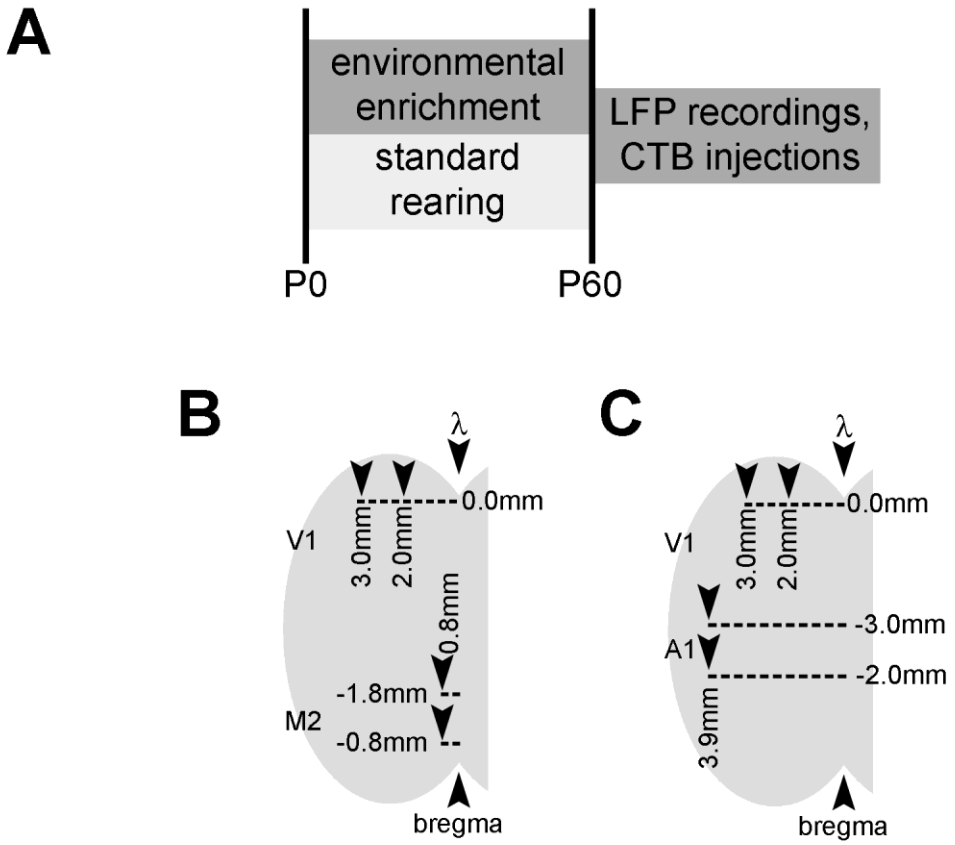

Figure 3.10 Experimental protocol for EE experiments in mice. A) Schematic diagram of the EE since birth protocol. B) Drawing showing the stereotaxic coordinates for placing EEG electrodes in secondary motor cortex/frontal eye field (M2) and primary visual cortex (V1). C) Drawing showing the stereotaxic coordinates for placing EEG electrodes in primary auditory cortex (A1) and primary visual cortex (V1). For panels B and C, M2 and A1 coordinates are referred to the bregma point, V1 coordinates to the lambda point.

3.2.1 Identification of monosynaptic connections between primary visual cortex and other cortical areas

To label connections between V1 and other cortical areas, I took advantage of Cholera Toxin β subunit (CTB), which, following intracortical injection, is both taken up by neuronal terminals and retrogradely transported to the soma and anterogradely transported from the cell body to synaptic terminals. Given that I was interested to analyze direct connections impinging on the *primary* visual cortex (V1), I stereotaxically injected a minimal amount (50nℓ) of CTB at a cortical depth of 600μm; this avoided diffusion of the tracer to the adjacent secondary visual cortex. Injection sites were located either 2.5mm or 3.0mm mediolateral (and 0.0mm anteroposterior) to the lambda point, which correspond to the monocular and binocular parts of V1, respectively. This allowed me to detect possible differences in the corticortical connectivity of these V1 subregions. After injection, I allowed 3 days for the tracer to be transported to neuronal somata before processing animals for immunohistochemistry for CTB, coupled to nuclear staining with YoYo-1 (Fig. 3.11-16).

From the observation of the acquired images, it can be appreciated that the dense staining around the injection site remains confined within the boundaries of the monocular or binocular V1 (Fig. 3.11A, left and right). Thus, labeled neurons and terminals in other cortical areas are very likely to be connected with V1, not with higher-order visual areas. A further proof confirming the identity of the injection site is the retrograde transport of CTB to the ipsilateral dLGN. The appearance of dLGN labeling confirmed the regional selectivity of the injection. Indeed, CTB delivery into the monocular and binocular V1 resulted in labeling of the ventral and dorsal part of the dLGN, respectively (Fig. 3.11B).

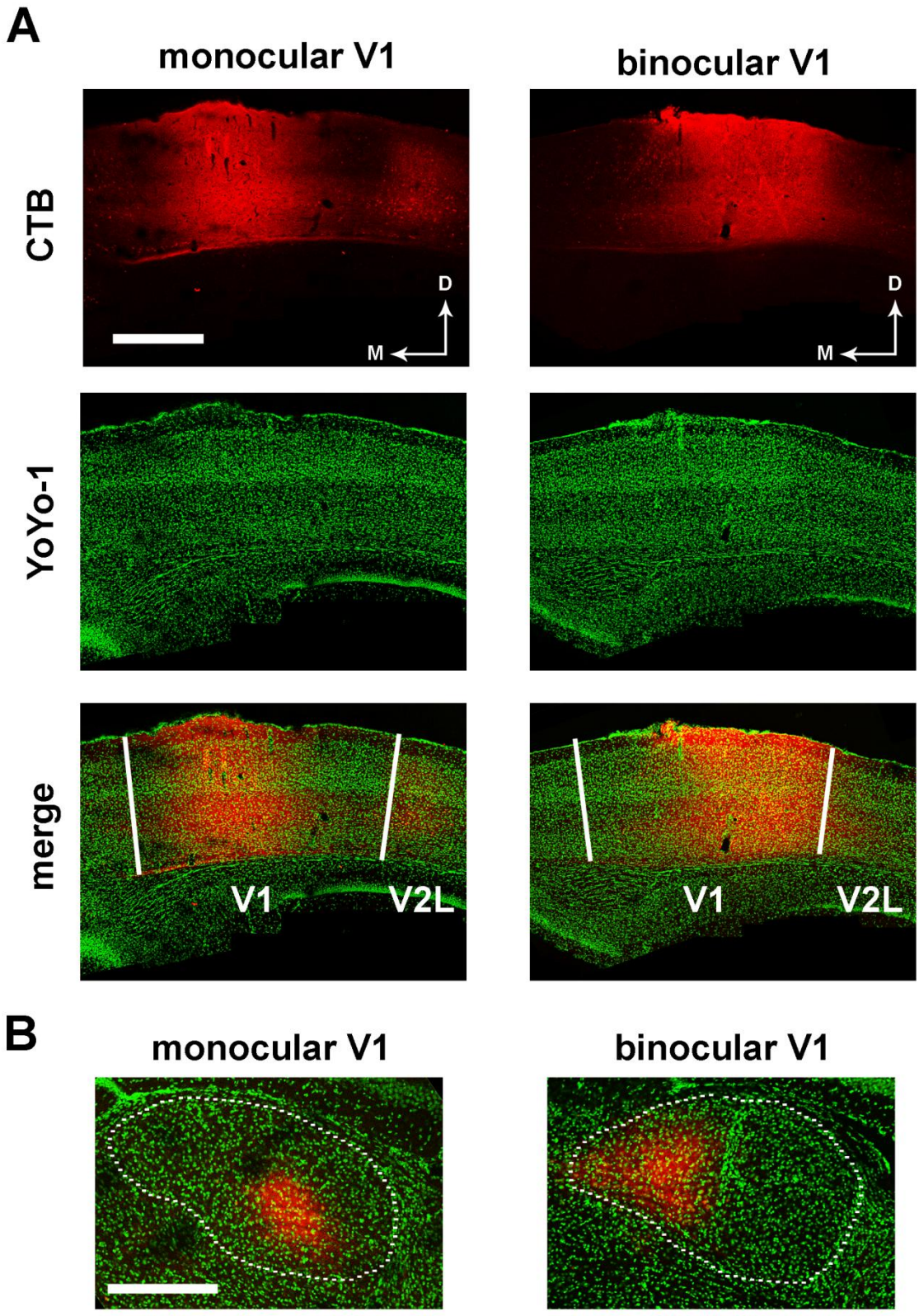

Figure 3.11 Anatomical tracing of corticocortical connections with primary visual cortex. A) Cholera toxin β subunit (CTB) injection sites in the monocular portion of primary visual cortex (left) and in the binocular portion of V1 (right). Scale bar is 500μm. B) Retrograde transport of CTB (red) injected into the monocular (left) and binocular (right) portions of primary visual cortex to the dorsal nucleus of dLGN, whose contour is indicated by the dashed line. Cell nuclei (green) are counterstained with YoYo-1. Scale bar is 100μm.

As expected, when CTB was injected into the monocular V1, stained cells were abundant across the whole thickness of the adjacent ispilateral lateral and medial secondary visual cortices (V2L and V2M, Fig. 3.12, left). On the other hand, projections from the binocular V1 to the V2M and V2L were less abundant (Fig. 3.12, right).

When the hemisphere contralateral to the injection site was examined, delivery of CTB to the monocular V1 resulted in the labeling of scattered cell bodies, located prefrentially in layers V-VI (Fig. 3.13, right). On the other hand, when the injection site was located into the binocular V1, in proximity to the border with V2L, *i.e.* comprising the cortical representation of the vertical meridian, stained somata were visible throughout the whole thickness of the V1 (Fig. 3.13, right).

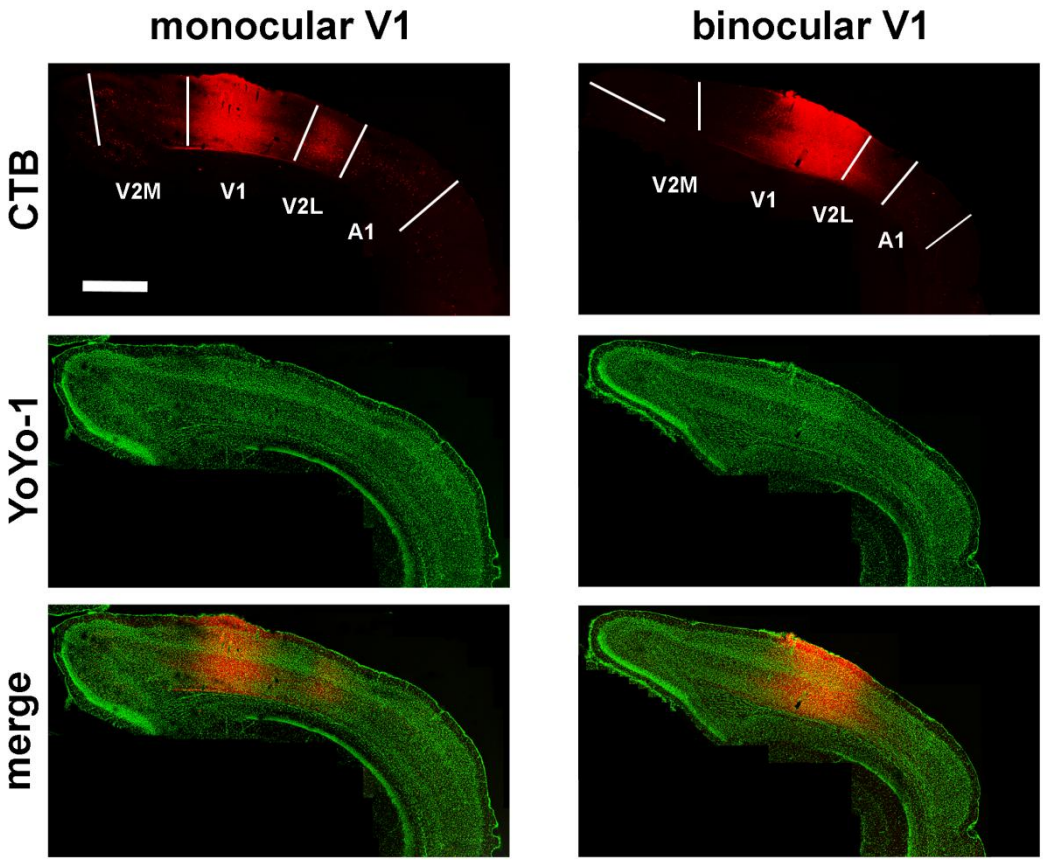

Figure 3.12 Corticocortical connections between V1 and adjacent cortical areas. Left, CTB injected into the monocular portion of V1 was retrogradely transported to layers II-VI of lateral secondary visual cortex (V2L), whereas in medial secondary visual cortex (V2M) only layer IV neurons were stained. Right, CTB injected into the binocular portion of V1 was retrogradely transported to layers V-VI of V2L, whereas in V2M labeling was virtually absent. Scale bar is 500μm.

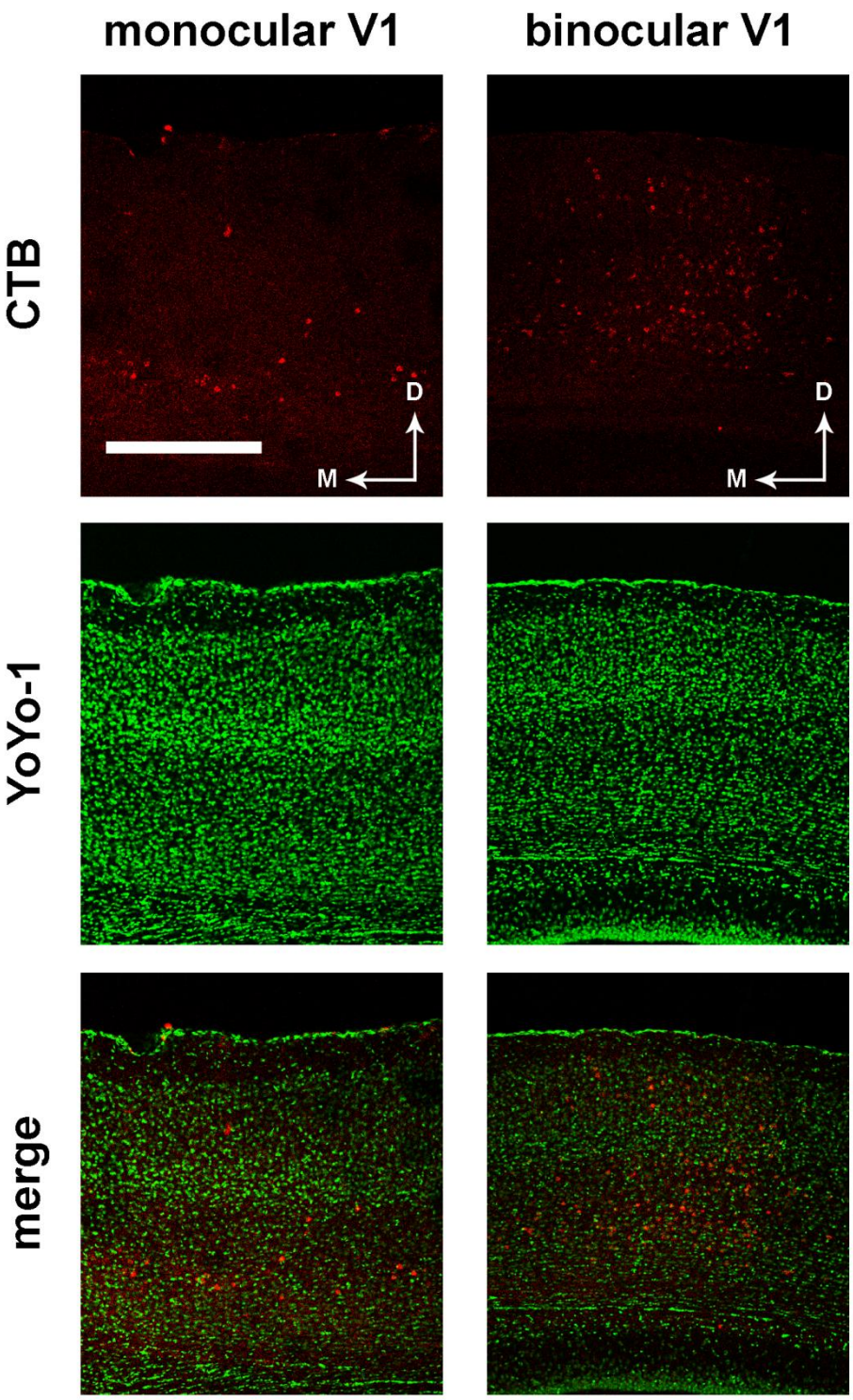

Figure 3.13 Connections from contralateral V1. Left, injection of CTB into the monocular V1 resulted in staining of layer V-VI neurons in contralateral V1. Right, CTB injected into the binocular portion of V1 was retrogradely transported to layers II-VI of contralateral V1. Scale bar is 1mm.

When I looked for cortical areas that displayed retrograde transport of CTB, I found three clearly labeled areas that are not directly related with processing of visual sensory information.

The first area was comprised in sections containing the temporal lobe and was identified as the primary somatosensory cortex (S1) (Paxinos, 2008) (Fig. 3.14A, B). Only the ipsilateral S1 was labeled. To investigate the possibility that stained neurons and terminals were located in the barrel field of S1, which receives input from the vibrissae, I combined CTB and vGluT2 stainings. Indeed, vGluT2 is a marker of thalamocortical afferents and thus precisely labels layer IV barrels of S1. From this experiment I could conclude that connections between V1 and S1 do not involve the barrel field, since CTB and vGluT2 labelings did not colocalize (data not shown).

Delivery of CTB to the monocular or binocular V1 resulted in different labeling patterns, since in the first case a light staining of neuronal terminals coming from the V1 and a few cell somata were observed in layers II-III and V (Fig. 3.14A), while in the second case, anterograde transport was more conspicuous and cell bodies were much more abundant, especially in layers II-III and V-VI (Fig. 3.14B).

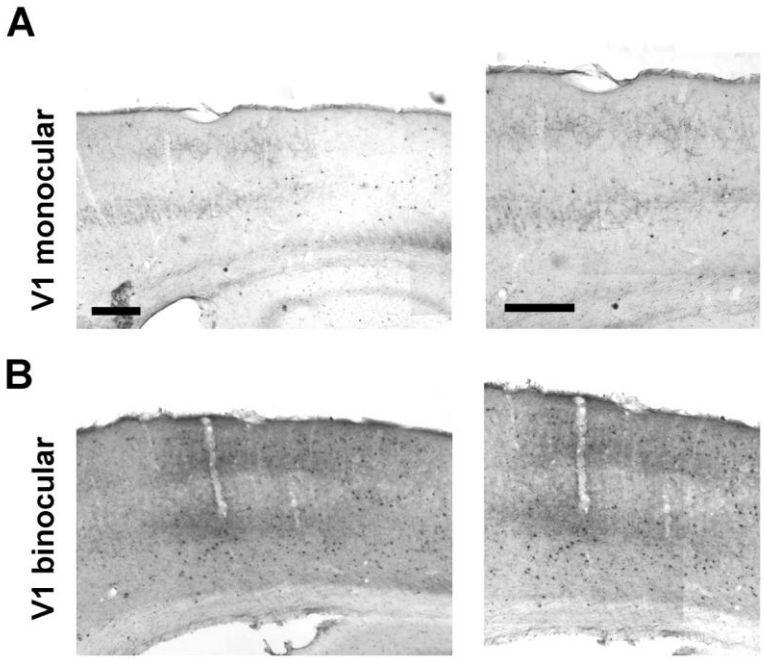

Figure 3.14 Connections between primary somatosensory cortex and V1. Left. Low-magnification images of CTB immunoreactivity in primary somatosensory cortex (S1). Right. Higher magnifications from images showed on the left side. Scale bars are 200μm. When CTB was injected into the monocular portion of V1, only projections from V1 to layers II-III and V, in addition to a few scattered cell somata. On the other hand, when the injection site was located in the binocular portion of V1, a more conspicuous anterograde staining, together with a higher number of cell somata, were visible.

The second area was apparent in anterior coronal sections at the level of the frontal lobe (Fig. 3.15A, B). In the hemisphere ipsilateral to the injected V1, CTB immunoreactivity was particularly prominent and was confined in a thin stripe close to the interhemispheric fissure and was distributed across all cortical layers (Fig. 3.15A, B), with no difference between injection sites located in monocular or binocular V1. Of note, a few cells were labeled also in the hemisphere contralateral to the injected site (Fig. 3.15A, B). I identified this area as the secondary motor cortex (M2) (Paxinos, 2008). This area is classified in rats and primates as "frontal eye field"(fef), and it is known to be involved in controlling voluntary eye movements, but also in multimodal sensory processing and in visual memory (Huerta et al., 1987; Guandalini, 1998).

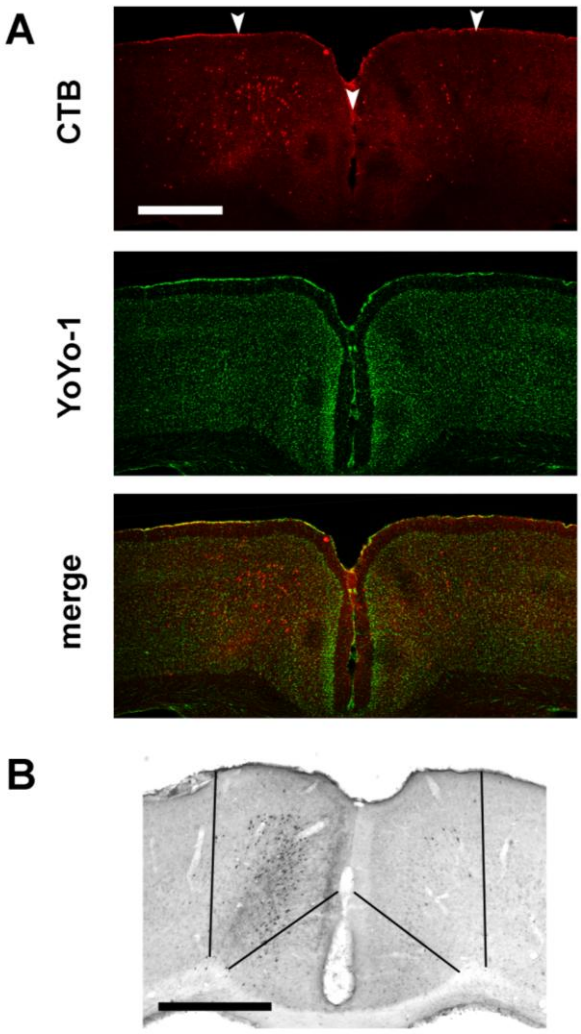

Figure 3.15 Projections from secondary motor cortex/frontal eye field to V1. A) Immunofluorescence images showing retrograde labeling of neuronal somata contained in the M2/fef area, whose boundaries are indicated by arrowheads. B) DAB detection of CTB immunoreactivity makes it possible to appreciate a dense anterograde labeling of projections coming from ipsilateral V1; black lines indicate M2/fef boundaries. Scale bars are 500μm.

The third area was comprised in sections containing the posteriormost part of the temporal lobe and was identified as the primary auditory cortex (A1) (Paxinos, 2008) (Fig. 3.16). In the hemisphere ipsilateral to the injected V1, labeled cells were located in layers IV-VI, with a few scattered cells in layers II-III (Fig. 3.16, left). In the contralateral hemisphere, neurons projecting to V1 were less abundant and preferentially located in layers V-VI (Fig. 3.16, right).

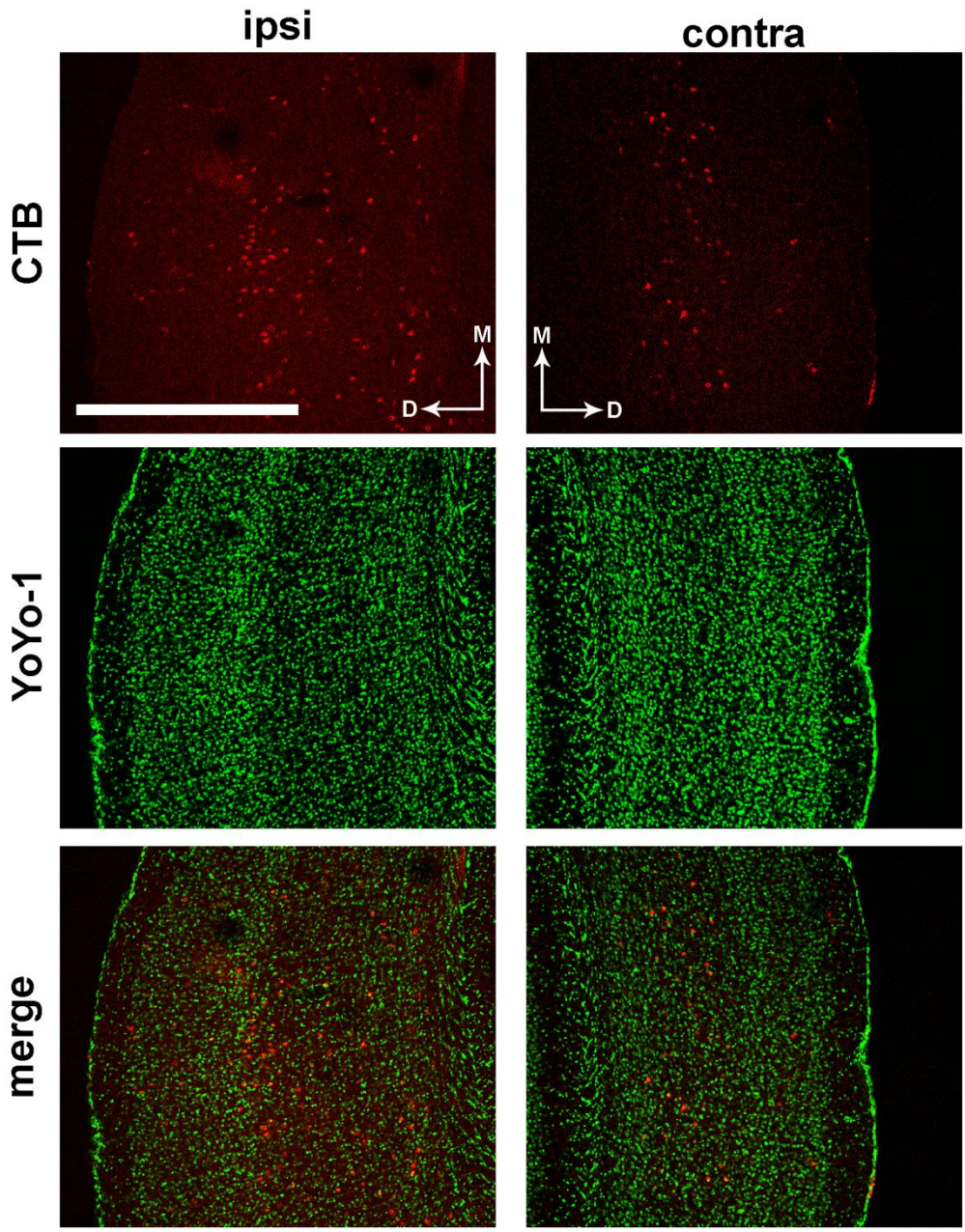

Figure 3.16 Projections from primary auditory cortex to V1. Left, immunofluorescence images showing retrograde transport of CTB injected in V1 to ipsilateral layers IV-VI of primary auditory cortex (red), with a few scattered somata in layer II-III. Right, in the hemisphere contralateral to the injection site, a few cells are labeled in layers V-VI. Nuclei are counterstained with YoYo-1 (green). Scale bar is 500μm.

An analogous set of experiments was performed in EE animals. Comparison of stained sections between EE and non-EE mice revealed the same pattern of labeling. This consisted again of both retrograde and anterograde transports of CTB from V1 to M2/fef and S1, in addition to retrograde transport to A1.

3.2.2 EE and functional coupling between cortical areas

On the basis of the anatomical tracing experiments described above, I investigated whether EE from birth could affect coupling of electrical activity between V1 and M2 or A1, using multichannel LFP recordings in freely moving adult mice.

After trace acquisition, computational analysis of LFP signals was used to quantitatively assess the extent of synchrony in activity between V1 and the two areas that I identified as being directly connected with it. In particular, I calculated two indexes, which result from linear cross correlation (CC) and mutual information (MI) functions. Both operations give an evaluation of the synchrony between signal amplitudes acquired from different cortical areas. It is worth noting that CC takes into account only linear interactions between signals, whereas MI is designed to consider also nonlinear dynamics (Mormann et al., 2003; Kraskov et al., 2004).

When I analyzed couples of signals coming from LFP recordings in V1 and M2, I found that EE since birth results in a pronounced desynchronization of regional neural activities in these areas. Indeed, the CC index decreased from 0.270±0.004 in non-EE mice to 0.137±0.001 in EE animals (Student's *t* test, $P<0.001$) (Fig. 3.17A). Analogously, the MI index was 0.060±0.002 in the non-EE group and this value decreased to 0.015±0.000 (Student's *t* test, $P<0.001$) (Fig. 3.17B).

The same analysis performed on recordings from V1 and A1 yelded a completely different result. In this case, EE was responsible for an increase in the CC index, which amounted to 0.199±0.006 in non-EE animals and to 0.321±0.004 in EE mice (Student's *t* test, $P<0.001$) (Fig.

3.17C). A consistent result came from MI calculation, which increased from 0.039±0.002 in non-EE mice to 0.054±0.002 in EE mice (Student's *t* test, P<0.001) (Fig. 3.17D).

Thus, LFP recordings showed that EE has specific effects on different cortical areas that are monosynaptically connected. In particular, synchrony of activity between V1 and M2, an area that is not responsible for direct processing of sensory information, is decreased. On the other hand, functional coupling between two important primary sensory areas –V1 and A1– is dramatically increased in adult animals subjected to EE since birth.

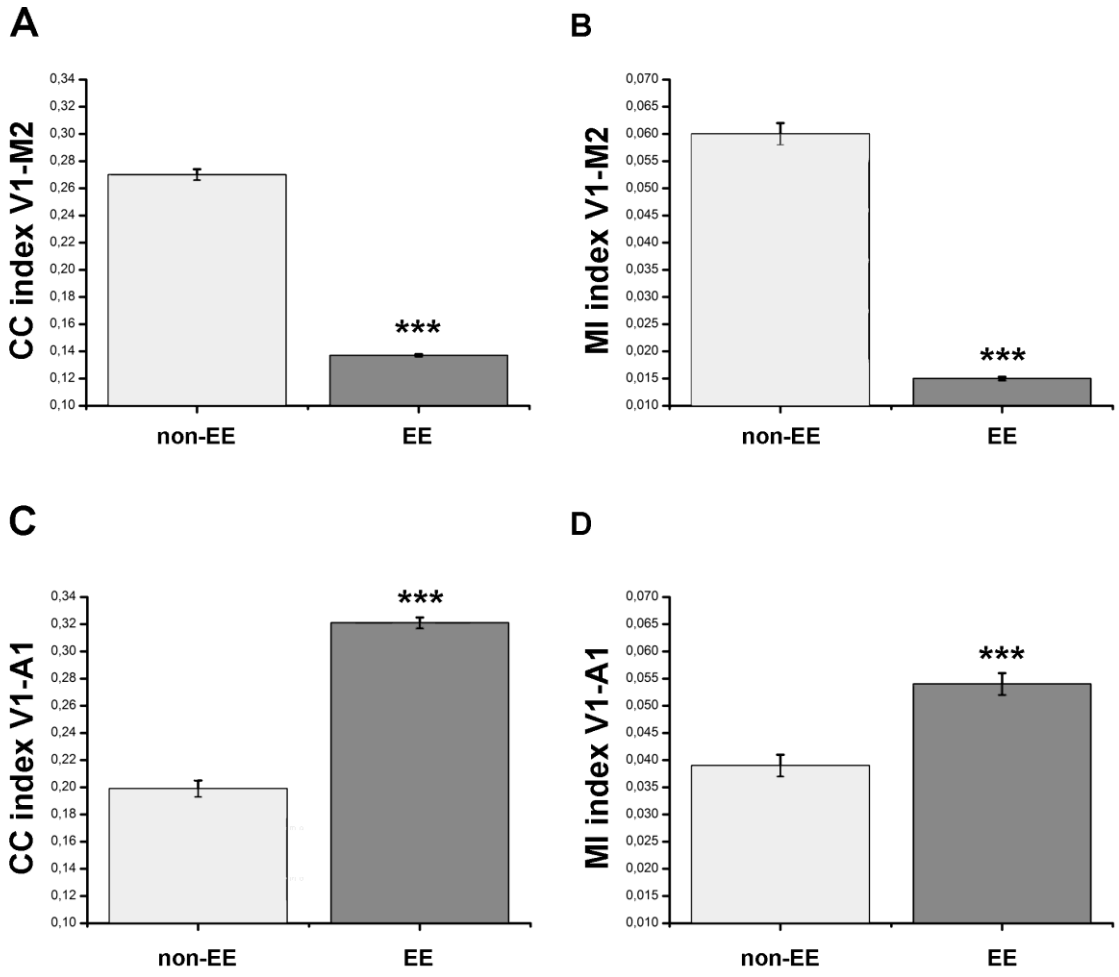

Figure 3.17 Quantitative analysis of synchrony between local activities in V1-M2 and V1-A1. A) Crosscorrelation between activities in V1 and M2 was decreased in EE mice compared to non-EE animals (EE, N=6, non-EE, N=8, Student's *t* test, P<0.001). B) Mutual information between activities in V1 and M2 was decreased in EE mice compared to non-EE animals (EE, N=6, non-EE, N=8, Student's *t* test, P<0.001). C) Crosscorrelation between activities in V1 and A1 was increased in EE mice compared to non-EE animals (EE, N=6, non-EE, N=6, Student's *t* test, P<0.001). D) Mutual information between activities in V1 and A1 was increased in EE mice compared to non-EE animals (EE, N=6, non-EE, N=6, Student's *t* test, P<0.001). Data are expressed as mean ± SEM.

4. DISCUSSION

4.1 EE potentiates thalamocortical transmission in the adult rat

EE is an experimental paradigm that is widely used to provide animals with a complex sensorimotor stimulation consisting of physical activity, different learning experiences and social interaction (van Praag et al., 2000). Indeed, enriched animals are reared in large groups, in a wide and stimulating environment containing several objects -that are frequently changed- and running wheels for voluntary physical exercise (van Praag et al., 2000; Will et al., 2004; Nithianantharajah and Hannan, 2006; Sale et al., 2009). Previous experiments have shown that exposure to EE in adulthood enhances plasticity of neural circuitry in both the normal and diseased brain (Will et al., 2004). In our laboratory, it has been demonstrated that EE can reinstate plasticity in the adult rat brain reverting amblyopia effects and restoring a normal visual function (Sale et al., 2007a). Moreover, EE stimulates axonal plasticity and synaptic reorganization following adult brain injury, reactivating plasticity of retinotectal projections following retinal lesions (Caleo et al., 2009). While EE action during development is beginning to be clarified both at the cortical level (Cancedda et al., 2004; Ciucci et al., 2007; Sale et al., 2007b) and in peripheral structures like the retina (Landi et al., 2007a; Landi et al., 2007b; Landi et al., 2009), the mechanisms by which EE acts on the adult brain are not fully understood. In particular, it is not known whether subcortical nuclei are affected by EE.

In the present work, I sought to determine whether changes in thalamocortical connections could contribute to the enhancement of plasticity observed following EE in adult brain. In particular, I compared the physiology of the geniculocortical pathway *in vivo* using animals reared in standard cages or exposed to EE for two weeks. I stimulated the geniculate and recorded cortical field potentials in correspondence with the major, short latency sink in layer IV-layer III, that corresponds to excitatory postsynaptic currents elicited directly by the thalamocortical afferents (Mitzdorf, 1985; Heynen and Bear, 2001). My data demonstrate for the

first time that EE affects the thalamic input to the visual cortex *in vivo*, and that this functional effect is associated with neurochemical modifications of excitatory and inhibitory neurotransmission.

First, my data indicate a difference in the input-output relationship of the thalamocortical system. Indeed, in EE rats the input-output curve was shifted upwards and EE animals required a lower stimulation intensity to reach saturation of response. This phenomenon can be explained by (i) an increase in the quantal size, (ii) an enhanced release probability at thalamocortical synapses, or (iii) an increased density of geniculocortical terminals. Intracellular recordings would be needed to address these issues. These possibilities (not mutually exclusive) are consistent with the upregulation of vGluT-2 expression in thalamocortical synapses in layer IV. Indeed, previous work had established a direct link between the level of glutamate transporter expression and both the amount of released glutamate and the likelihood of such release events (Murthy et al., 2001; Wilson et al., 2005; Takamori, 2006). The hypothesis of an increased release probability at geniculocortical synapses is supported by the conspicuous decrease of the Paired-Pulse Depression (PPD) ratio in enriched animals, especially at short interstimulus intervals. PPD at thalamocortical synapses is caused by presynaptic Ca^{2+}-dependent neurotransmitter depletion and postsynaptic GABAergic inhibition ((Rozas et al., 2001; Jia et al., 2004). After the first stimulation, this leaves a smaller population of synaptic vesicles available for release in response to a second, closely-spaced stimulus (Thomson, 2000). Thalamocortical synapses typically display PPD as they are characterized by a high release probability ((Castro-Alamancos and Connors, 1997; Gil et al., 1999; Thomson, 2000). Thus, my findings support the idea that EE impacts on the synaptic strength of thalamocortical connections by regulating vGluT-2 expression and hence release of glutamate from presynaptic geniculocortical afferents. On the other hand, a simple increase in the number of

thalamocortical afferents, with no change in synapse functional status, would not explain the effect on PPD, because in this case the ratio between the second and the first response would be unaffected.

A previous report by Rozas et al. (Rozas et al., 2001) found that acute bath application of the GABAA antagonist picrotoxin reduced the degree of PPD in visual cortical slices, pointing to a crucial role of synaptic inhibition in PPD. On the other hand, Rozas and collaborators did not exclude the possibility that changes in the probability of release at excitatory terminals could counterbalance changes in inhibition producing the effect I observed in the present study. One reasonable explanation for my findings is indeed that the enhancement of thalamocortical excitatory transmission could outweigh the decrease in intracortical inhibition, thus resulting in a net increase of PPD. Therefore, I explain the shift in the input-output curve and the increased PPD as signs of a selective potentiation of the thalamocortical afference to the visual cortex induced by EE.

My data also show that EE is able to affect also long-term plastic events, such as LTP of thalamocortical synapses induced after TBS of the thalamus. In non-EE animals I found a small, but highly significant (one-way ANOVA, $P<0.001$) enhancement of cortical field potentials induced by TBS of the dLGN, indicating that these experimental conditions are adequate for eliciting genuine LTP in controls. The magnitude of LTP that I observed in non-EE rats is lower than that reported by other authors, but this difference may depend on several experimental conditions, including age of the animal, type of anaesthesia, LTP-inducing protocol and location of the recording electrode (monocular vs. binocular visual cortex) (Heynen and Bear, 2001; Tsanov and Manahan-Vaughan, 2007; Kuo and Dringenberg, 2008). Remarkably, EE rats showed a potentiation 2.5-fold higher than non-EE animals, reinforcing previous data based on cortical slices in our laboratory (Sale et al., 2007a). The induction of LTP in EE rats had also

robust consequences on the cortical response to physiological visual stimuli. Indeed, after TBS stimulation EE rats showed a significant potentiation of the response to grating stimuli across a range of contrasts, while in standard animals we observed a potentiation of the VEP response only to optimal (90%) contrast gratings. These data provide further support for the idea that EE improves the capability of the visual system to react to relevant stimuli and change as a function of its activity.

Enhancement of plasticity is causally related to an EE-mediated reduction of inhibition in the adult cortex, as recovery of plasticity is prevented by intracortical infusion of benzodiazepines during the EE period (Sale et al., 2007a) and a reduction of the inhibitory tone in adult animals causes the reopening of ocular dominance plasticity in the visual cortex (Harauzov et al., 2010). Moreover, visual deprivation reactivates plasticity in adult rats and produces a significant decrease in the level of GABAA receptors relative to AMPA receptors (He et al., 2006). My data are consistent with this evidence, demonstrating a decrease in the inhibitory system marker vGAT in the visual cortex after EE. Moreover, the quantitative immunoblottings I did revealed an augmented expression of vGluT-1, demonstrating for the first time an EE-mediated effect on the levels of this intracortical excitatory marker. Therefore, changes in both glutamatergic and GABAergic systems contribute to the increase in the excitation/inhibition ratio that takes place after EE. The net result of these neurochemical modifications could be a reopening of the inhibitory "plasticity gate" that regulates expression of cortical LTP (Kirkwood and Bear, 1994a). These effects on the intracortical circuitry may cooperate with the potentiation of thalamocortical transmission. Thus, two different mechanisms can act concurrently to determine the enhancement of plasticity we observed in EE animals: (i) a potentiation of the thalamic input to the primary visual cortex and (ii) an increase in cortical excitability based on a higher excitation/inhibition balance.

The fact that enriched animals display a higher amount of LTP, compared to controls, suggests the possibility the occurrence of metaplasticity mechanisms triggered by EE. Indeed, adult visual cortex retains the possibility to express LTP (present data and Heynen and Bear, 2001), but a period of EE is able to increase the amount of LTP expressed by the thalamocortical pathway in response to electrical stimulation of the dLGN. Hence, EE is able to lower the activity threshold for potentiation of cortical response, which represents a metaplastic phenomenon, *i.e.* a modulation in the capability of a given neural system to express its plastic potential (Abraham, 2008). At the biochemical level, metaplasticity can be actuated by the shift in the cortical excitation/inihibition balance. The resulting higher excitatory tone can represent the functional basis for the increased magnitude of cortical LTP.

It is tempting to speculate that the crucial factor for the expression of metaplasticity in the cortex of enriched animals appears to be BDNF, since it has been demostrated that the cortical level of this neurotrophin is increased following EE (Sale et al., 2007b). Moreover, LTP induction in hippocampal slices is accompanied by an increase in BDNF secretion (Aicardi et al., 2004). This suggests that blockade of BDNF signaling during EE through pharmacological inhibition of the TrkB receptor, would antagonize the enhancement of cortical plasticity.

Administration of fluoxetine to standard-reared rats is able to reproduce the effect of EE on visual cortical plasticity (Maya Vetencourt et al., 2008), including the increase in BDNF level and in the excitation/inhibition ratio. This raises the possibility that enhancement of serotonergic activity is the preminent mediator of the effect of EE on metaplasticity, modulating BDNF secretion and cortical excitability, with the net effect of lowering the threshold for plasticity induction.

It can be concluded that a period of EE in adulthood has specific effects on the efficacy of thalamocortical inputs to the primary visual cortex and enhances activity-dependent synaptic

plasticity in this pathway. These physiological modifications are associated with changes in the expression of vesicular neurotransmitter transporters. These data indicate novel mechanisms by which experience modulates synaptic function and the degree of plasticity in the mature brain.

4.2 EE differentially affects crossmodal plasticity between cortical areas

The influence of EE on brain structure and physiology is well known (van Praag et al., 2000; Sale et al., 2009). Previous studies have focused only on the effects exerted by EE on the physiology of specific brain areas, such as the hippocampus or the primary visual cortex (van Praag et al., 2000; Sale et al., 2009). However, EE is a complex manipulation that has a global influence on the central nervous system, since it combines motor stimulation with social interaction, in addition to providing multimodal sensory inputs, coming from the continuous exploration of novel objects and from the periodical changes in the arrangement of the rearing space. Thus, EE is very likely to affect at once plasticity in multiple brain areas, which is quite different from other experimental manipulations, such as monocular deprivation or whisker trimming, that are designed to selectively induce plasticity in the circuits devoted to a specific sensory modality. To investigate the problem of crossmodal plasticity in response to EE , I adopted a protocol of prolonged enrichment, starting since birth and continuing until adulthood, to maximize the putative effect of EE on functional coupling between different areas. Indeed, early EE is known to accelerate visual system development (Cancedda et al., 2004). Hence, I hypothesized that EE could have an influence also on those corticocortical connections that have been described to exist in the cat between A1 and V1 (Innocenti and Clarke, 1984). In particular, it was tempting to speculate that EE could induce an enhancement in corticortical transmission during early development, which would result in the adult animal

in the maintenance of these connections, that would be otherwise lost, as a consequence of pruning processes (Innocenti and Clarke, 1984).

Crossmodal connections have been sparsely described in rodents and the majority of literature concerns subcortical inputs to sensory cortices. For example, auditory inputs to V1 coming from a pathway connecting the inferior colliculus with the dLGN have been found in congenitally anophtalmic mice (Chabot et al., 2008). Concerning corticocortical connections, work on the prairie vole (*Microtus ochrogaster*) has identified direct connections between A1 and V1 (Campi et al., 2009), which appear similar to what has been described in primates (Falchier et al., 2002). Thus, a systematic description of corticocortical connections that could provide a substrate for crossmodal plasticity is substantially lacking.

Using stereotaxical injections of the retrograde tracer cholera toxin β subunit, I was able to label cortical and subcortical areas that are monosynaptically connected with V1. Apart from the expected connection between V1 and dLGN, which provided an internal control to check the correct site of injection, I identified some interesting cortical areas that send input to the V1: the frontal eye field/secondary motor cortex (FEF/M2), the A1 and the trunk S1. A previous study in the rat had used anterograde tracer injections in FEF to show projections to the V1 (Guandalini, 1998). My results confirm this finding, using the retrogradely transported CTB. This area has been initially linked to the control of saccadic eye movements in primates (Bruce and Goldberg, 1985), but it has also a role in a higher order visual processing and short-term memory (Huerta et al., 1987; Felleman and Van Essen, 1991).

On the other hand, the direct connection between A1 and V1 is shown here for the first time in the mouse. Its existence had been hypothesized in anophtalmic mice (Laemle et al., 2006), but further work showed that it actually come from a subcortical link between the visual thalamus and the inferior colliculus (Chabot et al., 2008). Moreover, this pathway is shown here in

physiological conditions, without any significant alteration in visual and auditory functionalities. The connection I describe here can represent the homologous of the similar pathway that has been described in primates (Falchier et al., 2002). These data demonstrate that cortical areas can have strong direct connections, in addition to being indirectly coupled by their thalamic afferents and by subcortical diffuse projection nuclei.

The absence of easily recognisable differences in the extent of corticocortical connections between EE and non-EE animals should not surprise. Indeed, the most economical way to modulate functional coupling among different areas would be to change their level of activity - possibily through activity-dependent plasticity phenomena, instead of building or maintaining a higher number of fibers.

When considering the existence of these direct projections from the M2 and A1 to the V1, it was of interest to investigate whether their functional coupling could be affected by EE, thus resulting in crossmodal plasticity. This problem was investigated using multichannel LFP recordings in freely moving mice, subjected to EE since birth. To analyze LFP recordings, I evaluated the global neuronal activity pattern, instead of dividing the signal into the traditional frequency bands (δ, θ, α, β, γ). It has been proposed that this approach could be more informative, as during neural activity the different frequency bands coalesce and influence each other (Steriade, 2006). The results of this analysis showed that EE decreases linear and nonlinear correlation between regional neural activities in M2 and V1. Conversely, visuoacustic functional interactions between A1 and V1 are increased by the same rearing condition. The existence of these opposite effects on functional interaction of different cortical areas with V1 leads to hypothesize that different brain functions might be affected by EE in different ways. In particular, activity in V1 is less correlated to activity in M2 in response to EE. This could be explained by considering that M2 is connected also with secondary visual cortex in the rat and

with V4 extrastriatal visual area in the macaque (Stanton et al., 1995; Guandalini, 1998) and could be involved in higher-order visual processing. Therefore, EE could result in a loss of correlation between the first stages of visual processing, which take place in V1 and supeior visual functions that appear to require also input from farther cortical areas, such as M2. A somewhat similar result has been obtained using EEG recordings in humans, showing that coupling between visually evoked frontal and occipital neural activity is decreased during the execution of a simple motor task (Saron et al., 2001). On the other hand, correlation between A1 and V1 is increased in EE mice. This result is in line with previous electrophysiological findings, which demonstated the existence of auditory responses in visual neurons (Morrell, 1972; Fishman and Michael, 1973). In this case, cognitive stimulation provided by EE results in an increase in correlated activity between these two primary sensory areas. It would be interesting to further explore this phenomenon, using acute electrophysiological recordings to evaluate whether this pathway can undergo LTP/LTD, which would provide a basis for the increased correlation observed after EE.

In addition to a potentiation or depression of the specific corticocortical neural pathways – that could be sufficient to explain the increase in correlation between A1 and V1, it is tempting to speculate that EE might act also on the synchronizing influence of the thalamus on the cortex. The increase in the excitation/inhibition ratio that has been described to take place in the adult visual system, could be a common motif regulating cortical and subcortical plasticity. If so, the reduction in the inhibitory drive could also involve thalamic afferents, which are known to shape cortical activity during sleep and wakefulness (Steriade, 2006). Therefore, the various cortical areas could be able to express their functional individuality, which would result in the decorrelation observed between M2 and V1 and in the facilitation of potentiation of auditory input to the visual cortex.

Further studies are ongoing to compare single-channel EEGs of the recorded areas from EE and non-EE mice, together with Granger causality analysis (Antonucci et al., 2008) to establish whether interaction between areas has a preferential direction (*i.e.*, whether V1 drives M2/fef and A1 or *vice versa*).

An interesting feature of this experiment is that crossomodal plasticity was observed under physiological conditions, which is quite different from previous studies, which were mainly based on sensory deprivation (Toldi et al., 1994; Angelucci et al., 1997; Piche et al., 2007). In the case of sensory loss, crossmodal plasticity is more appropriately termed compensatory plasticity (Bavelier and Neville, 2002), since it is characterized by an improvement in the spared sensory modalities, based on functional recruitment of neural structures left unused by the lost modality. Instead, EE acts on the physiological properties of brain to modulate the expression of plasticity mechanisms, not causing an improvement in the absolute performance of a given sensory system (Sale et al., 2009), but rather affecting the activity pattern of cerebral areas (present work).

The crossmodal effect described here could also contribute to explain the great influence of EE on visual system physiology, which arrives to promote recovery from amblyopia (Sale et al., 2007b), which appears surprising when considering that vision is not the preferred sensory modality of rodents. This could be, at least in part, explained by the fact that M2/fef is connected with primary motor cortex (Guandalini, 1998) and could thus represent a "bridge" to convey to V1 information about changes in motor activity that might contribute to mediate plasticity.

It would be of interest to investigate whether the effect of EE on crossmodal plasticity can be simulated by acute electrical stimulation of these cortical areas, which would point to the involvement of activity-dependent mechanisms, such as long-term potentiation or depression

of corticocortical connections. Another intriguing experiment would be to block activity in one cortical area -*e.g.* A1- during EE, to investigate how correlation of activity with other connected regions -*e.g.* V1- is affected. Taking into account the clinical data on sensory loss, which describe the functional takeover of the deprived area by spared sensory modalities (Sadato et al., 1996; Finney et al., 2001), it can be hypothesized that the blocked area would express an increased correlation with connected regions.

The existence of a crossmodal effect of EE, raises the possibility that an important role in functional recovery of vision could arise from inputs from other cortical areas, whose activity is stimulated by EE. This could also be important for designing new "crossmodal"functional rehabilitation procols to enhance recovery from neurological lesions.

5. APPENDIX

A SENSITIVE PERIOD FOR ENVIRONMENTAL REGULATION OF EATING BEHAVIOUR AND LEPTIN SENSITIVITY

5.1 ABSTRACT

Western life style contributes to body weight dysregulation. Leptin downregulates food intake by modulating the activity of neural circuits in the hypothalamic arcuate nucleus (ARC) and resistance to this hormone is considered a permissive condition for obesity. Physical exercise modulates leptin sensitivity in DIO rats. The role of other life style components in modulating leptin sensitivity remains elusive.

Environmentally enriched (EE) mice were employed to explore the effects of life style change on leptin production/action and on other metabolic parameters. I analyzed: 1) adult mice exposed to EE. These showed decreased leptin, reduced adipose mass and increased food intake; 2) and 3) 50 days old mice exposed to either EE (YEE) or physical exercise (YW) since birth. They both showed decreased leptin. YEE showed no change in food intake, increased response to leptin administration and increased activation of STAT3 in the ARC. YW leptin-induced food intake response was intermediate between YST and YEE. YEE exhibited also an increased and decreased ratio of excitatory/inhibitory synapses onto α-MSH and AgRP neurons of the ARC, respectively; 4) animals as described in 2) and then placed in standard cages for one month. They showed no alterated leptin production/action, but presented changes in the excitatory/inhibitory synaptic contacts in the ARC similar to YEE. EE and physical activity resulted in improved insulin sensitivity.

In conclusion, EE and physical activity impacted on feeding behaviour, leptin production/action, insulin sensitivity, and EE affected ARC circuitry. The leptin-hypothalamic axis is maximally enhanced if environmental stimulation is applied during development.

5.2 INTRODUCTION

It is widely accepted that the prevalent life style model of western societies characterized by limited physical activity, excessive caloric intake, but also repetitive behavioural patterns contributes to the dysregulation of the otherwise homeostatic control of body weight (BW) (Coppari et al., 2009). Main player in this system is leptin, a hormone secreted in the periphery by fat cells (Zhang et al., 1994), that signals the status of body energy stores, downregulates feeding behaviour and promotes energy expenditure by activating signal transduction mediated by the Janus Kinase-signal transducers and activators of transcription pathway (JAK-STAT) in the arcuate nucleus of the hypothalamus (ARC), through its receptor (Ob-Rb). This in turn promotes excitation and inhibition of neurons expressing, respectively POMC, precursor of the most potent anorexigenic peptide ◎-Melanocyte Stimulating Hormone (MSH), and the orexigenic peptides Agouti Related Peptide (AgRP)/NPY (Elmquist and Flier, 2004; Pinto et al., 2004).

Such seemingly clear view of the complex regulation of feeding behaviour and BW is challenged by the fact that the majority of obese people exhibit high levels of circulating leptin (Maffei et al., 1995), to which they are apparently resistant. Leptin resistance is emerging as a permissive condition for obesity (Friedman, 2009) and efforts to enhance leptin sensitivity could be determinant in the treatment and in the prevention of this disorder.

Leptin resistance, often reported in standard housed mice (Scarpace and Zhang, 2009) especially if obese, was partially rescued by genetic modifications (5) or physical exercise (Patterson et al., 2009). However, mice employed in the studies investigating leptin regulation and action are usually reared in standard conditions that allow little physical activity and limited sensorial, emotional and cognitive stimulation. This certainly impinges on several metabolic functions, as Martin et al. (Martin et al., 2010) conclude from a meta-analysis of health

conditions of standard housed mice versus physically exercised or diet restricted ones. What is not as yet clear is whether rearing factors other than diet or locomotor activity may affect metabolism in rodents as several evidences indicate in humans. Indeed depression, anxiety, solitude, frustration, boredom, are considered important determinants of human emotional eating (van der Merwe, 2007; Luppino et al.), often leading to metabolic disorders

In this part of my work, I asked whether multifaceted modifications of the environment might influence metabolism and leptin sensitivity in wild type not obese animals. To address this issue I exposed mice to environmental enrichment (EE), a manipulation of the rearing environment including enhanced physical activity, sensory, cognitive, and social stimulation (van Praag et al., 2000), that exerts important effects on experience-dependent plasticity, including adult neurogenesis and synaptic connectivity (van Praag et al., 2000). To disentangle the contribution of locomotor activity from the other EE components, the effects of EE were compared with those of voluntary physical exercise alone.

My findings demonstrate for the first time that EE has an effect on glucose tolerance, feeding behaviour, and leptin sensitivity; this third aspect is observed only if EE is applied since birth. In the ARC of young mice these effects are associated with increased leptin receptor expression, enhanced activation of the STAT3 pathways and a shift of the excitation/inhibition balance towards the former in α-MSH neurons, and towards the latter in AgRP/NPY neurons. Intriguingly, also physical activity impacted on feeding behaviour, leptin production/action, and EE affected ARC circuitry.

5.3 MATERIALS AND METHODS

5.3.1 Animals

All animal protocols were approved by the local ethical committee. The experimental protocols followed the Principles of Laboratory Animal Care and a specific authorization was issued by Italian Ministry of Education (document number 129/2000-A) to CNR Neuroscience Institute, where animals were housed. C57/BL6 male mice were raised in our in-house colony and used for all studies. Four experimental groups were analysed: 1) young mice, referred to as YEE, born in EE and sacrificed at postnatal day (P) 50; 2) adult mice, referred to as AEE, moved to EE cages at P50 and sacrificed at P80; 3) mice born in EE, transferred to a standard cage at P50, and monitored until P80, referred to as EE/ST; 4) young mice, reared since birth with free access to a running wheel, referred to as YW. Each group was compared with standard animals, namely AST, YST and ST/ST.

Enriched environment consisted of a large cage (44 x 62 x 28 cm) with a wire mesh lid containing several food hoppers, a running wheel, and differently shaped objects (tunnels, shelters, stairs) that were repositioned once per day and completely substituted with others once per week. Every cage housed at least two dams, 10 pups, and two additional filler females. At weaning (P25), the females were moved to a different cage. A running wheel was installed on the lid of a standard cage for running wheel experiments. Standard environment consisted of a standard laboratory cage (26 x 42 x 18 cm) housing a maximum of 4 animals.

In both environmental conditions food and water were available *ad libitum*. Food intake was monitored every other day, whereas body weight measurements were obtained on a weekly basis. For the all the experimental groups, monitoring of BW and food intake started from weaning (P22). At sacrifice, brain, epigonadal white adipose tissue (WAT) and liver from each animal were dissected and processed for subsequent analisys.

5.3.2 Blood collection and plasma assays

Blood samples were taken from the tail vein of 2hr-fasted animals, collected in EDTA-coated tubes and centrifuged in a refrigerated microfuge. Plasma was collected and stored at -20°C for subsequent assays.

Plasma glucose was measured with a One-Touch Ultra glucometer (LifeScan, Milpitas, CA). Commercial ELISA kits were used to assess plasma levels of insulin (Linco Research, Inc., St. Charles, MO, USA) and leptin (R&D Sistems, Minneapolis, MN, USA).

5.3.3 IpGTT and AUC parameter

For intraperitoneal glucose tolerance tests (IpGTT), mice were fasted (given water only) for 2 h and then injected intraperitoneally (ip) with 1mg glucose/g of body weight. Blood glucose was measured via tail vein bleeds at 0, 15, 60 and 120 minutes post injection using a One-Touch Ultra glucometer (LifeScan, Milpitas, CA). Total area under curve (AUC) was calculated using the trapezoid model, as an indication of insulin sensitivity.

5.3.4 Acute leptin injection

At the end of the EE or standard rearing period, leptin sensitivity of young animals was assessed. One hour prior to dark onset, food was removed. At dark onset (7 pm) mice received an intraperitioneal injection of saline or murine leptin (Sigma, 3 mg/kg in 0.3 ml of PBS), and were individually caged and given weighted chow food. Food intake was monitored 14 hours after injection .

5.3.5 Isolation of total RNA and real time PCR

Total RNA was isolated from frozen tissues (epiWAT and hypothalami from A and Y mice) with Tripure (Roche Molecular Biochemicals) or from formaline-fixed tissues (hypothalami from Y and EE/ or ST/ST animals) with Agentcourt FormaPure Tube starter kit (Beckman Coulter). Its integrity was evaluated on a formaldehyde denaturing agarose gel. RNA was then treated with Rnase-free Dnase (Roche Molecular Biochemicals) to remove any contaminating genomic DNA. First-strand cDNA synthesis was performed using oligo hexamers (Pharmacia) (see ref. 31 for detailed protocols).

Taq-Man quantitative PCR (50 °C for 2 min, 95 °C for 10 min, followed by 40 cycles of 95 °C for 15 s 60 °C for for 1 min) was performed to amplify samples for leptin, SOCS3, ObRb, NPY, POMC and BDNF (protein coding exon). The relative abundance of mRNAs was calculated with TATA Binding Protein (TBP) mRNA as the invariant control. The assays were all purchased from Applied Biosystems (Switzerland).

5.3.6 Immunofluorescence

Animals were fasted for 2 hours before receiving 3 mg/kg i.p. leptin and 45min later they were anaesthetized with an overdose of Chloral Hydrate. Then, they were transcardially perfused with phosphate buffered saline, followed by 4% paraformaldehyde in 0.1M phosphate buffer (PB). Brains were quickly removed from the skull and post- fixed in the same fixative at 4°C for 4 h, then sunk in 30% sucrose in 0.1M PB at 4 °C. After cryoprotection, brains were frozen in isopenthane and stored -80 °C. 40μm-thick coronal sections comprising the ARC were cut on a cryostat (Leica, Germany) and processed for immunofluorescence.

For vGAT and vGluT2 immunofluorescence, free-floating sections were blocked for 2h at RT in 0.3% Triton X-100, 10% BSA in PBS, then incubated O/N at 4°C with 1:1000 rabbit anti-

mouse vGAT or vGluT2 antibodies (Synaptic Systems, Germany) diluted in 0.1% Triton X-100, 1% BSA in PBS. Sections were then revealed with 1:400 goat anti-rabbit secondary antibody conjugated to Alexa-568, diluted in 0.1% Triton, 1% BSA in PBS, for 2.5h at RT. For STAT3 and phosphoSTAT3 (pSTAT3) , sections were permeabilised in 100% Methanol at 4°C for 5min before blocking. The primary antibodies used were 1:250 rabbit anti-mouse STAT3 (Cell Signaling Technologies, USA) and 1:250 rabbit anti-mouse pSTAT3 (Cell Signaling Technologies) and incubation was O/N at 4°C. Sections were then revealed with the same secondary antibody solution described above. For double immunofluorescence experiments, free-floating sections were prepared and incubated with blocking solution as above, then reacted with 1:1000 anti-αMSH sheep primary antibody (Calbiochem, USA) or 1:1000 anti-AgRP guinea pig primary antibody (AbCam, UK), together with 1:1000 anti-vGluT2 or 1:1000 anti-vGAT rabbit primary antibodies, O/N at 4°C. The secondary antibodies used were 1:400 goat anti-rabbit Alexa-568, 1:400 donkey anti-sheep Alexa-488 (Molecular Probes, USA) and 1:200 donkey anti-guinea pig DyLight-488 (Jackson ImmunoResearch, USA); incubation lasted 2.5h at RT. Stained sections were mounted on glass slides, air-dried, soaked with VectaShield mounting medium (Vector Labs., USA) and covered with coverslips, then stored at 4°C in darkness to preserve fluorescence signal.

5.3.7 Quantitative analysis of immunolabeled cells and puncta

For each group of immunofluorescence sections, optimal acquisition parameters (photomultiplier gain, intensity offset, laser excitation intensity) were adjusted at the beginning of each experiment and held constant.

For quantification of pSTAT3- and STAT3-immunostained sections, at least 5 images for each experimental case were acquired with an Olympus confocal laser-scanning microscope

(Olympus, Japan), using the FluoView software (Olympus). A 40X oil objective (n.a.=1.3) guaranteeing coverage of the whole extension of each half of the ARC was used. The brightest focal plane for each section was chosen and images from this one, plus the two adjacent focal planes (z-step 1μm) were acquired. pSTAT3 and STAT3 images were stacked and the number of immunoreactive cells manually counted using the MetaMorph software (Universal Imaging Corp.,USA), with the operator blind to the experimental case. Given that the ARC changes its area on the rostrocaudal axis, the area of the ARC in each section was measured and used to normalize cell counts. For vGAT and vGluT2, a 60X oil objective (n.a.=1.4) was used, with a 2.5 digital zoom. To achieve an optimal resolution on the z axis, 15 sequential focal planes, spaced 0.125μm, were acquired. Each focal plane was then saved as a single TIFF image file in 8bit-grayscale mode. For vGAT and vGluT-2 immunoreactive puncta analysis, the images were processed using the "spots" function of the Imaris software (Bitplane, Switzerland). The "Spot quality threshold" and "minimum spot diameter" parameters were manually adjusted to optimize puncta detection, with the operator blind to the experimental case. The "minimum spot diameter" was kept constant for all cases. For double immunofluorescence quantification, single-cell images were acquired using a 60X oil objective and a 7.5 digital zoom. The number of focal planes, spaced 0.125μm, was adjusted to comprise the entire extension of the cell soma on the z axis. The number of vGluT2-or vGAT immunoreactive contacting the soma of AgRP or α-MSH positive neurons was manually counted using the MetaMorph software. Each punctum was considered to contact the cell soma when it was comprised within a distance of 1μm from it.

5.3.8 Statistical analysis

The number of mice in each experimental group is indicated in the figure legends. All values are expressed as means ± SEM. Pairwise comparisons of quantitative phenotypes between mice of different groups (e.g. ST versus EE) were assessed by 2-tailed Student's t-test. When more than 2 groups were analyzed, 1-way ANOVA and 2-way ANOVA followed by Bonferroni post-hoc for selected comparisons (e.g. ST vs EE saline- or leptin-injected) were used. For immunofluorescence analyses, the cell count value obtained for each experimental case was normalized on the average value of the control group (ST injected with saline) to obtain the relative percentage of the group respect to the control. Statistical evaluation of results was performed using GraphPad Prism version 3.00 for Windows (GraphPad Software, San Diego, CA).

5.4 RESULTS

5.4.1 Environmental enrichment (EE) effect on metabolism and feeding behaviour in adult mice.

Exposure of male adult mice (P50) to EE for 4 weeks (wks) resulted in no significant difference in BW (Table 5.1). A significant difference was evidenced in the weight of the fat depots, with AEE mice showing significantly lower values for this parameter as compared to adult mice reared in standard conditions (AST) (Table 5.1). No difference was found in the weight of other metabolically active organs including liver and brown adipose tissue (BAT) (Table 5.1).

Table 5.1 Metabolic assessment in adult ST and EE mice.

	AST (n=16)	AEE (n=14)	
Body weight (g)	25.7±0.6	25.4±0.4	
Weight gain P50-P80 (g)	1.74±0.42	1.99±0.37	
Fat pad (epidyd+ perirenal) (mg)	397±26	326±14	*
Liver (g)	1.29±0.04	1.25±0.05	
BAT (mg)	121±15	115±11	
Leptin (pg/ml)	1222±93	927±111	*
Leptin / fat pads (pg/ml/mg)	3.2±0.22	2.9±0.3	
Average food intake (g/mouse/day)	3.15±0.06	3.61±0.05	***
Fasted insulin (ng/ml)	0.72 ±0.05	0.71±0.16	
Fasted glucose (mg/dl)	124.7±5.0	138.7±5.	

t-test *P<0.05, ***P<0.001

Plasma leptin measured at the end of the EE rearing period was lower in AEE mice as compared to AST (Fig. 5.1A). When the individual leptin levels at 4 wks were normalized for the corresponding weight of the fat pads, no significant difference between the AEE and AST could be observed (Table 5.1), suggesting that the reduction in serum leptin likely results from the decrease in the adiposity herein described for the EE mice. When leptin mRNA abundance was assessed in the epididymal WAT of AEE and AST no significant difference was found (Fig 5.1B).

Lowering the levels of circulating leptin may result in increased food intake. Indeed average food intake was significantly higher (Table 5.1) in the AEE mice as expected in an animal exposed to a higher physical activity.

AEE showed similar insulin levels and moderately decreased levels of fasting glucose as compared to standard mice (Table 5.1). When an intra-peritoneal glucose tolerance test (IpGTT) was performed (Fig 5.1C), a significant increase in insulin sensitivity was observed (Fig 5.1D).

Taken together these data indicate that in the adult mouse EE improves glucose tolerance, reduces adipose mass, increases food intake and downregulates leptin production.

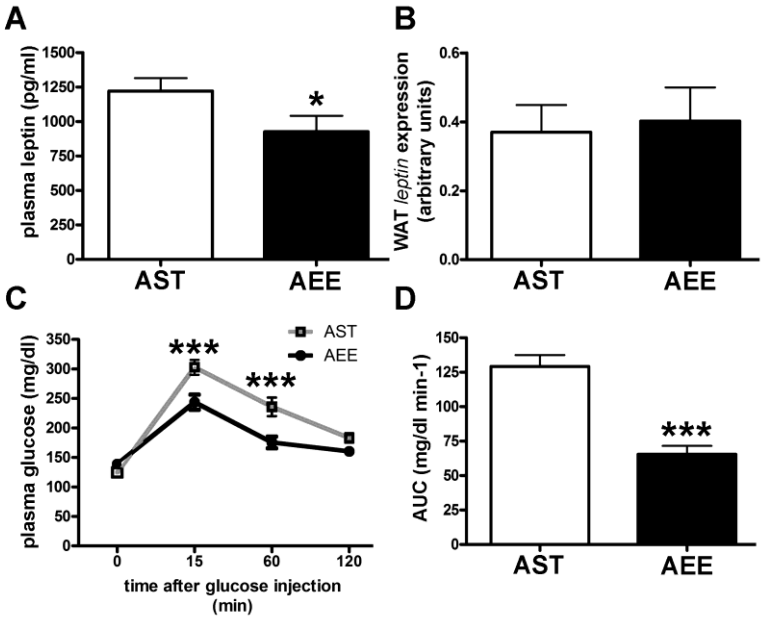

Figure 5.1 Effect of EE on leptin expression and glucose tolerance in adult mice. A) Plasma leptin at the end of EE in AST (n= 16) and AEE (n= 14; *t*-test P<0.05). B) WAT *leptin* gene expression in AST (n=11) and AEE (n=10). C) IpGTT at the end of EE in AST (n=11) and AEE (n=10; 2-way ANOVA, rearing effect P<0.001, time effect P<0.001, Bonferroni *post-hoc* test AST *vs* AEE P<0.001). D) AUC values (mg/dL min^{-1} over a 120-min test) for the glycemic responses of AST and AEE mice shown in C) (*t*-test P<0.001).

5.4.2 EE effect on metabolism and feeding behaviour in young mice.

To evaluate the effects of EE during development on metabolism and leptin production/action, I monitored a group of mice born in EE conditions (YEE) and sacrificed at P50. Yoked control mice were kept in standard conditions (YST). The weights of body, liver and BAT were identical in YEE and YST. No difference was evidenced in the weight of the gonadal fat pad (Table 5.2).

YEE mice showed similar plasma insulin and slightly lower level of fasting glucose (Table 5.2), and performed better during the IpGTT (Fig. 5.2A, B). Plasma leptin was lower in YEE than in YST, even when normalized to the weight of fat pads (Fig. 5.3A, B, Table 5.2). Abundance of WAT leptin mRNA was then assessed by real time PCR in WAT of YEE and YST but no

statistically significant difference was found (Fig. 5.3C). Other post transcriptional mechanisms could explain the different leptin levels in YEE mice. For instance, Ceccarini et al. (Ceccarini et al., 2009) reported that leptin uptake by megalin in the kidney and its binding to red bone marrow importantly accounts for its biodistribution, and may contribute to explain variation in its plasma levels. The diminished level of circulating leptin observed in YEE was not associated with increase in food intake (Fig. 5.3D).

These data indicate that during development EE has a positive effect on glucose tolerance, no effect on adipose mass or food intake, and reduces leptin production.

Table 5.2 Metabolic assessment in young ST and EE mice.

	YST (n=34)	YEE (n=37)
Body weight (g)	21.73±0.40	21.79±0.35
Weight gain P22-P50 (g)	12.97±0.45	11.43±0.48
Fat pad (epididymal) (mg)	208±10	213±11
Liver (g)	1.28±0.05	1.28±0.06
BAT (mg)	96±11	81±9
Leptin (pg/ml)	1406.6± 160.52	1010.0± 81.86 *
Leptin / epididymal fat pad (pg/ml/mg	7.09± 0.74	4.73± 0.42 **
Fasted Insulin (ng/ml)	0.65±0.1	0.53±0.07
Fasted Glucose (mg/dl)	159.8±6.87	141.9±6.60

t-test *P<0.05, **P<0.01

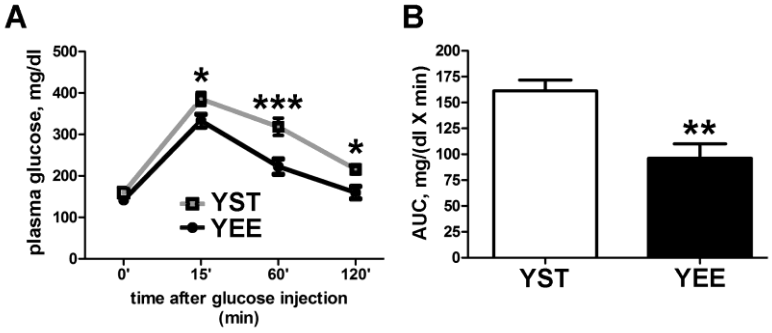

Figure 5.2 Improved glucose tolerance in young mice at the end of EE. A) IpGTT at the end of EE in YST (n=19) and YEE (n=15); 2-way ANOVA, rearing effect P<0.001, time effect P<0.001, Bonferroni *post-hoc* test YST *vs* YEE, * P<0.05, ***P<0.001). B) AUC values (mg/dL min^{-1} over a 120-min test) for the glycemic responses of YST and YEE mice shown in A) (*t*-test P<0.002).

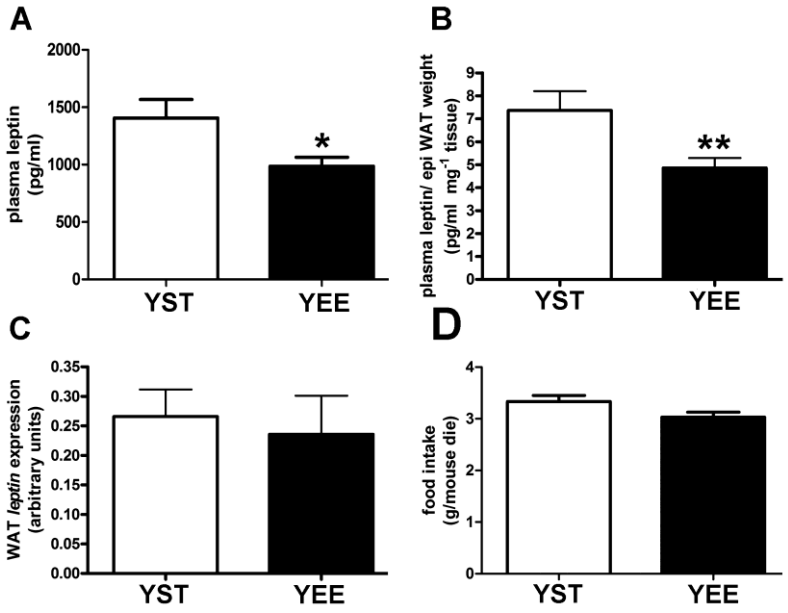

Figure 5.3 Effect of EE on metabolic parameters in young mice. A) Plasma leptin is decreased in YEE (n=37) compared to YST (n=34; *t*-test P<0.05). B) Plasma leptin /epididymal fat weight (pg/ml mg^{-1} tissue) for YST and YEE (*t*-test P<0.01). C) *Leptin* gene expression in epidydimal WAT of YST (n=19) and YEE (n=17). D) Average food intake in YST and YEE mice.

5.4.3 EE effect on leptin response and hypothalamic gene expression in young mice.

I then analyzed the effect of leptin administration on food consumption. Food intake assessed 14 hours after injection of leptin or vehicle was reduced by 38% in YEE, and by 13% in YST (as compared to corresponding vehicle-treated animals) (Fig. 5.4A). The relatively small reduction of food intake measured in YST should not surprise given that leptin effects in wild type animals on food intake are often cumulative and become significant only after 2-3 days of chronic treatment (Zhang et al., 2008). The effect of EE was then investigated on the hypothalamic expression of genes directly implicated in eating behaviour. These included: the long isoform of leptin receptor (Ob-Rb), the orexigenic peptide NPY, the α-MSH precursor POMC and orexin. Real time PCR revealed no significant difference in the abundance of POMC and NPY transcripts between YEE and YST, while Ob-Rb and orexin expression was upregulated in YEE (Fig. 5.4B).

Next I asked whether the activation state of molecules involved in leptin signalling might differ between the 2 groups. Upon leptin injection the number of pSTAT3-positive neurons in the ARC was strongly upregulated by EE (Fig. 5.4C). In particular leptin stimulation resulted in STAT3 phosphorylation in 72% of STAT3 positive cells in YEE (234% of saline treated), whereas in YST pSTAT3 was activated only in 38% of STAT3 positive neurons (190% of saline treated). No significant difference was found in the number of neurons expressing STAT3 in YEE and YST (Fig. 5.4D).

These data are consistent with the above stated hypothesis that EE increases leptin sensitivity in young mice.

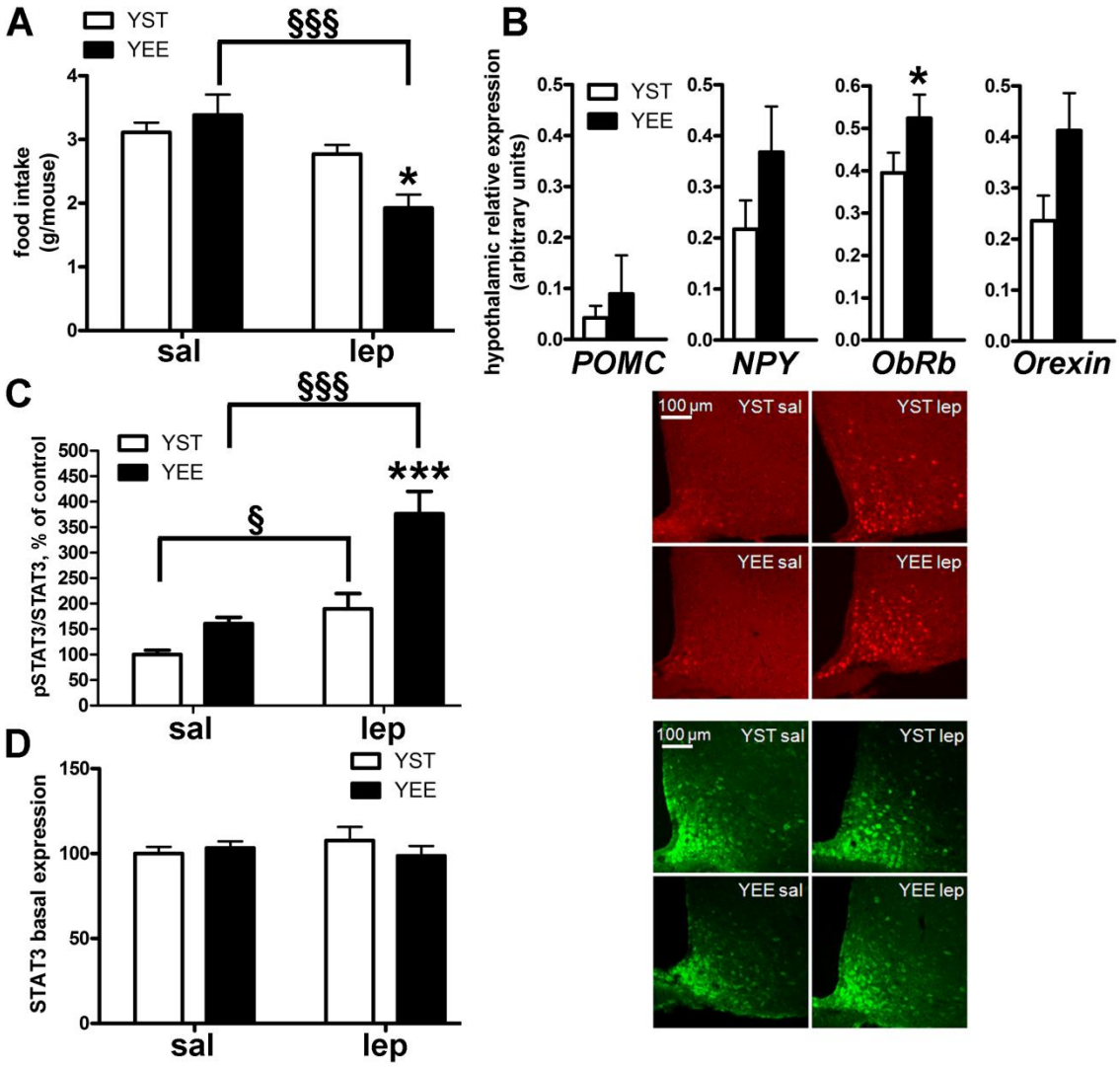

Figure 5.4 EE enhances response to exogenous leptin administration in young mice. A) Food intake assessed 14 hours after ip leptin injection in YST and YEE. (2-way ANOVA, treatment effect P<0.01, interaction P<0.05; Bonferroni *post-hoc* tests: YST *vs* YEE, *P<0.05; saline *vs* leptin §§§P<0.001). B) Hypothalamic gene expression in YST (n=15) and YEE (n=13; *t*-test P<0.05). C) *Left*, histogram showing the ratio of pSTAT3 positive cells to the total number of STAT3 positive neurons 45 min after leptin or saline injection in the ARC of YST (saline n=8, leptin n=6) and YEE (saline n=7, leptin n=6; 2-way ANOVA, rearing effect P<0.001, treatment effect P<0.001, interaction P=0.037; Bonferroni *post-hoc* tests: YST *vs* YEE ***P<0.001; leptin *vs* saline §P<0.05, §§§P<0.001). *Right*, representative immunofluorescence showing pSTAT3 activation in the ARC after saline or leptin injection. D) *Left*, total number of STAT3-positive neurons in the ARC of YEE and YST after saline or leptin injection (2-way ANOVA NS). *Right*, representative immunofluorescence showing STAT3 expression in the ARC of YEE and YST.

5.4.4 EE effect on ARC synaptic connectivity in young mice.

Considering that fasting and genetic leptin deficiency affect energy balance also by significantly interfering with the synaptic plasticity of the ARC (Bouret et al., 2004; Pinto et al., 2004; Sternson et al., 2005) I analyzed whether EE impacts on ARC synaptic organization.

In the cerebral cortex and in the hippocampus (Mora et al., 2007), EE modifies synaptic organization of neural circuits, and enhances the expression of Brain Derived Neurotrophic Factor (BDNF) (Sale et al., 2009) a neurotrophin important for synaptic plasticity. When hypothalamic BDNF expression was assessed, I found significantly increased level in YEE as compared to YST (Fig. 5.5A).

I then searched for modifications in the neural circuitry of the ARC. To this end I assessed the number of excitatory and inhibitory synapses in YEE and YST by immunofluorescence, counting the puncta labelled with the specific markers vGluT2 and vGAT corresponding to excitatory and inhibitory synaptic terminals, respectively. I found that in the ARC of YEE the number of excitatory synaptic terminals is significantly higher than in YST and the number of inhibitory synaptic terminals is reduced (Fig. 5.6A, B), thus lowering the ratio between excitatory and inhibitory synapses (Fig. 5.6C).

I next asked if excitatory and inhibitory synapses on neurons expressing α-MSH and AgRP were differentially affected by EE by double immunolabeling for α-MSH or AgRP and vGluT2 or vGAT. As shown in figure 5.5B ratio of vGluT2/vGAT positive puncta is significantly higher on α-MSH positive neurons of YEE as compared to YST. On the other hand, YEE exhibit a significantly lower ratio of vGluT2/vGAT positive puncta on AgRP neurons (Fig. 5.5C). The YEE effects observed with the ratio are recapitulated by the absolute numbers of immunoreactive puncta in each of the 4 double immunofluorescence experiments shown in Fig. 5.7.

These data establish that upon EE young mice ARC undergoes a change in its overall synaptic connectivity and a cell specific alteration in neurons, that are key in the regulation of energy homeostasis.

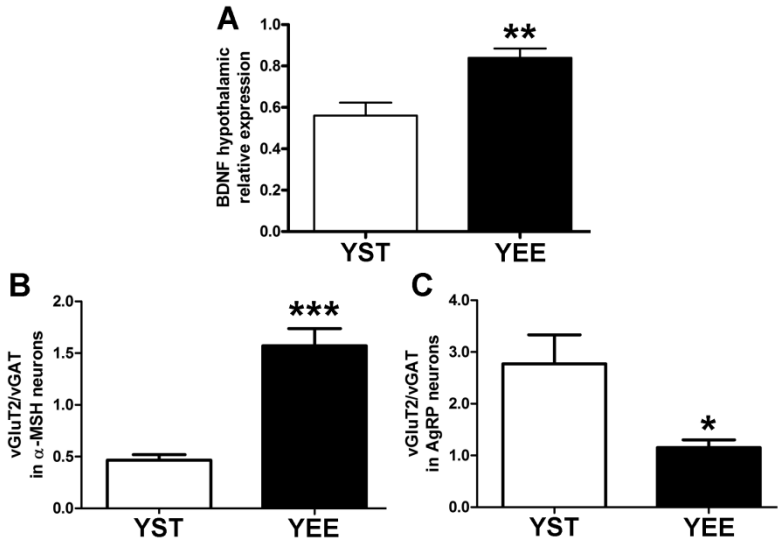

Figure 5.5 *BDNF* expression and excitation/inhibition ratio on α-MSH and AgRP neurons of YST and YEE mice. A) *BDNF* hypothalamic expression in YST (n=12) and YEE (n=7; *t*-test P<0.01). B) Histogram of the ratio between excitatory and inhibitory synapses on α-MSH neurons in the ARC of YEE (n=11) and YST (n=9), *t*-test P<0.001. C) Histogram of the ratio between excitatory and inhibitory synapses on AgRP neurons in the ARC of YEE (n=7) and YST (n=6) *t*-test P<0.05.

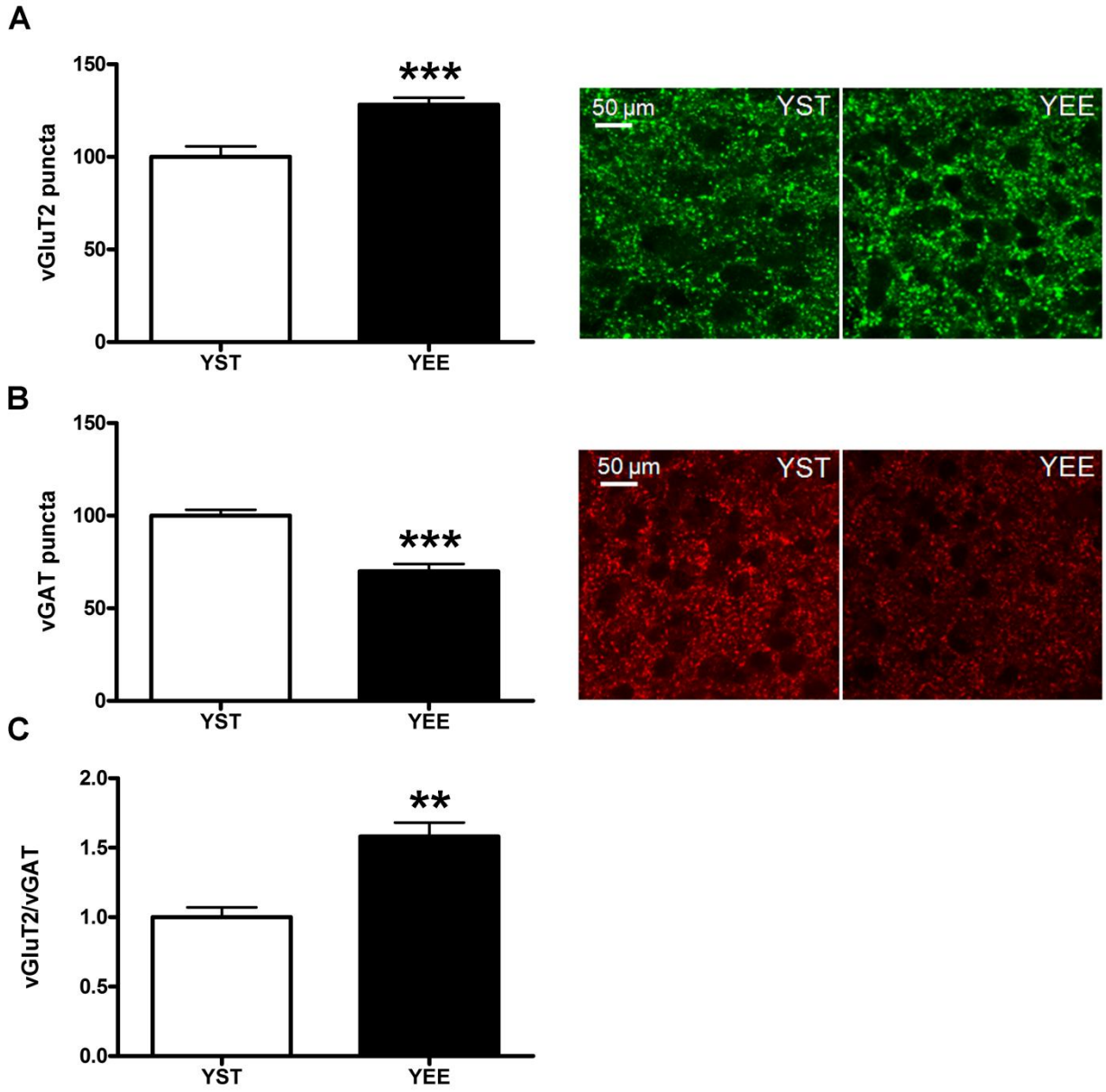

Figure 5.6 Synaptic connectivity in the ARC of YEE and YST mice. A) Left, increased total number of excitatory vGluT2-immunoreactive synapses in the ARC of YEE (YEE n=13, YST n=11; t-test P<0.001); right, representative immunofluorescence showing vGluT2 expression in the ARC of YEE and YST mice. B) Left, decreased total number of inhibitory vGAT-immunoreactive synapses in the ARC of YEE (t-test, P<0.001); right, representative immunofluorescence showing vGluT2 expression in the ARC of YEE and YST mice. C) increased ratio between excitatory and inhibitory synapses in the ARC of YEE mice compared to YST (t-test P<0.01).

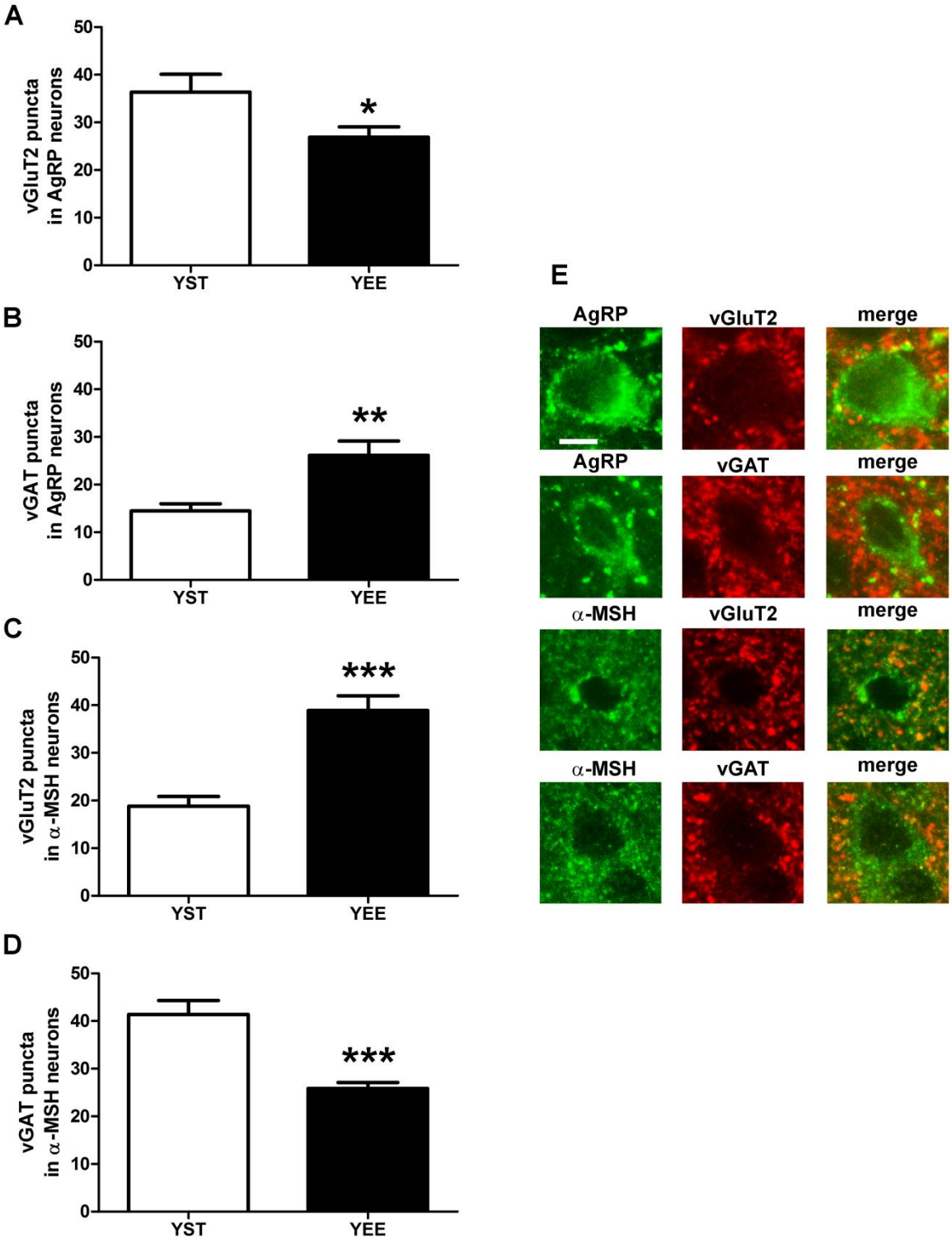

Figure 5.7 Excitatory and inhibitory synapses on α-MSH and AgRP neurons in the ARC of YEE and YST mice. A) Decreased number of excitatory vGluT2-immunoreactive synapses on AgRP neurons in the ARC of YEE (n=9) and YST (n=8), *t*-test P<0.05. B) Increased number of inhibitory vGAT-immunoreactive synapses on AgRP neurons in the ARC of YEE (n=7) and YST (n=6), *t*-test P<0.01. C) Increased number of excitatory vGluT2-immunoreactive synapses on α-MSH neurons in the ARC of YEE (n=11) and YST (n=9), *t*-test P<0.001. D) Decreased number of inhibitory vGAT-immunoreactive synapses on α-MSH neurons in the ARC of YEE (n=13) and YST (n=9), *t*-test P<0.001. E) Representative confocal microscopy images showing double immunofluorescence for AgRP or α-MSH (green) and vGluT2 or vGAT (red). Scale bar is 10μm.

5.4.5 How EE experienced during development affects metabolism and feeding behaviour in the adult.

I next asked whether EE effects could persist once animals are removed from this condition. Mice enriched since birth were then transferred to a standard cage at P50 and monitored until P80 (EE/ST). A group of controls (ST/ST) was kept in standard cages during the whole period.

Despite displaying similar BW at P50, the 2 groups diverged afterwards, in that EE/ST showed a higher weight gain between P50 and P80 ending up with a significantly higher weight as compared to ST/ST (Table 5.3). No difference was observed in the weight of epigonadal fat, BAT or liver (Table 5.3). ST/ST and ST/EE showed similar level of fasting glucose and insulin (Table 5.3). IpGTT and AUC calculation revealed a significantly improved glucose tolerance in EE/ST as compared to ST/ST mice (Fig. 5.8A, B).

The increased BW observed in EE/ST can be explained considering that they ate significantly more between P50 and P80 (Fig. 5.8C). Interestingly, food intake increased abruptly after animal transfer to standard rearing. This sharp change of food consumption was associated with a concomitant rise in leptin levels, that increased 3 days after the transition from EE to ST conditions (P53) with respect to the levels observed one day before the end of EE (P49, Fig. 5.8D). ST/ST did not show significantly increased leptin over this time window. At P80 there was no difference in plasma leptin between EE/ST and ST/ST (Table 5.3).

Taken together, these data indicate that EE experienced during developmental age leaves a metabolic imprint on the adult mouse, that shows enhanced glucose tolerance.

Table 5.3 Metabolic assessment in EE/ST and ST/ST mice.

	ST/ST (n=12)	EE/ST (n=19)	
Body weight (g)	25.1±0.5	27.3±0.6	**
Weight Gain P50-P80 (g)	1.55± 0.36	3.97± 0.36	***
Fat pad (epididymal) (mg)	0.38±0.02	0.35±0.02	
Liver (g)	1.52±0.07	1.57±0.06	
BAT (mg)	98±8	103±6	
Leptin (pg/ml)	2259±209	2106±148	
Leptin /epididymal fat pad (pg/ml/mg)	6.38±0.51	7.13±0.78	
Average food intake (g/mouse/day)	3.64±0.06	4.29±0.06	***
Fasted Insulin (ng/ml)	0.71±0.16	0.67±0.17	
Fasted Glucose (mg/dl)	162.6±6.	154.4±5.1	

t-test **P<0.01, ***P<0.001

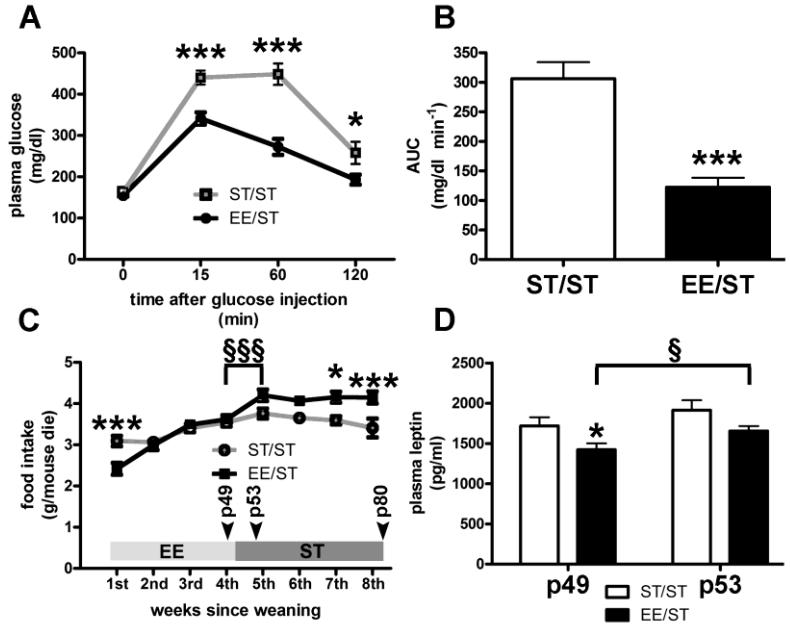

Figure 5.8 How EE experienced in the youth affects food intake and metabolic parameters in adulthood. A) IpGTT in ST/ST (n=13) and EE/ST (n=19): 2-way ANOVA, rearing effect P<0.0001, time effect P<0.0001, interaction, P<0.0001; Bonferroni *post- hoc* test, ST/ST *vs* EE/ST *P<0.05, ***P<0.001). B) AUC values (mg/dL min^{-1} over a 120-min test) for the glycemic responses of ST/ST and EE/ST shown in A) (t-test P<0.001). C) Weekly food intake of ST/ST and EE/ST over the 8 post-weaning wks. Bar indicates rearing condition over time. (2-way ANOVA, rearing effect P<0.01, time effect P<0.0001, interaction P<0.0001; Bonferroni *post-hoc* tests: ST/ST *vs* EE/ST, * P<0.05, ** P<0.01, *** P<0.001; Bonferroni *post-hoc* test applied to time course comparison §§ P<0.01. D) Plasma leptin at the end of EE (P49) and 3 days after moving to ST (P53) in EE/ST and ST/ST; 2-way ANOVA, time effect P<0.05, rearing effect P<0.01; Bonferroni *post-hoc* test, EE/ST *vs* ST/ST *P<0.05; Bonferroni *post-hoc* test applied to P49 *vs* P53 §P<0.05.

5.4.5 How EE experienced during development affects leptin response in the adult.

Food intake measured 14 hrs following leptin injection was not significantly different in P80 EE/ST and ST/ST (Fig. 5.9A). The assessment of leptin sensitivity in terms of STAT3 activation following leptin injection mirrored this scenario: EE/ST and ST/ST did not exhibit significant difference in the percentage of STAT3 positive neurons showing staining for pSTAT3 (Fig. 5.9B). No significant difference was found in the number of neurons expressing STAT3 in EE/ST and ST/ST (Fig. 5.9C).

These data show that EE effects on leptin sensitivity observed in the developing young animals do not persist through adulthood upon standard rearing conditions.

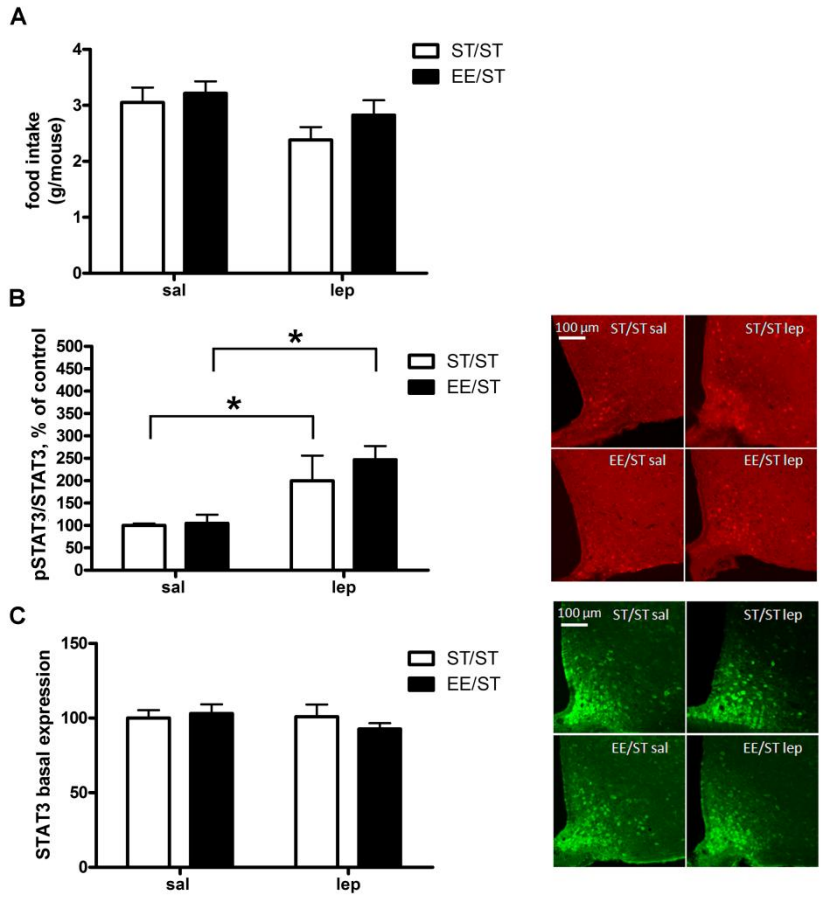

Figure 5.9 Leptin response of ST/ST and EE/ST mice. A) Food intake assessed 14 hours after ip leptin injection in ST/ST (n=12) and EE/ST (n=19). B) Histogram of the ratio of pSTAT3 positive cells to the total number of STAT3 positive neurons 45min after leptin or saline injection in the ARC of ST/ST (saline n=7, leptin n=5) and EE/ST (saline n=9, leptin n=10); 2-way ANOVA, rearing effect NS, treatment effect P<0.001, interaction NS; Bonferroni *post-hoc* test: leptin *vs* saline *P<0.05. C) Total number of STAT3-positive neurons in the ARC of EE/ST and ST/ST after saline or leptin injection; 2-way ANOVA NS.

5.4.6 How EE experienced during development affects ARC synaptic connectivity in the adult.

EE/ST mice showed a significantly lower number of inhibitory terminals (vGAT-positive) in the ARC with respect to ST/ST (Fig. 5.10B). No difference was found in the number of excitatory synaptic terminals (vGluT2-positive, Fig. 5.10A). The ratio between excitatory and inhibitory puncta was significantly higher in EE/ST as compared to ST/ST (Fig. 5.10C).

When neuron-specific investigations were performed, I found that only the reduction in vGAT puncta on α-MSH neurons and the increase in vGluT2 puncta on AgRP positive neurons were significant in EE/ST as compared to ST/ST (Fig. 5.11A, D). Nonetheless excitation/inhibition ratio for EE/ST was respectively higher in α-MSH (Fig. 5.12A) and lower in AgRP neurons (Fig. 5.12B). Hypothalamic BDNF gene expression was similar in EE/ST and ST/ST (0.63±0.14 and 0.55±0.05 arbitrary units)

These results indicate that ARC circuits retain a persistent, although attenuated, trace of the rearing condition experienced during development consisting in an altered ratio between excitatory and inhibitory synaptic density affecting both α-MSH and AgRP neurons.

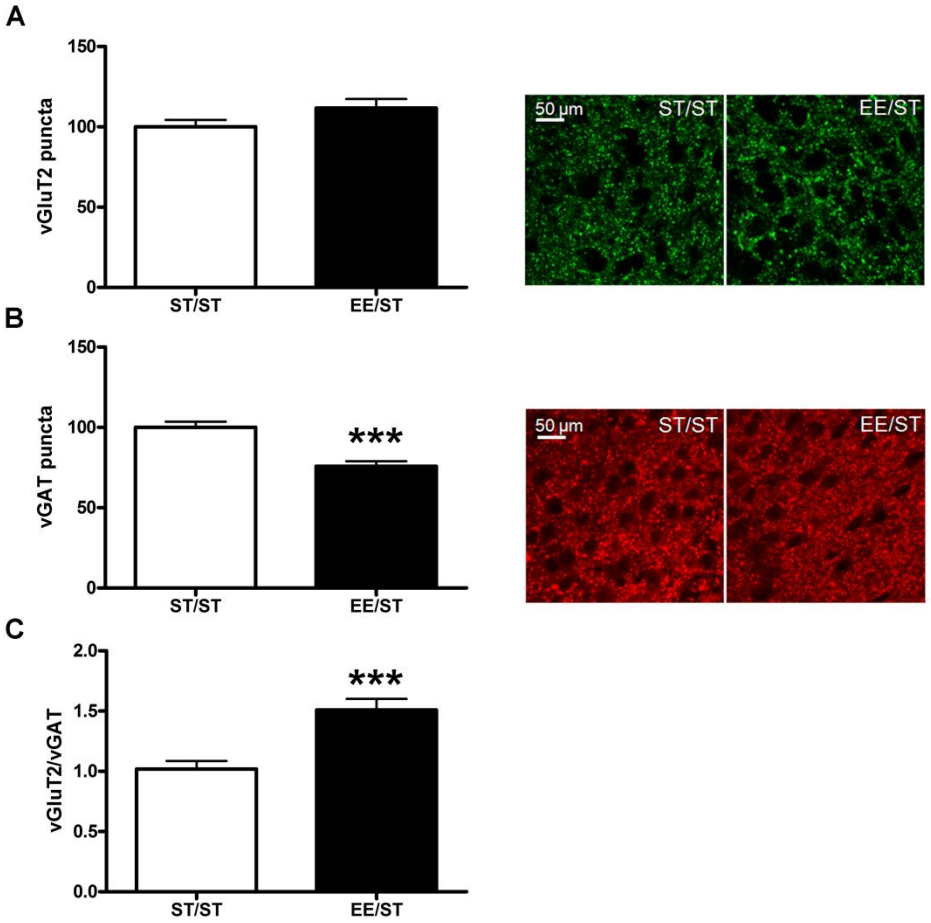

Figure 5.10 Synaptic connectivity in the ARC of EE/ST and ST/ST mice. A) *Left*, the total number of excitatory vGluT2-immunoreactive synapses in the ARC of EE/ST (n=12) and ST/ST (n=19) is not significantly different (*t*-test P=0.297); *right*, representative immunofluorescence showing vGluT2 expression in the ARC of EE/ST and ST/ST mice. B) *Left*, decrease in the total number of inhibitory vGAT-immunoreactive synapses in the ARC of EE/ST compared to ST/ST mice (*t*-test P=0.001); *right*, representative immunofluorescence showing vGAT expression in the ARC of EE/ST and ST/ST mice. C) Increased ratio between excitatory and inhibitory synapses in the ARC of EE/ST mice compared to ST/ST mice (*t*-test P<0.001).

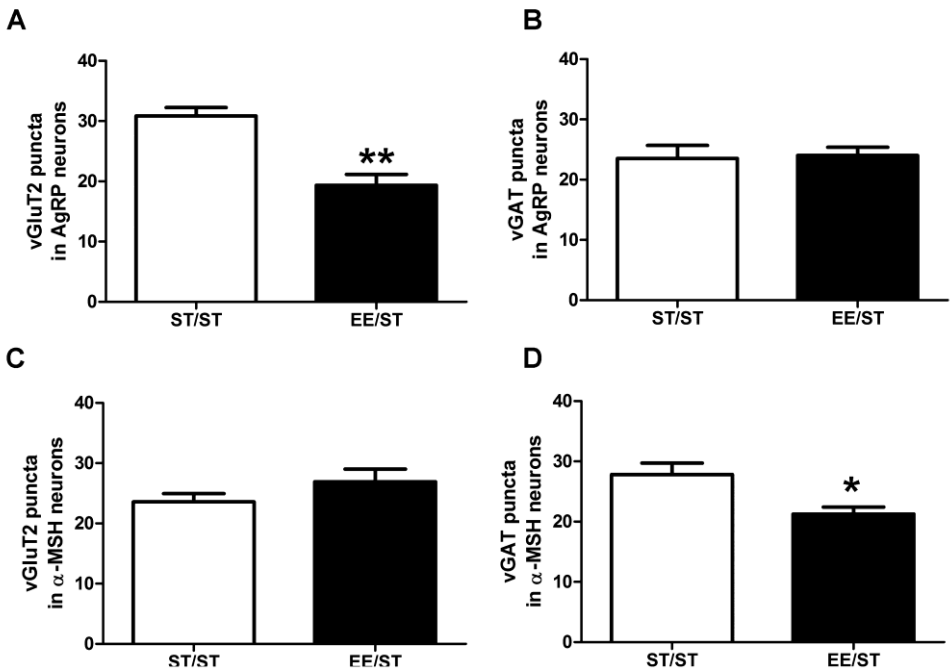

Figure 5.11 Excitatory and inhibitory synapses in α-MSH and AgRP neurons in the ARC of EE/ST and ST/ST mice. A) Decreased number of excitatory vGluT2-immunoreactive synapses in AgRP neurons in the ARC of EE/ST (n=4) mice compared to ST/ST (n=4) mice; *t*-test P<0.01. B) Lack of significant difference in inhibitory vGAT-immunoreactive synapses in AgRP neurons in the ARC of EE/ST and ST/ST mice. C) Lack of significant difference in excitatory vGluT2-immunoreactive synapses in αMSH neurons in the ARC of EE/ST and ST/ST mice. D) Decreased number of inhibitory vGAT-immunoreactive synapses in α-MSH neurons in the ARC of YEE mice (*t*-test P<0.05).

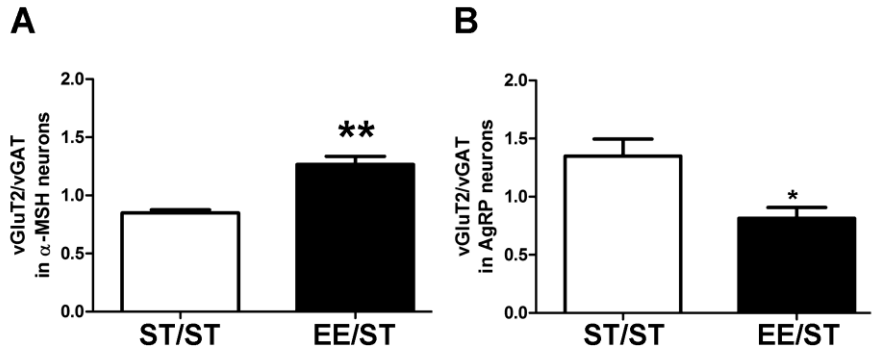

Figure 5.12 Excitation/inhibition ratio on α-MSH and AgRP neurons of ST/ST and EE/ST mice. A) Histogram showing the increase in the ratio between excitatory and inhibitory synapses on α-MSH neurons in the ARC of EE/ST (n=4) and ST/ST (n=4); *t*-test P<0.01. B) Histogram showing the decrease in the ratio between excitatory and inhibitory synapses on AgRP neurons in the ARC of EE/ST (*t*-test P<0.05).

5.4.7 Comparison between physical exercise and EE.

To assess whether in young mice the effects of EE on feeding behaviour, leptin production and responsiveness, glucose tolerance and synaptic organization of the ARC were simply due to enhanced physical activity, I studied how voluntary physical exercise (free access to a running wheel) by itself could impact on these parameters.

Young physically exercised mice (YW) did not show a significantly altered BW as compared to YEE or to YST, despite a trend towards an increased food intake (Fig. 5.13A). Their adiposity (weight of epididymal fat pad /BW) was lower than that observed in both YST and YEE (Fig. 5.13B). IpGTT revealed that, similarly to YEE, YW displayed a better glucose tolerance as compared to YST (Fig. 5.13D, E).

YW showed lower leptin concentration than YST (Fig. 5.13C). Leptin sensitivity assessed as food intake following leptin injection, was intermediate between that of YST and that of YEE. If I assume the leptin induced change in food intake in YST as 100%, a 200% change was observed in YW and a 300% in YEE (Fig. 5.13F). Following leptin injection, the ratio between pSTAT3 and STAT3 positive neurons in YW was similar to YST and lower than YEE. However if fold change from saline to leptin treatment are considered this parameter underwent a 2.55 fold change in YW, which is respectively similar and higher to what observed in YEE (2.34) and YST (1.9) (Fig. 5.13G).

Differently from what observed with EE, no effect of voluntary physical exercise was observed on the total number of excitatory and inhibitory synapses in the ARC (Fig. 5.13H).

Taken data together these data suggest that physical exercise by itself quantitatively accounts for only some of the changes in metabolism and leptin sensitivity observed upon EE.

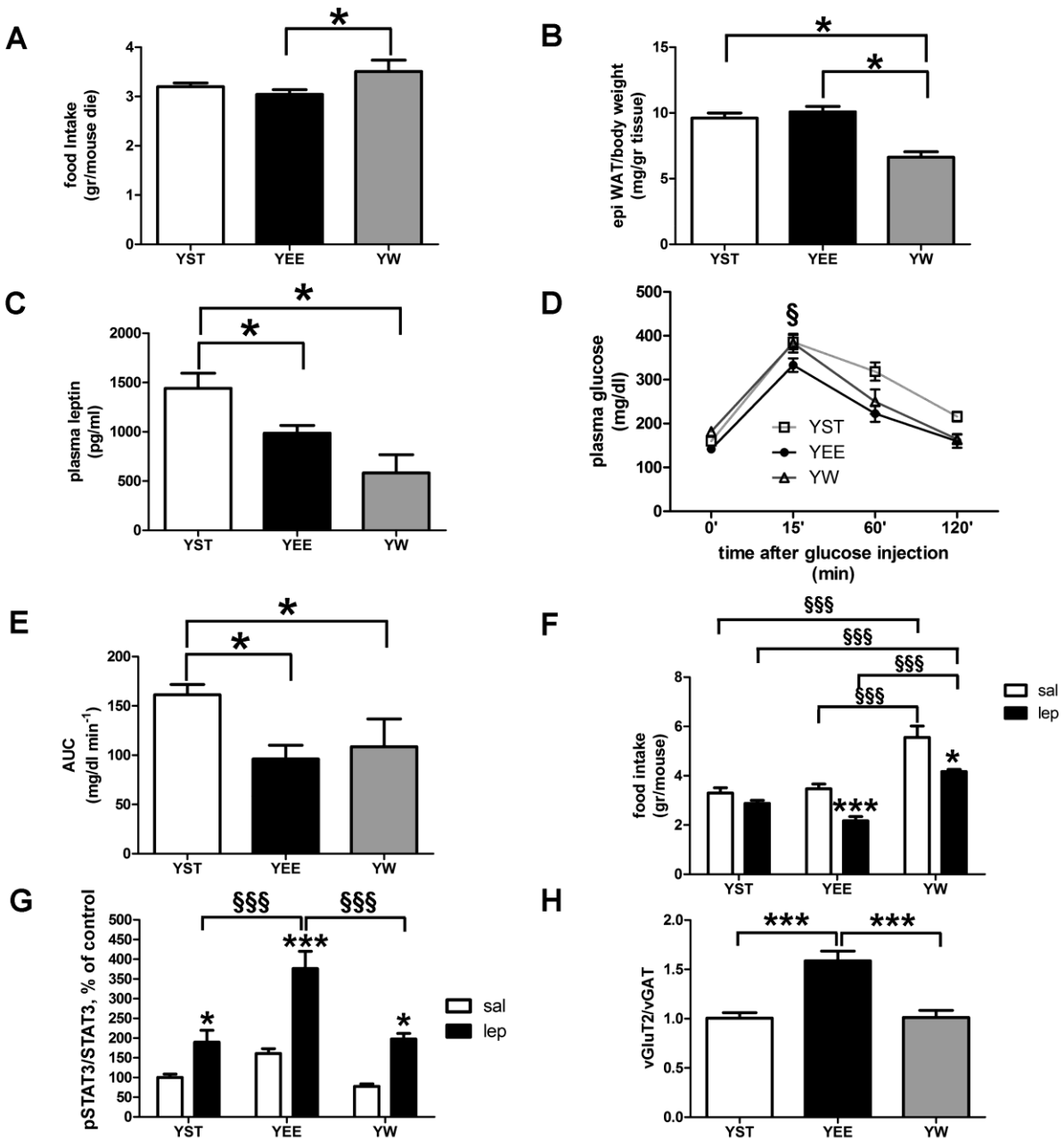

Figure 5.13 Effects of physical exercise on metabolism, leptin response and ARC synaptic connectivity in YW mice. A) Average food intake between P25 and P50 (1-way ANOVA followed by Bonferroni *post-hoc* test, YST *vs* YW *P<0.05). B) Weight of epididymal fat pad /body weight (adiposity) (1-way ANOVA followed by Bonferroni *post-hoc* test, *P<0.05). C) Plasma leptin at P50 (1-way ANOVA followed by Bonferroni *post-hoc* test, *P<0.05). D) IpGTT at the end of EE in YST, YEE and YW; 2-way ANOVA, rearing effect P<0.001, time effect P<0.001; Bonferroni *post-hoc* test, YST *vs* YW, *P<0.05). E) AUC values (mg/dL min^{-1} over a 120-min test) for the glycemic responses of YST, YEE and YW shown in D) (1-way ANOVA, Bonferroni *post hoc* test *P<0.05). F) Food intake assessed 14 hours after ip leptin injection in YST, YEE and YW. 2-way ANOVA: treatment effect P<0.0001, interaction P<0.0001, Bonferroni *post-hoc* tests: saline *vs* leptin *P<0.05; ***P<0.001, YW *vs* YEE or YST §§§P<0.001. G) Histogram showing the ratio of pSTAT3 positive cells to the total number of STAT3 positive neurons 45min after leptin or saline injection in the ARC of YST, YEE and YW (saline n=3, leptin n=4). 2-way ANOVA, rearing effect P<0.001, treatment effect P<0.001; Bonferroni *post-hoc* test, saline *vs* leptin *P<0.05, YW *vs* YEE §§§P<0.001. H) Ratio between excitatory and inhibitory synapses in the ARC of YW mice compared to YST and YEE. (1-way ANOVA, Bonferroni *post-hoc* test ***P<0.001).

5.5 DISCUSSION

The present results revealed that exposing mice to EE impacts on their feeding behaviour, leptin production/action and insulin sensitivity. The former two outcomes depend on the age at which EE is experienced, since EE in adulthood does not seem to affect the leptin system, whereas EE since birth results in an enhanced response to exogenous leptin, superior to that found in physically exercised mice.

The ARC of young EE mice exhibits also important changes in synaptic connectivity with an increased excitation/inhibition ratio in α-MSH neurons and decreased excitation/inhibition ratio in AgRP neurons.

Although food intake is known to be regulated by numerous factors and molecular pathways, the response of adult mice to EE is largely predictable using the leptin controller system as a paradigm. Indeed, this condition resulted in reduction of fat mass, consequent reduction of leptin production and increased food intake. The observed scenario mirrors the introduction of a more dynamic life style in sedentary individuals: despite an augmented appetite, BW is well maintained with a beneficial effect on insulin sensitivity.

When compared to YST, YEE mice exhibited similar fat depots, reduced plasma leptin, and similar food intake, thus suggesting that the leptin controller system had been adjusted to a different set point with an augmented sensitivity. Indeed YEE leptin response in terms of food intake was more pronounced than in the YST. Consistently YEE showed increased Ob-Rb hypothalamic expression, and enhanced response to leptin injection as assessed by ARC STAT3 phosphorylation and food intake reduction. An increased expression of leptin receptor may well explain the empowered leptin signalling and STAT3 is considered the main effector of leptin signalling in the ARC (Vaisse et al., 1996; Friedman, 2009). YEE also showed an increased hypothalamic expression of orexin. Despite the positive effect on food intake described for this

peptide, orexin deficient mice exhibit obesity, indicating that orexin may exert an overall catabolic influence over energy balance (Hara et al., 2001).

Mice reared in EE since birth constitute therefore the first non genetic non pathological model of enhanced leptin sensitivity. Genetic models with enhanced leptin sensitivity/response include, among others, mice deficient for cytokine signalling 3 (SOCS3) gene (Mori et al., 2004; Zhang et al., 2008) and mice in which the orexin-OXR2 receptor signalling is enhanced (Funato et al., 2009).

Patterson et al. recently (Patterson et al., 2009) reported that leptin resistance is reduced in Diet Induced Obese (DIO) rats exposed to post-weaning voluntary exercise as compared to control sedentary rats, thus attenuating the development of obesity typical of this model. These data are in the same line of my findings, although obtained in a pathological model genetically predisposed to become obese and characterized by leptin resistance (Levin et al., 1997). Indeed, the increase in leptin sensitivity, herein obtained for YEE, indicates the possibility of manipulating this parameter even in physiological conditions, as long as this manipulation is applied early in life. Besides, our data underscore 3 important differences between the effects of EE and voluntary physical exercise. First, the effects of locomotor activity on leptin sensitivity were less pronounced than those observed in YEE. Second, some of YW features (reduced adiposity, increased food intake) totally differed from what found in YEE and cannot be interpreted following the intermediate phenotype paradigm, thus suggesting that physical exercise outcomes are not totally contained within the EE condition and viceversa. Third, physical exercise did not modify the overall density of both excitatory or inhibitory synaptic contacts in the ARC, whereas EE increases the former and reduces the latter. Thus, components of EE other than physical exercise could play a role in regulating feeding behaviour and the related mechanisms in developing mice. If we picture this concept as a Wenn diagram we could

say that the 2 conditions share an intersection but maintain distinct areas of effect. In this regard, evidence exists that EE and voluntary exercise affect different phases of the neurogenic process in the hippocampus (Olson et al., 2006).

When animals were removed from EE and kept in a standard cage for one month the enhancement in leptin sensitivity disappeared but the hypothalamic structural modifications persisted to some extent and could represent a long lasting trace of a rearing condition experienced during development.

Interestingly, EE/ST food intake increased significantly when they were placed in a standard cage, and a concomitant rise in leptin was determined. These results suggest that the improved leptin sensitivity observed in the YEE suddenly dropped upon environmental change; consequently the hypothalamus sensed leptin concentrations as abnormally low and animals were induced to compensate an imbalance in their leptin controller system by eating more.

It is tempting to speculate about the existence of a leptin inhibitory signal promoted by EE and rapidly downregulated upon its discontinuation. Leptin can be considered the ideal afferent signal that informs the center (hypothalamus) about the status of the energy stores (WAT). This putative leptin modulator would complement leptin action and inform the periphery (WAT) about the status of the CNS, the privileged target of EE and the integration center of body functions. The nature of this signal that we can imagine as a circulating factor or a nervous input has yet to be established. Of note, recent data (Stanley et al., 2010) indicate clear anatomic connections between POMC neurons in the ARC and WAT.

In young mice, EE modified the excitatory/inhibitory synaptic connectivity in the ARC overall. Specifically, α-MSH and AgRP neurons respectively displayed an enhancement and a decrease of the excitation/inhibition ratio. ARC synaptic plasticity and changes in feeding

behaviour/energy homeostasis were first linked by Pinto et al. (Pinto et al., 2004), who found changes in the excitation/inhibition of POMC and NPY cells of the *ob*/*ob* mouse, consistent with the typical overfeeding behaviour of this model. They demonstrated that leptin treatment was able to rescue the *ob*/*ob* ARC phenotype and that treatment of wild type animals with the orexigenic peptide ghrelin led to enhanced inhibition of POMC neurons. Nutritional state has been also implied in the rapid reorganization of ARC synaptic connectivity. Studies in non human primates (Horvath, 2006) indicate that fasting results in an altered synaptic balance that favours the activity of NPY and orexin neurons. Further, the strength of the excitatory input from the ventro-medial hypothalamic area to ARC POMC neurons was reduced by fasting in mice (Sternson et al., 2005). In female mice estradiol (E2) triggers a robust increase in the number of excitatory inputs to POMC neurons in the ARC, that is leptin independent (Gao et al., 2007). All changes so far described resulted from a real (fasting) or perceived state of starvation (*ob*/*ob* mouse) or following a hormonal treatment.

These results provide the first demonstration that a change in rearing conditions and "life style" may interfere with the neural circuitry that underlies energy homeostasis. Indeed EE has an overall action on ARC synaptic connectivity that leads to the opposite functional outcome seen upon ghrelin treatment, starvation and leptin deficiency. Enhanced leptin sensitivity, herein observed in EE mice, could mediate the effects of EE on ARC synaptology; however I cannot exclude that the observed changes are leptin independent, but STAT3 dependent, as previously demonstrated for E2 (Gao et al., 2007). An enhanced basal activation of STAT3 was in fact observed in YEE as compared to YST.

These results are in agreement with the observation that the effect of EE on visual cortex plasticity involves a modulation of the excitation/inhibition balance (Sale et al., 2009).

Overall these findings indicate that diet-independent changes in lifestyle occurring early in life are able to modulate leptin sensitivity and leave metabolic and synaptic imprints. This may have important implications for the use of leptin and behavioural therapy in treatment and, especially, prevention of obesity.

6. REFERENCES

Abraham WC (2008) Metaplasticity: tuning synapses and networks for plasticity. Nat Rev Neurosci 9:387.

Abraham WC, Williams JM (2003) Properties and mechanisms of LTP maintenance. Neuroscientist 9:463-474.

Abraham WC, Logan B, Greenwood JM, Dragunow M (2002) Induction and experience-dependent consolidation of stable long-term potentiation lasting months in the hippocampus. J Neurosci 22:9626-9634.

Aicardi G, Argilli E, Cappello S, Santi S, Riccio M, Thoenen H, Canossa M (2004) Induction of long-term potentiation and depression is reflected by corresponding changes in secretion of endogenous brain-derived neurotrophic factor. Proc Natl Acad Sci U S A 101:15788-15792.

Amitai Y (2001) Thalamocortical synaptic connections: efficacy, modulation, inhibition and plasticity. Rev Neurosci 12:159-173.

Angelucci A, Clasca F, Bricolo E, Cramer KS, Sur M (1997) Experimentally induced retinal projections to the ferret auditory thalamus: development of clustered eye-specific patterns in a novel target. J Neurosci 17:2040-2055.

Antonini A, Stryker MP (1996) Plasticity of geniculocortical afferents following brief or prolonged monocular occlusion in the cat. J Comp Neurol 369:64-82.

Antonini A, Stryker MP (1998) Effect of sensory disuse on geniculate afferents to cat visual cortex. Vis Neurosci 15:401-409.

Antonini A, Fagiolini M, Stryker MP (1999) Anatomical correlates of functional plasticity in mouse visual cortex. J Neurosci 19:4388-4406.

Antonucci F, Di Garbo A, Novelli E, Manno I, Sartucci F, Bozzi Y, Caleo M (2008) Botulinum neurotoxin E (BoNT/E) reduces CA1 neuron loss and granule cell dispersion, with no effects on chronic seizures, in a mouse model of temporal lobe epilepsy. Exp Neurol 210:388-401.

Artola A, Singer W (1987) Long-term potentiation and NMDA receptors in rat visual cortex. Nature 330:649-652.

Artola A, Singer W (1990) The Involvement of N-Methyl-D-Aspartate Receptors in Induction and Maintenance of Long-Term Potentiation in Rat Visual Cortex. Eur J Neurosci 2:254-269.

Barria A, Muller D, Derkach V, Griffith LC, Soderling TR (1997) Regulatory phosphorylation of AMPA-type glutamate receptors by CaM-KII during long-term potentiation. Science 276:2042-2045.

Bartoletti A, Medini P, Berardi N, Maffei L (2004) Environmental enrichment prevents effects of dark-rearing in the rat visual cortex. Nat Neurosci 7:215-216.

Bavelier D, Neville HJ (2002) Cross-modal plasticity: where and how? Nat Rev Neurosci 3:443-452.

Bear MF, Kleinschmidt A, Gu QA, Singer W (1990) Disruption of experience-dependent synaptic modifications in striate cortex by infusion of an NMDA receptor antagonist. J Neurosci 10:909-925.

Beaulieu C, Colonnier M (1987) Effect of the richness of the environment on the cat visual cortex. J Comp Neurol 266:478-494.

Bender VA, Bender KJ, Brasier DJ, Feldman DE (2006) Two coincidence detectors for spike timing-dependent plasticity in somatosensory cortex. J Neurosci 26:4166-4177.

Bennett EL, Rosenzweig MR, Diamond MC, Morimoto H, Hebert M (1974) Effects of successive environments on brain measures. Physiol Behav 12:621-631.

Berardi N, Pizzorusso T, Maffei L (2000) Critical periods during sensory development. Curr Opin Neurobiol 10:138-145.

Berardi N, Braschi C, Capsoni S, Cattaneo A, Maffei L (2007) Environmental enrichment delays the onset of memory deficits and reduces neuropathological hallmarks in a mouse model of Alzheimer-like neurodegeneration. J Alzheimers Dis 11:359-370.

Berardi N, Cellerino A, Domenici L, Fagiolini M, Pizzorusso T, Cattaneo A, Maffei L (1994) Monoclonal antibodies to nerve growth factor affect the postnatal development of the visual system. Proc Natl Acad Sci U S A 91:684-688.

Bernstein L (1973) A study of some enriching variables in a free-environment for rats. J Psychosom Res 17:85-88.

Bidlingmaier M, Strasburger CJ (2010) Growth hormone. Handb Exp Pharmacol:187-200.

Bienenstock EL, Cooper LN, Munro PW (1982) Theory for the development of neuron selectivity: orientation specificity and binocular interaction in visual cortex. J Neurosci 2:32-48.

Blakemore C, Van Sluyters RC (1974) Reversal of the physiological effects of monocular deprivation in kittens: further evidence for a sensitive period. J Physiol 237:195-216.

Bliss TV, Gardner-Medwin AR (1973) Long-lasting potentiation of synaptic transmission in the dentate area of the unanaestetized rabbit following stimulation of the perforant path. J Physiol 232:357-374.

Bliss TV, Lomo T (1973) Long-lasting potentiation of synaptic transmission in the dentate area of the anaesthetized rabbit following stimulation of the perforant path. J Physiol 232:331-356.

Bortolotto ZA, Bashir ZI, Davies CH, Collingridge GL (1994) A molecular switch activated by metabotropic glutamate receptors regulates induction of long-term potentiation. Nature 368:740-743.

Bouret SG, Draper SJ, Simerly RB (2004) Trophic action of leptin on hypothalamic neurons that regulate feeding. Science 304:108-110.

Bozzi Y, Pizzorusso T, Cremisi F, Rossi FM, Barsacchi G, Maffei L (1995) Monocular deprivation decreases the expression of messenger RNA for brain-derived neurotrophic factor in the rat visual cortex. Neuroscience 69:1133-1144.

Brosch M, Selezneva E, Scheich H (2005) Nonauditory events of a behavioral procedure activate auditory cortex of highly trained monkeys. J Neurosci 25:6797-6806.

Bruce CJ, Goldberg ME (1985) Primate frontal eye fields. I. Single neurons discharging before saccades. J Neurophysiol 53:603-635.

Bruckner G, Bringmann A, Hartig W, Koppe G, Delpech B, Brauer K (1998) Acute and long-lasting changes in extracellular-matrix chondroitin-sulphate proteoglycans induced by injection of chondroitinase ABC in the adult rat brain. Exp Brain Res 121:300-310.

Bruckner G, Grosche J, Schmidt S, Hartig W, Margolis RU, Delpech B, Seidenbecher CI, Czaniera R, Schachner M (2000) Postnatal development of perineuronal nets in wild-type mice and in a mutant deficient in tenascin-R. J Comp Neurol 428:616-629.

Buzas P, Eysel UT, Adorjan P, Kisvarday ZF (2001) Axonal topography of cortical basket cells in relation to orientation, direction, and ocular dominance maps. J Comp Neurol 437:259-285.

Cabelli RJ, Hohn A, Shatz CJ (1995) Inhibition of ocular dominance column formation by infusion of NT-4/5 or BDNF. Science 267:1662-1666.

Caleo M, Maffei L (2002) Neurotrophins and plasticity in the visual cortex. Neuroscientist 8:52-61.

Caleo M, Lodovichi C, Maffei L (1999) Effects of nerve growth factor on visual cortical plasticity require afferent electrical activity. Eur J Neurosci 11:2979-2984.

Caleo M, Medini P, von Bartheld CS, Maffei L (2003) Provision of brain-derived neurotrophic factor via anterograde transport from the eye preserves the physiological responses of axotomized geniculate neurons. J Neurosci 23:287-296.

Caleo M, Tropea D, Rossi C, Gianfranceschi L, Maffei L (2009) Environmental enrichment promotes fiber sprouting after deafferentation of the superior colliculus in the adult rat brain. Exp Neurol 216:515-519.

Caleo M, Restani L, Gianfranceschi L, Costantin L, Rossi C, Rossetto O, Montecucco C, Maffei L (2007) Transient synaptic silencing of developing striate cortex has persistent effects on visual function and plasticity. J Neurosci 27:4530-4540.

Campi KL, Bales KL, Grunewald R, Krubitzer L (2009) Connections of auditory and visual cortex in the prairie vole (Microtus ochrogaster): evidence for multisensory processing in primary sensory areas. Cereb Cortex 20:89-108.

Cancedda L, Putignano E, Impey S, Maffei L, Ratto GM, Pizzorusso T (2003) Patterned vision causes CRE-mediated gene expression in the visual cortex through PKA and ERK. J Neurosci 23:7012-7020.

Cancedda L, Putignano E, Sale A, Viegi A, Berardi N, Maffei L (2004) Acceleration of visual system development by environmental enrichment. J Neurosci 24:4840-4848.

Caporale N, Dan Y (2008) Spike timing-dependent plasticity: a Hebbian learning rule. Annu Rev Neurosci 31:25-46.

Carmignoto G, Vicini S (1992) Activity-dependent decrease in NMDA receptor responses during development of the visual cortex. Science 258:1007-1011.

Carroll RC, Beattie EC, von Zastrow M, Malenka RC (2001) Role of AMPA receptor endocytosis in synaptic plasticity. Nat Rev Neurosci 2:315-324.

Castren E, Zafra F, Thoenen H, Lindholm D (1992) Light regulates expression of brain-derived neurotrophic factor mRNA in rat visual cortex. Proc Natl Acad Sci U S A 89:9444-9448.

Castro-Alamancos MA, Connors BW (1997) Distinct forms of short-term plasticity at excitatory synapses of hippocampus and neocortex. Proc Natl Acad Sci U S A 94:4161-4166.

Ceccarini G, Flavell RR, Butelman ER, Synan M, Willnow TE, Bar-Dagan M, Goldsmith SJ, Kreek MJ, Kothari P, Vallabhajosula S, Muir TW, Friedman JM (2009) PET imaging of leptin biodistribution and metabolism in rodents and primates. Cell Metab 10:148-159.

Celio MR, Blumcke I (1994) Perineuronal nets--a specialized form of extracellular matrix in the adult nervous system. Brain Res Brain Res Rev 19:128-145.

Celio MR, Spreafico R, De Biasi S, Vitellaro-Zuccarello L (1998) Perineuronal nets: past and present. Trends Neurosci 21:510-515.

Chabot N, Charbonneau V, Laramee ME, Tremblay R, Boire D, Bronchti G (2008) Subcortical auditory input to the primary visual cortex in anophthalmic mice. Neurosci Lett 433:129-134.

Chattopadhyaya B, Di Cristo G, Higashiyama H, Knott GW, Kuhlman SJ, Welker E, Huang ZJ (2004) Experience and activity-dependent maturation of perisomatic GABAergic innervation in primary visual cortex during a postnatal critical period. J Neurosci 24:9598-9611.

Chen WS, Bear MF (2007) Activity-dependent regulation of NR2B translation contributes to metaplasticity in mouse visual cortex. Neuropharmacology 52:200-214.

Christie BR, Abraham WC (1992) Priming of associative long-term depression in the dentate gyrus by theta frequency synaptic activity. Neuron 9:79-84.

Chun D, Gall CM, Bi X, Lynch G (2001) Evidence that integrins contribute to multiple stages in the consolidation of long term potentiation in rat hippocampus. Neuroscience 105:815-829.

Ciucci F, Putignano E, Baroncelli L, Landi S, Berardi N, Maffei L (2007) Insulin-like growth factor 1 (IGF-1) mediates the effects of enriched environment (EE) on visual cortical development. PLoS One 2:e475.

Clem RL, Barth A (2006) Pathway-specific trafficking of native AMPARs by in vivo experience. Neuron 49:663-670.

Cohen AS, Abraham WC (1996) Facilitation of long-term potentiation by prior activation of metabotropic glutamate receptors. J Neurophysiol 76:953-962.

Cohen AS, Coussens CM, Raymond CR, Abraham WC (1999a) Long-lasting increase in cellular excitability associated with the priming of LTP induction in rat hippocampus. J Neurophysiol 82:3139-3148.

Cohen LG, Weeks RA, Sadato N, Celnik P, Ishii K, Hallett M (1999b) Period of susceptibility for cross-modal plasticity in the blind. Ann Neurol 45:451-460.

Cohen LG, Celnik P, Pascual-Leone A, Corwell B, Falz L, Dambrosia J, Honda M, Sadato N, Gerloff C, Catala MD, Hallett M (1997) Functional relevance of cross-modal plasticity in blind humans. Nature 389:180-183.

Collingridge GL, Kehl SJ, McLennan H (1983) The antagonism of amino acid-induced excitations of rat hippocampal CA1 neurones in vitro. J Physiol 334:19-31.

Coppari R, Ramadori G, Elmquist JK (2009) The role of transcriptional regulators in central control of appetite and body weight. Nat Clin Pract Endocrinol Metab 5:160-166.

Corson J, Nahmani M, Lubarsky K, Badr N, Wright C, Erisir A (2009) Sensory activity differentially modulates N-methyl-D-aspartate receptor subunits 2A and 2B in cortical layers. Neuroscience 163:920-932.

Crowley JC, Katz LC (1999) Development of ocular dominance columns in the absence of retinal input. Nat Neurosci 2:1125-1130.

Dan Y, Poo MM (2004) Spike timing-dependent plasticity of neural circuits. Neuron 44:23-30.

Daw NW, Gordon B, Fox KD, Flavin HJ, Kirsch JD, Beaver CJ, Ji Q, Reid SN, Czepita D (1999) Injection of MK-801 affects ocular dominance shifts more than visual activity. J Neurophysiol 81:204-215.

Desai NS, Cudmore RH, Nelson SB, Turrigiano GG (2002) Critical periods for experience-dependent synaptic scaling in visual cortex. Nat Neurosci 5:783-789.

Di Cristo G, Berardi N, Cancedda L, Pizzorusso T, Putignano E, Ratto GM, Maffei L (2001) Requirement of ERK activation for visual cortical plasticity. Science 292:2337-2340.

Diamond MC, Lindner B, Raymond A (1967) Extensive cortical depth measurements and neuron size increases in the cortex of environmentally enriched rats. J Comp Neurol 131:357-364.

Doron N, Wollberg Z (1994) Cross-modal neuroplasticity in the blind mole rat Spalax ehrenbergi: a WGA-HRP tracing study. Neuroreport 5:2697-2701.

Dudek SM, Bear MF (1992) Homosynaptic long-term depression in area CA1 of hippocampus and effects of N-methyl-D-aspartate receptor blockade. Proc Natl Acad Sci U S A 89:4363-4367.

Elmquist JK, Flier JS (2004) Neuroscience. The fat-brain axis enters a new dimension. Science 304:63-64.

Enoki R, Hu YL, Hamilton D, Fine A (2009) Expression of long-term plasticity at individual synapses in hippocampus is graded, bidirectional, and mainly presynaptic: optical quantal analysis. Neuron 62:242-253.

Ethell IM, Ethell DW (2007) Matrix metalloproteinases in brain development and remodeling: synaptic functions and targets. J Neurosci Res 85:2813-2823.

Fagiolini M, Hensch TK (2000) Inhibitory threshold for critical-period activation in primary visual cortex. Nature 404:183-186.

Fagiolini M, Pizzorusso T, Berardi N, Domenici L, Maffei L (1994) Functional postnatal development of the rat primary visual cortex and the role of visual experience: dark rearing and monocular deprivation. Vision Res 34:709-720.

Fagiolini M, Pizzorusso T, Porciatti V, Cenni M, Maffei L (1997) Transplant of Schwann cells allows normal development of the visual cortex of dark-reared rats. Eur J Neurosci 9:102-112.

Fagiolini M, Fritschy JM, Low K, Mohler H, Rudolph U, Hensch TK (2004) Specific GABAA circuits for visual cortical plasticity. Science 303:1681-1683.

Falchier A, Clavagnier S, Barone P, Kennedy H (2002) Anatomical evidence of multimodal integration in primate striate cortex. J Neurosci 22:5749-5759.

Farlie PG, Dringen R, Rees SM, Kannourakis G, Bernard O (1995) bcl-2 transgene expression can protect neurons against developmental and induced cell death. Proc Natl Acad Sci U S A 92:4397-4401.

Fawcett JW, Asher RA (1999) The glial scar and central nervous system repair. Brain Res Bull 49:377-391.

Felleman DJ, Van Essen DC (1991) Distributed hierarchical processing in the primate cerebral cortex. Cereb Cortex 1:1-47.

Ferchmin PA, Bennett EL (1975) Direct contact with enriched environment is required to alter cerebral weights in rats. J Comp Physiol Psychol 88:360-367.

Fine I, Wade AR, Brewer AA, May MG, Goodman DF, Boynton GM, Wandell BA, MacLeod DI (2003) Long-term deprivation affects visual perception and cortex. Nat Neurosci 6:915-916.

Finney EM, Fine I, Dobkins KR (2001) Visual stimuli activate auditory cortex in the deaf. Nat Neurosci 4:1171-1173.

Fishman MC, Michael P (1973) Integration of auditory information in the cat's visual cortex. Vision Res 13:1415-1419.

Flint AC, Maisch US, Weishaupt JH, Kriegstein AR, Monyer H (1997) NR2A subunit expression shortens NMDA receptor synaptic currents in developing neocortex. J Neurosci 17:2469-2476.

Fox K (1992) A critical period for experience-dependent synaptic plasticity in rat barrel cortex. J Neurosci 12:1826-1838.

Frenkel MY, Bear MF (2004) How monocular deprivation shifts ocular dominance in visual cortex of young mice. Neuron 44:917-923.

Frey U, Krug M, Reymann KG, Matthies H (1988) Anisomycin, an inhibitor of protein synthesis, blocks late phases of LTP phenomena in the hippocampal CA1 region in vitro. Brain Res 452:57-65.

Frey U, Schollmeier K, Reymann KG, Seidenbecher T (1995) Asymptotic hippocampal long-term potentiation in rats does not preclude additional potentiation at later phases. Neuroscience 67:799-807.

Frick KM, Fernandez SM (2003) Enrichment enhances spatial memory and increases synaptophysin levels in aged female mice. Neurobiol Aging 24:615-626.

Friedman JM (2009) Leptin at 14 y of age: an ongoing story. Am J Clin Nutr 89:973S-979S.

Funato H, Tsai AL, Willie JT, Kisanuki Y, Williams SC, Sakurai T, Yanagisawa M (2009) Enhanced orexin receptor-2 signaling prevents diet-induced obesity and improves leptin sensitivity. Cell Metab 9:64-76.

Galli L, Maffei L (1988) Spontaneous impulse activity of rat retinal ganglion cells in prenatal life. Science 242:90-91.

Gandhi SP, Yanagawa Y, Stryker MP (2008) Delayed plasticity of inhibitory neurons in developing visual cortex. Proc Natl Acad Sci U S A 105:16797-16802.

Gao Q, Mezei G, Nie Y, Rao Y, Choi CS, Bechmann I, Leranth C, Toran-Allerand D, Priest CA, Roberts JL, Gao XB, Mobbs C, Shulman GI, Diano S, Horvath TL (2007) Anorectic estrogen mimics leptin's effect on the rewiring of melanocortin cells and Stat3 signaling in obese animals. Nat Med 13:89-94.

Gianfranceschi L, Siciliano R, Walls J, Morales B, Kirkwood A, Huang ZJ, Tonegawa S, Maffei L (2003) Visual cortex is rescued from the effects of dark rearing by overexpression of BDNF. Proc Natl Acad Sci U S A 100:12486-12491.

Gil Z, Connors BW, Amitai Y (1999) Efficacy of thalamocortical and intracortical synaptic connections: quanta, innervation, and reliability. Neuron 23:385-397.

Glazewski S (1998) Experience-dependent changes in vibrissae evoked responses in the rodent barrel cortex. Acta Neurobiol Exp (Wars) 58:309-320.

Glazewski S, Fox K (1996) Time course of experience-dependent synaptic potentiation and depression in barrel cortex of adolescent rats. J Neurophysiol 75:1714-1729.

Globus A, Rosenzweig MR, Bennett EL, Diamond MC (1973) Effects of differential experience on dendritic spine counts in rat cerebral cortex. J Comp Physiol Psychol 82:175-181.

Gould E, Beylin A, Tanapat P, Reeves A, Shors TJ (1999) Learning enhances adult neurogenesis in the hippocampal formation. Nat Neurosci 2:260-265.

Gray EG (1959) Electron microscopy of synaptic contacts on dendrite spines of the cerebral cortex. Nature 183:1592-1593.

Green EJ, Greenough WT (1986) Altered synaptic transmission in dentate gyrus of rats reared in complex environments: evidence from hippocampal slices maintained in vitro. J Neurophysiol 55:739-750.

Greenough WT, Volkmar FR (1973) Pattern of dendritic branching in occipital cortex of rats reared in complex environments. Exp Neurol 40:491-504.

Greenough WT, Volkmar FR, Juraska JM (1973) Effects of rearing complexity on dendritic branching in frontolateral and temporal cortex of the rat. Exp Neurol 41:371-378.

Greenough WT, Cohen NJ, Juraska JM (1999) New neurons in old brains: learning to survive? Nat Neurosci 2:203-205.

Gu QA, Bear MF, Singer W (1989) Blockade of NMDA-receptors prevents ocularity changes in kitten visual cortex after reversed monocular deprivation. Brain Res Dev Brain Res 47:281-288.

Guandalini P (1998) The corticocortical projections of the physiologically defined eye field in the rat medial frontal cortex. Brain Res Bull 47:377-385.

Guimaraes A, Zaremba S, Hockfield S (1990) Molecular and morphological changes in the cat lateral geniculate nucleus and visual cortex induced by visual deprivation are revealed by monoclonal antibodies Cat-304 and Cat-301. J Neurosci 10:3014-3024.

Gustafsson B, Wigstrom H, Abraham WC, Huang YY (1987) Long-term potentiation in the hippocampus using depolarizing current pulses as the conditioning stimulus to single volley synaptic potentials. J Neurosci 7:774-780.

Guzzetta A, Baldini S, Bancale A, Baroncelli L, Ciucci F, Ghirri P, Putignano E, Sale A, Viegi A, Berardi N, Boldrini A, Cioni G, Maffei L (2009) Massage accelerates brain development and the maturation of visual function. J Neurosci 29:6042-6051.

Hara J, Beuckmann CT, Nambu T, Willie JT, Chemelli RM, Sinton CM, Sugiyama F, Yagami K, Goto K, Yanagisawa M, Sakurai T (2001) Genetic ablation of orexin neurons in mice results in narcolepsy, hypophagia, and obesity. Neuron 30:345-354.

Harauzov A, Spolidoro M, DiCristo G, De Pasquale R, Cancedda L, Pizzorusso T, Viegi A, Berardi N, Maffei L (2010) Reducing intracortical inhibition in the adult visual cortex promotes ocular dominance plasticity. J Neurosci 30:361-371.

Hardingham N, Fox K (2006) The role of nitric oxide and GluR1 in presynaptic and postsynaptic components of neocortical potentiation. J Neurosci 26:7395-7404.

He HY, Hodos W, Quinlan EM (2006) Visual deprivation reactivates rapid ocular dominance plasticity in adult visual cortex. J Neurosci 26:2951-2955.

He HY, Ray B, Dennis K, Quinlan EM (2007) Experience-dependent recovery of vision following chronic deprivation amblyopia. Nat Neurosci 10:1134-1136.

Hebb D (1947) The effects of early experience on problem-soling at maturity. American Psyhchology 2:306-307.

Hebb D (1949) The Organization of Behavior. New York: Wiley.

Hensch TK (2005) Critical period plasticity in local cortical circuits. Nat Rev Neurosci 6:877-888.

Hensch TK, Stryker MP (2004) Columnar architecture sculpted by GABA circuits in developing cat visual cortex. Science 303:1678-1681.

Hensch TK, Fagiolini M, Mataga N, Stryker MP, Baekkeskov S, Kash SF (1998) Local GABA circuit control of experience-dependent plasticity in developing visual cortex. Science 282:1504-1508.

Herron CE, Lester RA, Coan EJ, Collingridge GL (1986) Frequency-dependent involvement of NMDA receptors in the hippocampus: a novel synaptic mechanism. Nature 322:265-268.

Heynen AJ, Bear MF (2001) Long-term potentiation of thalamocortical transmission in the adult visual cortex in vivo. J Neurosci 21:9801-9813.

Heynen AJ, Yoon BJ, Liu CH, Chung HJ, Huganir RL, Bear MF (2003) Molecular mechanism for loss of visual cortical responsiveness following brief monocular deprivation. Nat Neurosci 6:854-862.

Hockfield S, Kalb RG, Zaremba S, Fryer H (1990) Expression of neural proteoglycans correlates with the acquisition of mature neuronal properties in the mammalian brain. Cold Spring Harb Symp Quant Biol 55:505-514.

Hockly E, Cordery PM, Woodman B, Mahal A, van Dellen A, Blakemore C, Lewis CM, Hannan AJ, Bates GP (2002) Environmental enrichment slows disease progression in R6/2 Huntington's disease mice. Ann Neurol 51:235-242.

Hofer SB, Mrsic-Flogel TD, Bonhoeffer T, Hubener M (2006) Prior experience enhances plasticity in adult visual cortex. Nat Neurosci 9:127-132.

Hofer SB, Mrsic-Flogel TD, Bonhoeffer T, Hubener M (2009) Experience leaves a lasting structural trace in cortical circuits. Nature 457:313-317.

Holtmaat A, Svoboda K (2009) Experience-dependent structural synaptic plasticity in the mammalian brain. Nat Rev Neurosci 10:647-658.

Holtmaat AJ, Trachtenberg JT, Wilbrecht L, Shepherd GM, Zhang X, Knott GW, Svoboda K (2005) Transient and persistent dendritic spines in the neocortex in vivo. Neuron 45:279-291.

Horton JC, Hocking DR (1996) An adult-like pattern of ocular dominance columns in striate cortex of newborn monkeys prior to visual experience. J Neurosci 16:1791-1807.

Horvath TL (2006) Synaptic plasticity in energy balance regulation. Obesity (Silver Spring) 14 Suppl 5:228S-233S.

Huang YY, Wigstrom H, Gustafsson B (1987) Facilitated induction of hippocampal long-term potentiation in slices perfused with low concentrations of magnesium. Neuroscience 22:9-16.

Huang YY, Colino A, Selig DK, Malenka RC (1992) The influence of prior synaptic activity on the induction of long-term potentiation. Science 255:730-733.

Huang ZJ, Di Cristo G, Ango F (2007) Development of GABA innervation in the cerebral and cerebellar cortices. Nat Rev Neurosci 8:673-686.

Huang ZJ, Kirkwood A, Pizzorusso T, Porciatti V, Morales B, Bear MF, Maffei L, Tonegawa S (1999) BDNF regulates the maturation of inhibition and the critical period of plasticity in mouse visual cortex. Cell 98:739-755.

Hubel DH, Wiesel TN (1962) Receptive fields, binocular interaction and functional architecture in the cat's visual cortex. J Physiol 160:106-154.

Hubel DH, Wiesel TN (1963) Shape and arrangement of columns in cat's striate cortex. J Physiol 165:559-568.

Hubel DH, Wiesel TN (1964) Effects of Monocular Deprivation in Kittens. Naunyn Schmiedebergs Arch Exp Pathol Pharmakol 248:492-497.

Hubel DH, Wiesel TN (1968) Receptive fields and functional architecture of monkey striate cortex. J Physiol 195:215-243.

Hubel DH, Wiesel TN (1970) The period of susceptibility to the physiological effects of unilateral eye closure in kittens. J Physiol 206:419-436.

Hubel DH, Wiesel TN, LeVay S (1977) Plasticity of ocular dominance columns in monkey striate cortex. Philos Trans R Soc Lond B Biol Sci 278:377-409.

Huemmeke M, Eysel UT, Mittmann T (2002) Metabotropic glutamate receptors mediate expression of LTP in slices of rat visual cortex. Eur J Neurosci 15:1641-1645.

Huerta MF, Krubitzer LA, Kaas JH (1987) Frontal eye field as defined by intracortical microstimulation in squirrel monkeys, owl monkeys, and macaque monkeys. II. Cortical connections. J Comp Neurol 265:332-361.

Ibata K, Sun Q, Turrigiano GG (2008) Rapid synaptic scaling induced by changes in postsynaptic firing. Neuron 57:819-826.

Ickes BR, Pham TM, Sanders LA, Albeck DS, Mohammed AH, Granholm AC (2000) Long-term environmental enrichment leads to regional increases in neurotrophin levels in rat brain. Exp Neurol 164:45-52.

Innocenti GM, Clarke S (1984) Bilateral transitory projection to visual areas from auditory cortex in kittens. Brain Res 316:143-148.

Isaac JT, Nicoll RA, Malenka RC (1995) Evidence for silent synapses: implications for the expression of LTP. Neuron 15:427-434.

Jacob V, Brasier DJ, Erchova I, Feldman D, Shulz DE (2007) Spike timing-dependent synaptic depression in the in vivo barrel cortex of the rat. J Neurosci 27:1271-1284.

Jankowsky JL, Xu G, Fromholt D, Gonzales V, Borchelt DR (2003) Environmental enrichment exacerbates amyloid plaque formation in a transgenic mouse model of Alzheimer disease. J Neuropathol Exp Neurol 62:1220-1227.

Jia F, Xie X, Zhou Y (2004) Short-term depression of synaptic transmission from rat lateral geniculate nucleus to primary visual cortex in vivo. Brain Res 1002:158-161.

Jiang B, Akaneya Y, Ohshima M, Ichisaka S, Hata Y, Tsumoto T (2001) Brain-derived neurotrophic factor induces long-lasting potentiation of synaptic transmission in visual cortex in vivo in young rats, but not in the adult. Eur J Neurosci 14:1219-1228.

Kampa BM, Clements J, Jonas P, Stuart GJ (2004) Kinetics of Mg2+ unblock of NMDA receptors: implications for spike-timing dependent synaptic plasticity. J Physiol 556:337-345.

Katz LC, Shatz CJ (1996) Synaptic activity and the construction of cortical circuits. Science 274:1133-1138.

Kelleher RJ, 3rd, Govindarajan A, Tonegawa S (2004a) Translational regulatory mechanisms in persistent forms of synaptic plasticity. Neuron 44:59-73.

Kelleher RJ, 3rd, Govindarajan A, Jung HY, Kang H, Tonegawa S (2004b) Translational control by MAPK signaling in long-term synaptic plasticity and memory. Cell 116:467-479.

Kind PC, Mitchell DE, Ahmed B, Blakemore C, Bonhoeffer T, Sengpiel F (2002) Correlated binocular activity guides recovery from monocular deprivation. Nature 416:430-433.

Kirkwood A, Bear MF (1994a) Hebbian synapses in visual cortex. J Neurosci 14:1634-1645.

Kirkwood A, Bear MF (1994b) Homosynaptic long-term depression in the visual cortex. J Neurosci 14:3404-3412.

Kirkwood A, Lee HK, Bear MF (1995) Co-regulation of long-term potentiation and experience-dependent synaptic plasticity in visual cortex by age and experience. Nature 375:328-331.

Kirkwood A, Rioult MC, Bear MF (1996) Experience-dependent modification of synaptic plasticity in visual cortex. Nature 381:526-528.

Klausberger T, Roberts JD, Somogyi P (2002) Cell type- and input-specific differences in the number and subtypes of synaptic GABA(A) receptors in the hippocampus. J Neurosci 22:2513-2521.

Knudsen EI, Knudsen PF (1990) Sensitive and critical periods for visual calibration of sound localization by barn owls. J Neurosci 10:222-232.

Knudsen EI, Brainard MS (1991) Visual instruction of the neural map of auditory space in the developing optic tectum. Science 253:85-87.

Koester HJ, Sakmann B (1998) Calcium dynamics in single spines during coincident pre- and postsynaptic activity depend on relative timing of back-propagating action potentials and subthreshold excitatory postsynaptic potentials. Proc Natl Acad Sci U S A 95:9596-9601.

Komai S, Matsuyama T, Matsumoto K, Kato K, Kobayashi M, Imamura K, Yoshida S, Ugawa S, Shiosaka S (2000) Neuropsin regulates an early phase of schaffer-collateral long-term potentiation in the murine hippocampus. Eur J Neurosci 12:1479-1486.

Konur S, Yuste R (2004) Imaging the motility of dendritic protrusions and axon terminals: roles in axon sampling and synaptic competition. Mol Cell Neurosci 27:427-440.

Korte M, Carroll P, Wolf E, Brem G, Thoenen H, Bonhoeffer T (1995) Hippocampal long-term potentiation is impaired in mice lacking brain-derived neurotrophic factor. Proc Natl Acad Sci U S A 92:8856-8860.

Krahe TE, Medina AE, de Bittencourt-Navarrete RE, Colello RJ, Ramoa AS (2005) Protein synthesis-independent plasticity mediates rapid and precise recovery of deprived eye responses. Neuron 48:329-343.

Kraskov A, Stogbauer H, Grassberger P (2004) Estimating mutual information. Phys Rev E Stat Nonlin Soft Matter Phys 69:066138.

Kudo M, Moriya M, Mizuno N (1997) Auditory projections from the IC to the SCN by way of the LG in the mole, Mogera. Neuroreport 8:3405-3409.

Kuo MC, Dringenberg HC (2008) Histamine facilitates in vivo thalamocortical long-term potentiation in the mature visual cortex of anesthetized rats. Eur J Neurosci 27:1731-1738.

Laemle LK, Strominger NL, Carpenter DO (2006) Cross-modal innervation of primary visual cortex by auditory fibers in congenitally anophthalmic mice. Neurosci Lett 396:108-112.

Landi S, Cenni MC, Maffei L, Berardi N (2007a) Environmental enrichment effects on development of retinal ganglion cell dendritic stratification require retinal BDNF. PLoS One 2:e346.

Landi S, Ciucci F, Maffei L, Berardi N, Cenni MC (2009) Setting the pace for retinal development: environmental enrichment acts through insulin-like growth factor 1 and brain-derived neurotrophic factor. J Neurosci 29:10809-10819.

Landi S, Sale A, Berardi N, Viegi A, Maffei L, Cenni MC (2007b) Retinal functional development is sensitive to environmental enrichment: a role for BDNF. Faseb J 21:130-139.

Lazarov O, Robinson J, Tang YP, Hairston IS, Korade-Mirnics Z, Lee VM, Hersh LB, Sapolsky RM, Mirnics K, Sisodia SS (2005) Environmental enrichment reduces Abeta levels and amyloid deposition in transgenic mice. Cell 120:701-713.

Lee DS, Lee JS, Oh SH, Kim SK, Kim JW, Chung JK, Lee MC, Kim CS (2001a) Cross-modal plasticity and cochlear implants. Nature 409:149-150.

Lee HK, Barbarosie M, Kameyama K, Bear MF, Huganir RL (2000) Regulation of distinct AMPA receptor phosphorylation sites during bidirectional synaptic plasticity. Nature 405:955-959.

Lee HK, Takamiya K, He K, Song L, Huganir RL (2010) Specific roles of AMPA receptor subunit GluR1 (GluA1) phosphorylation sites in regulating synaptic plasticity in the CA1 region of hippocampus. J Neurophysiol 103:479-489.

Lee R, Kermani P, Teng KK, Hempstead BL (2001b) Regulation of cell survival by secreted proneurotrophins. Science 294:1945-1948.

Lein ES, Hohn A, Shatz CJ (2000) Dynamic regulation of BDNF and NT-3 expression during visual system development. J Comp Neurol 420:1-18.

Lendvai B, Stern EA, Chen B, Svoboda K (2000) Experience-dependent plasticity of dendritic spines in the developing rat barrel cortex in vivo. Nature 404:876-881.

Lessard N, Pare M, Lepore F, Lassonde M (1998) Early-blind human subjects localize sound sources better than sighted subjects. Nature 395:278-280.

Letzkus JJ, Kampa BM, Stuart GJ (2006) Learning rules for spike timing-dependent plasticity depend on dendritic synapse location. J Neurosci 26:10420-10429.

Levi-Montalcini R (1965) Growth regulation of sympathetic nerve cells. Arch Ital Biol 103:832-846.

Levi DM, Li RW (2009a) Improving the performance of the amblyopic visual system. Philos Trans R Soc Lond B Biol Sci 364:399-407.

Levi DM, Li RW (2009b) Perceptual learning as a potential treatment for amblyopia: a mini-review. Vision Res 49:2535-2549.

Levin BE, Dunn-Meynell AA, Balkan B, Keesey RE (1997) Selective breeding for diet-induced obesity and resistance in Sprague-Dawley rats. Am J Physiol 273:R725-730.

Lewin GR, Barde YA (1996) Physiology of the neurotrophins. Annu Rev Neurosci 19:289-317.

Lewis TL, Maurer D (2009) Effects of early pattern deprivation on visual development. Optom Vis Sci 86:640-646.

Lisman J, Schulman H, Cline H (2002) The molecular basis of CaMKII function in synaptic and behavioural memory. Nat Rev Neurosci 3:175-190.

Lodovichi C, Berardi N, Pizzorusso T, Maffei L (2000) Effects of neurotrophins on cortical plasticity: same or different? J Neurosci 20:2155-2165.

Lu Y, Christian K, Lu B (2008) BDNF: a key regulator for protein synthesis-dependent LTP and long-term memory? Neurobiol Learn Mem 89:312-323.

Luppino FS, de Wit LM, Bouvy PF, Stijnen T, Cuijpers P, Penninx BW, Zitman FG (2010) Overweight, obesity, and depression: a systematic review and meta-analysis of longitudinal studies. Arch Gen Psychiatry 67:220-229.

Lynch MA (2004) Long-term potentiation and memory. Physiol Rev 84:87-136.

Maffei A, Turrigiano GG (2008) Multiple modes of network homeostasis in visual cortical layer 2/3. J Neurosci 28:4377-4384.

Maffei A, Nelson SB, Turrigiano GG (2004) Selective reconfiguration of layer 4 visual cortical circuitry by visual deprivation. Nat Neurosci 7:1353-1359.

Maffei A, Lambo ME, Turrigiano GG (2010) Critical period for inhibitory plasticity in rodent binocular V1. J Neurosci 30:3304-3309.

Maffei A, Nataraj K, Nelson SB, Turrigiano GG (2006) Potentiation of cortical inhibition by visual deprivation. Nature 443:81-84.

Maffei L, Berardi N, Domenici L, Parisi V, Pizzorusso T (1992) Nerve growth factor (NGF) prevents the shift in ocular dominance distribution of visual cortical neurons in monocularly deprived rats. J Neurosci 12:4651-4662.

Maffei M, Fei H, Lee GH, Dani C, Leroy P, Zhang Y, Proenca R, Negrel R, Ailhaud G, Friedman JM (1995) Increased expression in adipocytes of ob RNA in mice with lesions of the hypothalamus and with mutations at the db locus. Proc Natl Acad Sci U S A 92:6957-6960.

Mainardi M, Landi S, Berardi N, Maffei L, Pizzorusso T (2009) Reduced responsiveness to long-term monocular deprivation of parvalbumin neurons assessed by c-Fos staining in rat visual cortex. PLoS One 4:e4342.

Majdan M, Shatz CJ (2006) Effects of visual experience on activity-dependent gene regulation in cortex. Nat Neurosci 9:650-659.

Majewska A, Tashiro A, Yuste R (2000a) Regulation of spine calcium dynamics by rapid spine motility. J Neurosci 20:8262-8268.

Majewska A, Brown E, Ross J, Yuste R (2000b) Mechanisms of calcium decay kinetics in hippocampal spines: role of spine calcium pumps and calcium diffusion through the spine neck in biochemical compartmentalization. J Neurosci 20:1722-1734.

Malenka RC, Kauer JA, Zucker RS, Nicoll RA (1988) Postsynaptic calcium is sufficient for potentiation of hippocampal synaptic transmission. Science 242:81-84.

Manahan-Vaughan D (1997) Group 1 and 2 metabotropic glutamate receptors play differential roles in hippocampal long-term depression and long-term potentiation in freely moving rats. J Neurosci 17:3303-3311.

Manahan-Vaughan D, Kulla A, Frey JU (2000) Requirement of translation but not transcription for the maintenance of long-term depression in the CA1 region of freely moving rats. J Neurosci 20:8572-8576.

Markram H, Toledo-Rodriguez M, Wang Y, Gupta A, Silberberg G, Wu C (2004) Interneurons of the neocortical inhibitory system. Nat Rev Neurosci 5:793-807.

Martin B, Ji S, Maudsley S, Mattson MP (2010) "Control" laboratory rodents are metabolically morbid: why it matters. Proc Natl Acad Sci U S A 107:6127-6133.

Mataga N, Nagai N, Hensch TK (2002) Permissive proteolytic activity for visual cortical plasticity. Proc Natl Acad Sci U S A 99:7717-7721.

Mataga N, Mizuguchi Y, Hensch TK (2004) Experience-dependent pruning of dendritic spines in visual cortex by tissue plasminogen activator. Neuron 44:1031-1041.

Matsuzaki M (2007) Factors critical for the plasticity of dendritic spines and memory storage. Neurosci Res 57:1-9.

Matsuzaki M, Honkura N, Ellis-Davies GC, Kasai H (2004) Structural basis of long-term potentiation in single dendritic spines. Nature 429:761-766.

Maya Vetencourt JF, Sale A, Viegi A, Baroncelli L, De Pasquale R, O'Leary OF, Castren E, Maffei L (2008) The antidepressant fluoxetine restores plasticity in the adult visual cortex. Science 320:385-388.

Mitchell DE, Gingras G, Kind PC (2001) Initial recovery of vision after early monocular deprivation in kittens is faster when both eyes are open. Proc Natl Acad Sci U S A 98:11662-11667.

Mitzdorf U (1985) Current source-density method and application in cat cerebral cortex: investigation of evoked potentials and EEG phenomena. Physiol Rev 65:37-100.

Mizutani A, Saito H, Matsuki N (1996) Possible involvement of plasmin in long-term potentiation of rat hippocampal slices. Brain Res 739:276-281.

Mockett B, Coussens C, Abraham WC (2002) NMDA receptor-mediated metaplasticity during the induction of long-term depression by low-frequency stimulation. Eur J Neurosci 15:1819-1826.

Mora F, Segovia G, del Arco A (2007) Aging, plasticity and environmental enrichment: structural changes and neurotransmitter dynamics in several areas of the brain. Brain Res Rev 55:78-88.

Mori H, Hanada R, Hanada T, Aki D, Mashima R, Nishinakamura H, Torisu T, Chien KR, Yasukawa H, Yoshimura A (2004) Socs3 deficiency in the brain elevates leptin sensitivity and confers resistance to diet-induced obesity. Nat Med 10:739-743.

Mormann F, Andrzejak RG, Kreuz T, Rieke C, David P, Elger CE, Lehnertz K (2003) Automated detection of a preseizure state based on a decrease in synchronization in intracranial electroencephalogram recordings from epilepsy patients. Phys Rev E Stat Nonlin Soft Matter Phys 67:021912.

Morrell F (1972) Visual system's view of acoustic space. Nature 238:44-46.

Mower GD, Berry D, Burchfiel JL, Duffy FH (1981) Comparison of the effects of dark rearing and binocular suture on development and plasticity of cat visual cortex. Brain Res 220:255-267.

Mrsic-Flogel TD, Hofer SB, Ohki K, Reid RC, Bonhoeffer T, Hubener M (2007) Homeostatic regulation of eye-specific responses in visual cortex during ocular dominance plasticity. Neuron 54:961-972.

Mulkey RM, Malenka RC (1992) Mechanisms underlying induction of homosynaptic long-term depression in area CA1 of the hippocampus. Neuron 9:967-975.

Mulkey RM, Herron CE, Malenka RC (1993) An essential role for protein phosphatases in hippocampal long-term depression. Science 261:1051-1055.

Murthy VN, Schikorski T, Stevens CF, Zhu Y (2001) Inactivity produces increases in neurotransmitter release and synapse size. Neuron 32:673-682.

Nagy V, Bozdagi O, Matynia A, Balcerzyk M, Okulski P, Dzwonek J, Costa RM, Silva AJ, Kaczmarek L, Huntley GW (2006) Matrix metalloproteinase-9 is required for hippocampal late-phase long-term potentiation and memory. J Neurosci 26:1923-1934.

Nahmani M, Erisir A (2005) VGluT2 immunochemistry identifies thalamocortical terminals in layer 4 of adult and developing visual cortex. J Comp Neurol 484:458-473.

Nakamura K, Hioki H, Fujiyama F, Kaneko T (2005) Postnatal changes of vesicular glutamate transporter (VGluT)1 and VGluT2 immunoreactivities and their colocalization in the mouse forebrain. J Comp Neurol 492:263-288.

Nevian T, Sakmann B (2004) Single spine Ca2+ signals evoked by coincident EPSPs and backpropagating action potentials in spiny stellate cells of layer 4 in the juvenile rat somatosensory barrel cortex. J Neurosci 24:1689-1699.

Nicoll RA, Oliet SH, Malenka RC (1998) NMDA receptor-dependent and metabotropic glutamate receptor-dependent forms of long-term depression coexist in CA1 hippocampal pyramidal cells. Neurobiol Learn Mem 70:62-72.

Niemeyer W, Starlinger I (1981) Do the blind hear better? Investigations on auditory processing in congenital or early acquired blindness. II. Central functions. Audiology 20:510-515.

Nishiyama M, Hong K, Mikoshiba K, Poo MM, Kato K (2000) Calcium stores regulate the polarity and input specificity of synaptic modification. Nature 408:584-588.

Nithianantharajah J, Hannan AJ (2006) Enriched environments, experience-dependent plasticity and disorders of the nervous system. Nat Rev Neurosci 7:697-709.

Nithianantharajah J, Levis H, Murphy M (2004) Environmental enrichment results in cortical and subcortical changes in levels of synaptophysin and PSD-95 proteins. Neurobiol Learn Mem 81:200-210.

Noguchi J, Matsuzaki M, Ellis-Davies GC, Kasai H (2005) Spine-neck geometry determines NMDA receptor-dependent Ca2+ signaling in dendrites. Neuron 46:609-622.

O'Connor JJ, Rowan MJ, Anwyl R (1995) Tetanically induced LTP involves a similar increase in the AMPA and NMDA receptor components of the excitatory postsynaptic current: investigations of the involvement of mGlu receptors. J Neurosci 15:2013-2020.

O'Leary DM, O'Connor JJ (1998) Priming of long-term potentiation by prior activation of group I and II metabotropic glutamate receptors in the rat dentate gyrus in vitro. Brain Res 809:91-96.

Oh MC, Derkach VA, Guire ES, Soderling TR (2006) Extrasynaptic membrane trafficking regulated by GluR1 serine 845 phosphorylation primes AMPA receptors for long-term potentiation. J Biol Chem 281:752-758.

Olson AK, Eadie BD, Ernst C, Christie BR (2006) Environmental enrichment and voluntary exercise massively increase neurogenesis in the adult hippocampus via dissociable pathways. Hippocampus 16:250-260.

Oray S, Majewska A, Sur M (2004) Dendritic spine dynamics are regulated by monocular deprivation and extracellular matrix degradation. Neuron 44:1021-1030.

Patterson CM, Bouret SG, Dunn-Meynell AA, Levin BE (2009) Three weeks of postweaning exercise in DIO rats produces prolonged increases in central leptin sensitivity and signaling. Am J Physiol Regul Integr Comp Physiol 296:R537-548.

Patterson SL, Abel T, Deuel TA, Martin KC, Rose JC, Kandel ER (1996) Recombinant BDNF rescues deficits in basal synaptic transmission and hippocampal LTP in BDNF knockout mice. Neuron 16:1137-1145.

Paxinos G, Franklin, K. (2008) The mouse brain in stereotaxic coordinates: Elsevier.

Pham TM, Winblad B, Granholm AC, Mohammed AH (2002) Environmental influences on brain neurotrophins in rats. Pharmacol Biochem Behav 73:167-175.

Philpot BD, Cho KK, Bear MF (2007) Obligatory role of NR2A for metaplasticity in visual cortex. Neuron 53:495-502.

Piche M, Robert S, Miceli D, Bronchti G (2004) Environmental enrichment enhances auditory takeover of the occipital cortex in anophthalmic mice. Eur J Neurosci 20:3463-3472.

Piche M, Chabot N, Bronchti G, Miceli D, Lepore F, Guillemot JP (2007) Auditory responses in the visual cortex of neonatally enucleated rats. Neuroscience 145:1144-1156.

Pinto S, Roseberry AG, Liu H, Diano S, Shanabrough M, Cai X, Friedman JM, Horvath TL (2004) Rapid rewiring of arcuate nucleus feeding circuits by leptin. Science 304:110-115.

Pizzorusso T, Medini P, Berardi N, Chierzi S, Fawcett JW, Maffei L (2002) Reactivation of ocular dominance plasticity in the adult visual cortex. Science 298:1248-1251.

Pizzorusso T, Medini P, Landi S, Baldini S, Berardi N, Maffei L (2006) Structural and functional recovery from early monocular deprivation in adult rats. Proc Natl Acad Sci U S A 103:8517-8522.

Polat U (2008) Restoration of underdeveloped cortical functions: evidence from treatment of adult amblyopia. Restor Neurol Neurosci 26:413-424.

Porciatti V, Burr DC, Morrone MC, Fiorentini A (1992) The effects of aging on the pattern electroretinogram and visual evoked potential in humans. Vision Res 32:1199-1209.

Porciatti V, Bonanni P, Fiorentini A, Guerrini R (2000) Lack of cortical contrast gain control in human photosensitive epilepsy. Nat Neurosci 3:259-263.

Ptito M, Fumal A, de Noordhout AM, Schoenen J, Gjedde A, Kupers R (2008) TMS of the occipital cortex induces tactile sensations in the fingers of blind Braille readers. Exp Brain Res 184:193-200.

Putignano E, Lonetti G, Cancedda L, Ratto G, Costa M, Maffei L, Pizzorusso T (2007) Developmental downregulation of histone posttranslational modifications regulates visual cortical plasticity. Neuron 53:747-759.

Quinlan EM, Olstein DH, Bear MF (1999a) Bidirectional, experience-dependent regulation of N-methyl-D-aspartate receptor subunit composition in the rat visual cortex during postnatal development. Proc Natl Acad Sci U S A 96:12876-12880.

Quinlan EM, Philpot BD, Huganir RL, Bear MF (1999b) Rapid, experience-dependent expression of synaptic NMDA receptors in visual cortex in vivo. Nat Neurosci 2:352-357.

Rampon C, Tang YP, Goodhouse J, Shimizu E, Kyin M, Tsien JZ (2000a) Enrichment induces structural changes and recovery from nonspatial memory deficits in CA1 NMDAR1-knockout mice. Nat Neurosci 3:238-244.

Rampon C, Jiang CH, Dong H, Tang YP, Lockhart DJ, Schultz PG, Tsien JZ, Hu Y (2000b) Effects of environmental enrichment on gene expression in the brain. Proc Natl Acad Sci U S A 97:12880-12884.

Raymond CR, Thompson VL, Tate WP, Abraham WC (2000) Metabotropic glutamate receptors trigger homosynaptic protein synthesis to prolong long-term potentiation. J Neurosci 20:969-976.

Reichardt LF (2006) Neurotrophin-regulated signalling pathways. Philos Trans R Soc Lond B Biol Sci 361:1545-1564.

Rittenhouse CD, Shouval HZ, Paradiso MA, Bear MF (1999) Monocular deprivation induces homosynaptic long-term depression in visual cortex. Nature 397:347-350.

Roberts EB, Meredith MA, Ramoa AS (1998) Suppression of NMDA receptor function using antisense DNA block ocular dominance plasticity while preserving visual responses. J Neurophysiol 80:1021-1032.

Roder B, Stock O, Bien S, Neville H, Rosler F (2002) Speech processing activates visual cortex in congenitally blind humans. Eur J Neurosci 16:930-936.

Roder B, Teder-Salejarvi W, Sterr A, Rosler F, Hillyard SA, Neville HJ (1999) Improved auditory spatial tuning in blind humans. Nature 400:162-166.

Rosenzweig MR, Bennett EL, Krech D (1964) Cerebral Effects of Environmental Complexity and Training among Adult Rats. J Comp Physiol Psychol 57:438-439.

Rosenzweig MR, Krech D, Bennett EL, Zolman JF (1962) Variation in environmental complexity and brain measures. J Comp Physiol Psychol 55:1092-1095.

Rosenzweig MR, Bennett EL, Hebert M, Morimoto H (1978) Social grouping cannot account for cerebral effects of enriched environments. Brain Res 153:563-576.

Rossi FM, Bozzi Y, Pizzorusso T, Maffei L (1999) Monocular deprivation decreases brain-derived neurotrophic factor immunoreactivity in the rat visual cortex. Neuroscience 90:363-368.

Rozas C, Frank H, Heynen AJ, Morales B, Bear MF, Kirkwood A (2001) Developmental inhibitory gate controls the relay of activity to the superficial layers of the visual cortex. J Neurosci 21:6791-6801.

Sacks O (1985) "To see and not to see". In: The man who mistook his wife for a hat. New York: Summit Books.

Sadato N, Pascual-Leone A, Grafman J, Deiber MP, Ibanez V, Hallett M (1998) Neural networks for Braille reading by the blind. Brain 121 (Pt 7):1213-1229.

Sadato N, Pascual-Leone A, Grafman J, Ibanez V, Deiber MP, Dold G, Hallett M (1996) Activation of the primary visual cortex by Braille reading in blind subjects. Nature 380:526-528.

Saghatelyan AK, Dityatev A, Schmidt S, Schuster T, Bartsch U, Schachner M (2001) Reduced perisomatic inhibition, increased excitatory transmission, and impaired long-term potentiation in mice deficient for the extracellular matrix glycoprotein tenascin-R. Mol Cell Neurosci 17:226-240.

Sale A, Berardi N, Maffei L (2009) Enrich the environment to empower the brain. Trends Neurosci 32:233-239.

Sale A, Cenni MC, Ciucci F, Putignano E, Chierzi S, Maffei L (2007a) Maternal enrichment during pregnancy accelerates retinal development of the fetus. PLoS One 2:e1160.

Sale A, Putignano E, Cancedda L, Landi S, Cirulli F, Berardi N, Maffei L (2004) Enriched environment and acceleration of visual system development. Neuropharmacology 47:649-660.

Sale A, Maya Vetencourt JF, Medini P, Cenni MC, Baroncelli L, De Pasquale R, Maffei L (2007b) Environmental enrichment in adulthood promotes amblyopia recovery through a reduction of intracortical inhibition. Nat Neurosci 10:679-681.

Saron CD, Schroeder CE, Foxe JJ, Vaughan HG, Jr. (2001) Visual activation of frontal cortex: segregation from occipital activity. Brain Res Cogn Brain Res 12:75-88.

Sawtell NB, Frenkel MY, Philpot BD, Nakazawa K, Tonegawa S, Bear MF (2003) NMDA receptor-dependent ocular dominance plasticity in adult visual cortex. Neuron 38:977-985.

Scarpace PJ, Zhang Y (2009) Leptin resistance: a prediposing factor for diet-induced obesity. Am J Physiol Regul Integr Comp Physiol 296:R493-500.

Schilling G, Savonenko AV, Coonfield ML, Morton JL, Vorovich E, Gale A, Neslon C, Chan N, Eaton M, Fromholt D, Ross CA, Borchelt DR (2004) Environmental, pharmacological, and genetic modulation of the HD phenotype in transgenic mice. Exp Neurol 187:137-149.

Schmucker C, Kleijnen J, Grosselfinger R, Riemsma R, Antes G, Lange S, Lagreze W (2010) Effectiveness of early in comparison to late(r) treatment in children with amblyopia or its risk factors: a systematic review. Ophthalmic Epidemiol 17:7-17.

Schuett S, Bonhoeffer T, Hubener M (2001) Pairing-induced changes of orientation maps in cat visual cortex. Neuron 32:325-337.

Seeburg DP, Feliu-Mojer M, Gaiottino J, Pak DT, Sheng M (2008) Critical role of CDK5 and Polo-like kinase 2 in homeostatic synaptic plasticity during elevated activity. Neuron 58:571-583.

Shi S, Hayashi Y, Esteban JA, Malinow R (2001) Subunit-specific rules governing AMPA receptor trafficking to synapses in hippocampal pyramidal neurons. Cell 105:331-343.

Shimizu C, Yoshida S, Shibata M, Kato K, Momota Y, Matsumoto K, Shiosaka T, Midorikawa R, Kamachi T, Kawabe A, Shiosaka S (1998) Characterization of recombinant and brain neuropsin, a plasticity-related serine protease. J Biol Chem 273:11189-11196.

Sjostrom PJ, Turrigiano GG, Nelson SB (2001) Rate, timing, and cooperativity jointly determine cortical synaptic plasticity. Neuron 32:1149-1164.

Smith GB, Heynen AJ, Bear MF (2009) Bidirectional synaptic mechanisms of ocular dominance plasticity in visual cortex. Philos Trans R Soc Lond B Biol Sci 364:357-367.

Song S, Miller KD, Abbott LF (2000) Competitive Hebbian learning through spike-timing-dependent synaptic plasticity. Nat Neurosci 3:919-926.

Stanley S, Pinto S, Segal J, Perez CA, Viale A, DeFalco J, Cai X, Heisler LK, Friedman JM (2010) Identification of neuronal subpopulations that project from hypothalamus to both liver and adipose tissue polysynaptically. Proc Natl Acad Sci U S A 107:7024-7029.

Stanton GB, Bruce CJ, Goldberg ME (1995) Topography of projections to posterior cortical areas from the macaque frontal eye fields. J Comp Neurol 353:291-305.

Steriade M (2006) Grouping of brain rhythms in corticothalamic systems. Neuroscience 137:1087-1106.

Sternson SM, Shepherd GM, Friedman JM (2005) Topographic mapping of VMH --> arcuate nucleus microcircuits and their reorganization by fasting. Nat Neurosci 8:1356-1363.

Stryker MP, Harris WA (1986) Binocular impulse blockade prevents the formation of ocular dominance columns in cat visual cortex. J Neurosci 6:2117-2133.

Sullivan FR, Bird ED, Alpay M, Cha JH (2001) Remotivation therapy and Huntington's disease. J Neurosci Nurs 33:136-142.

Sur M, Garraghty PE, Roe AW (1988) Experimentally induced visual projections into auditory thalamus and cortex. Science 242:1437-1441.

Sutton MA, Ito HT, Cressy P, Kempf C, Woo JC, Schuman EM (2006) Miniature neurotransmission stabilizes synaptic function via tonic suppression of local dendritic protein synthesis. Cell 125:785-799.

Sweatt JD (2004) Mitogen-activated protein kinases in synaptic plasticity and memory. Curr Opin Neurobiol 14:311-317.

Takamori S (2006) VGLUTs: 'exciting' times for glutamatergic research? Neurosci Res 55:343-351.

Thomas GM, Huganir RL (2004) MAPK cascade signalling and synaptic plasticity. Nat Rev Neurosci 5:173-183.

Thomson AM (2000) Facilitation, augmentation and potentiation at central synapses. Trends Neurosci 23:305-312.

Toldi J, Farkas T, Volgyi B (1994) Neonatal enucleation induces cross-modal changes in the barrel cortex of rat. A behavioural and electrophysiological study. Neurosci Lett 167:1-4.

Trachtenberg JT, Trepel C, Stryker MP (2000) Rapid extragranular plasticity in the absence of thalamocortical plasticity in the developing primary visual cortex. Science 287:2029-2032.

Trachtenberg JT, Chen BE, Knott GW, Feng G, Sanes JR, Welker E, Svoboda K (2002) Long-term in vivo imaging of experience-dependent synaptic plasticity in adult cortex. Nature 420:788-794.

Tropea D, Kreiman G, Lyckman A, Mukherjee S, Yu H, Horng S, Sur M (2006) Gene expression changes and molecular pathways mediating activity-dependent plasticity in visual cortex. Nat Neurosci 9:660-668.

Tsanov M, Manahan-Vaughan D (2007) Intrinsic, light-independent and visual activity-dependent mechanisms cooperate in the shaping of the field response in rat visual cortex. J Neurosci 27:8422-8429.

Tsay D, Yuste R (2004) On the electrical function of dendritic spines. Trends Neurosci 27:77-83.

Tumpel S, Wiedemann LM, Krumlauf R (2009) Hox genes and segmentation of the vertebrate hindbrain. Curr Top Dev Biol 88:103-137.

Turrigiano GG (2008) The self-tuning neuron: synaptic scaling of excitatory synapses. Cell 135:422-435.

Turrigiano GG, Nelson SB (2004) Homeostatic plasticity in the developing nervous system. Nat Rev Neurosci 5:97-107.

Turrigiano GG, Leslie KR, Desai NS, Rutherford LC, Nelson SB (1998) Activity-dependent scaling of quantal amplitude in neocortical neurons. Nature 391:892-896.

Tzounopoulos T, Rubio ME, Keen JE, Trussell LO (2007) Coactivation of pre- and postsynaptic signaling mechanisms determines cell-specific spike-timing-dependent plasticity. Neuron 54:291-301.

Ulrich HP, Klein U, von Figura K (1979) Degradation of even-numbered reduced and non-reduced hyaluronate oligosaccharides with D-glucuronic acid or N-acetyl-D-glucosamine as non-reducing terminal by chondroitin ABC and AC lyases. Hoppe Seylers Z Physiol Chem 360:1457-1463.

Vaisse C, Halaas JL, Horvath CM, Darnell JE, Jr., Stoffel M, Friedman JM (1996) Leptin activation of Stat3 in the hypothalamus of wild-type and ob/ob mice but not db/db mice. Nat Genet 14:95-97.

van Dellen A, Blakemore C, Deacon R, York D, Hannan AJ (2000) Delaying the onset of Huntington's in mice. Nature 404:721-722.

Van der Loos H, Woolsey TA (1973) Somatosensory cortex: structural alterations following early injury to sense organs. Science 179:395-398.

van der Merwe MT (2007) Psychological correlates of obesity in women. Int J Obes (Lond) 31 Suppl 2:S14-18; discussion S31-12.

van Praag H, Kempermann G, Gage FH (1999) Running increases cell proliferation and neurogenesis in the adult mouse dentate gyrus. Nat Neurosci 2:266-270.

van Praag H, Kempermann G, Gage FH (2000) Neural consequences of environmental enrichment. Nat Rev Neurosci 1:191-198.

Volgyi B, Farkas T, Toldi J (1993) Compensation of a sensory deficit inflicted upon newborn and adult animals. A behavioural study. Neuroreport 4:827-829.

von Melchner L, Pallas SL, Sur M (2000) Visual behaviour mediated by retinal projections directed to the auditory pathway. Nature 404:871-876.

Wallace W, Bear MF (2004) A morphological correlate of synaptic scaling in visual cortex. J Neurosci 24:6928-6938.

Weeber EJ, Beffert U, Jones C, Christian JM, Forster E, Sweatt JD, Herz J (2002) Reelin and ApoE receptors cooperate to enhance hippocampal synaptic plasticity and learning. J Biol Chem 277:39944-39952.

Wiesel TN, Hubel DH, Lam DM (1974) Autoradiographic demonstration of ocular-dominance columns in the monkey striate cortex by means of transneuronal transport. Brain Res 79:273-279.

Wigstrom H, Gustafsson B (1986) Postsynaptic control of hippocampal long-term potentiation. J Physiol (Paris) 81:228-236.

Will B, Galani R, Kelche C, Rosenzweig MR (2004) Recovery from brain injury in animals: relative efficacy of environmental enrichment, physical exercise or formal training (1990-2002). Prog Neurobiol 72:167-182.

Wilson NR, Kang J, Hueske EV, Leung T, Varoqui H, Murnick JG, Erickson JD, Liu G (2005) Presynaptic regulation of quantal size by the vesicular glutamate transporter VGLUT1. J Neurosci 25:6221-6234.

Wong-Riley MT, Welt C (1980) Histochemical changes in cytochrome oxidase of cortical barrels after vibrissal removal in neonatal and adult mice. Proc Natl Acad Sci U S A 77:2333-2337.

Xiao MY, Zhou Q, Nicoll RA (2001) Metabotropic glutamate receptor activation causes a rapid redistribution of AMPA receptors. Neuropharmacology 41:664-671.

Yazaki-Sugiyama Y, Kang S, Cateau H, Fukai T, Hensch TK (2009) Bidirectional plasticity in fast-spiking GABA circuits by visual experience. Nature 462:218-221.

Yoon BJ, Smith GB, Heynen AJ, Neve RL, Bear MF (2009) Essential role for a long-term depression mechanism in ocular dominance plasticity. Proc Natl Acad Sci U S A 106:9860-9865.

Zhang LI, Tao HW, Holt CE, Harris WA, Poo M (1998) A critical window for cooperation and competition among developing retinotectal synapses. Nature 395:37-44.

Zhang R, Dhillon H, Yin H, Yoshimura A, Lowell BB, Maratos-Flier E, Flier JS (2008) Selective inactivation of Socs3 in SF1 neurons improves glucose homeostasis without affecting body weight. Endocrinology 149:5654-5661.

Zhang Y, Proenca R, Maffei M, Barone M, Leopold L, Friedman JM (1994) Positional cloning of the mouse obese gene and its human homologue. Nature 372:425-432.

Zheng W, Knudsen EI (1999) Functional selection of adaptive auditory space map by GABAA-mediated inhibition. Science 284:962-965.

Zhou Q, Homma KJ, Poo MM (2004) Shrinkage of dendritic spines associated with long-term depression of hippocampal synapses. Neuron 44:749-757.